

MODELING OF TIME DOMAIN REPRESENTED SIGNALS WITH
MULTITONE SIGNALS

A THESIS SUBMITTED TO
THE GRADUATE SCHOOL OF NATURAL AND APPLIED SCIENCES
OF
MIDDLE EAST TECHNICAL UNIVERSITY

BY

GÖKHAN CANSIZ

IN PARTIAL FULLFILLMENT OF THE REQUIREMENTS
FOR
THE DEGREE OF MASTER OF SCIENCE
IN
ELECTRICAL AND ELECTRONICS ENGINEERING

MARCH 2014

Approval of the thesis:

IDENTIFICATION OF MEMORY TERMS IN A POWER AMPLIFIER

submitted by **GÖKHAN CANSIZ** in partial fulfillment of the requirements for the degree of **Master of Science in Electrical and Electronics Engineering Department, Middle East Technical University** by,

Prof. Dr. Canan Özgen
Dean, Graduate School of **Natural and Applied Sciences** _____

Prof. Dr. Gönül Turhan Sayan
Head of Department, **Electrical and Electronics Eng.** _____

Prof. Dr. Şimşek Demir
Supervisor, **Electrical and Electronics Eng. Dept., METU** _____

Examining Committee Members:

Prof. Dr. Canan Toker
Electrical and Electronics Eng. Dept., METU _____

Prof. Dr. Şimşek Demir
Electrical and Electronics Eng. Dept., METU _____

Prof. Dr. Sencer Koç
Electrical and Electronics Eng. Dept., METU _____

Asst. Prof. Dr. Ahmet Hayrettin Yüzer
Electrical and Electronics Eng. Dept., KBU _____

Bülent Şen, M.Sc.
Senior Lead Design Engineer, ASELSAN _____

Date: 10/03/2014

I hereby declare that all information in this document has been obtained and presented in accordance with academic rules and ethical conduct. I also declare that, as required by these rules and conduct, I have fully cited and referenced all material and results that are not original to this work.

Name, Last name : Gökhan CANSIZ

Signature :

ABSTRACT

MODELING OF TIME DOMAIN REPRESENTED SIGNALS WITH MULTITONE SIGNALS

Cansız, Gökhan

M. Sc., Department of Electrical and Electronics Engineering

Supervisor: Prof. Dr. Şimşek Demir

March 2014, 121 pages

Signals in certain systems, such as the transmitted signal in a cellular communication system, are strongly time dependent, non-deterministic and stochastically not well defined. Predicting the performance of the transmitter with such a signal at its input is important for efficient operation. Therefore, it is crucial to model a given time dependent waveform by multi-tone signals, which enables analytical derivations.

In this thesis, multi-tone representation is employed to model the varying envelope arbitrary waveforms. Number, amplitude, phase of the tones and spacing between tones are considered as parameters for the multi-tone stimuli. To prove the validity of the multi-tone representation, CCDF curve is considered as a figure of merit for comparison. Different nonlinear amplifiers are excited with an arbitrary waveform and its multi-tone representation in the simulation environment. At the output of the amplifier, similar nonlinear behaviors such as, in-band and out of band distortion powers are observed. After proving that original and model signal have similar nonlinear responses, modulation performance of the arbitrary waveform and model signal in a transmitter chain is investigated for different drive levels.

Keywords: Multi-tone signals, Modeling, Arbitrary Waveform

ÖZ

ZAMAN DÜZLEMİNDE TANIMLANMIŞ BİR SİNYALİN ÇOK TONLU SİNYALLER İLE MODELLENMESİ

Cansız, Gökhan

Yüksek Lisans, Elektrik ve Elektronik Mühendisliği Bölümü

Tez Yöneticisi: Prof. Dr. Şimşek Demir

Mart 2014, 121 sayfa

Mobil haberleşme sistemlerindeki iletim sinyallerinde olduğu gibi belirli bazı sistemlerde zaman düzleminde tanımlanmış, rastgele ve stokastik olarak iyi tanımlanmamış sinyaller kullanılır. Bu tarz bir işaretle çalışan bir göndericinin performansını öngörmek, verimli bir çalışma için önem arz etmektedir. Bu yüzden, zaman düzleminde tanımlanmış işaretleri, çok tonlu sinyaller ile ifade edebilmek, analitik çıkarımları mümkün kıldığı için önemlidir.

Bu tezde, değişken zarflı rastgele sinyalleri modelleyebilmek için çok tonlu gösterim kullanılır. Tonların sayısı, genliği, fazı ve tonlar arasındaki mesafe çok tonlu gösterim için parametre olarak alınır. Çok tonlu sinyalin geçerliliğini kanıtlamak amacı ile, bütünleyici birikimli dağılım fonksiyonu karşılaştırma amacı ile başarımlı ölçüsü olarak kullanılır. Farklı doğrusal olmayan yükselteçler, simülasyon ortamında rastgele sinyal ve onun çok tonlu modeli ile uyarılmıştır. Yükselteç çıkışında bant içi ve bant dışı bozunum gücü gibi benzer doğrusal olmayan davranışlar gözlemlenmiştir. Sinyallerin benzer doğrusal olmayan davranışlara yol açtığını gösterdikten sonra, bir gönderici bloğu altında rastgele sinyalin ve onun çok tonlu gösteriminin modülasyon performansları farklı giriş seviyeleri için araştırılmıştır.

Anahtar Kelimeler: Çok tonlu sinyal, modelleme, Rastgele Sinyal

To My Family,

ACKNOWLEDGEMENTS

First of all, I would like to express my deepest gratitude to my family for their loving and continued support.

I cannot express enough thanks to my advisor, Prof. Dr. Şimşek Demir for his excellent guiding, caring, patience and encouragement throughout the thesis. I had an outstanding research activity under his supervision.

I am grateful to ASELSAN Electronic Industries for giving me opportunity to improve my engineering capabilities and for providing me every kind of hardware, software and financial support.

I would also like to thank Turkish Scientific and Technological Research Council (TUBİTAK) for their monetary support throughout my study.

TABLE OF CONTENTS

ABSTRACT.....	v
ÖZ	vi
ACKNOWLEDGEMENTS	viii
TABLE OF CONTENTS	ix
LIST OF TABLES	xi
LIST OF FIGURES	xiii
LIST OF ABBREVIATIONS	xviii
CHAPTERS	
1. INTRODUCTION	1
2. POWER AMPLIFIER CHARACTERISTICS AND MODELING.....	5
2.1 Power Amplifier Characteristics	5
2.1.1 Intermodulation Products	6
2.1.2 Intercept Points.....	8
2.1.3 Compression Points.....	10
2.1.4 AM-AM and AM-PM Conversion Rate	10
2.1.5 ACPR	11
2.1.6 Efficiency	12
2.2 Power Amplifier Models	14
2.2.1 Polynomial Model.....	14
2.2.2 Saleh Model	18
2.2.3 Rapp Model.....	19
2.2.4 Ghorbani Model	20
3. MULTI-TONE MODELLING	23
3.1 Properties of Multi-Tone Stimuli	24
3.2 Parameters of the Multi-Tone Model	27
3.2.1 Effect of Phase Variations of Tones	29

3.2.2	Effect of Spacing between Tones.....	32
3.2.3	Effect of Amplitudes of Tones.....	34
3.2.4	Effect of Number of Tones.....	37
3.3	Parameter Selection Criteria.....	38
3.4	Properties of the Amplifiers Used in Simulations.....	41
3.5	Properties of Waveforms Used in Simulations.....	50
4.	VERIFICATION OF MULTI-TONE MODELS WITH AMPLIFIERS.....	57
4.1	Multi-Tone Models for WCDMA Signal.....	58
4.1.1	3-Tone Model for WCDMA signal.....	58
4.1.2	5-Tone Model for WCDMA signal.....	63
4.1.3	7-Tone Model for WCDMA signal.....	67
4.1.4	9-Tone Model for WCDMA signal.....	71
4.2	Multi-Tone Models for CDMA Signal.....	76
4.2.1	5-Tone Model for CDMA signal.....	76
4.2.2	7-Tone Model for CDMA signal.....	82
4.2.3	9-Tone Model for CDMA signal.....	86
5.	EVM & BER MEASUREMENT.....	91
5.1	SIMULATED BER and EVM RESULTS.....	96
6.	CONCLUSION & FUTURE WORK.....	107
	REFERENCES.....	111
	APPENDICES.....	115

LIST OF TABLES

TABLES

Table 3-1 Characteristics of two 5-tone signal with same channel power, tone phases and spacings	36
Table 3-2 Intermodulation distortion products under two equal amplitude tone with 1 MHz tone spacing for the amplifier board GVA-63+	44
Table 3-3 Intermodulation distortion products under two equal amplitude tone with 1 MHz tone spacing for the amplifier board PMA-545G1+	48
Table 4-1 WCDMA parameters for different drive levels of GVA-63+	61
Table 4-2 3-tone model parameters for different drive levels of GVA-63+	61
Table 4-3 WCDMA parameters for different drive levels of PMA-545G1+	62
Table 4-4 3-tone model parameters for different drive levels of PMA-545G1+	62
Table 4-5 5-tone model parameters for different drive levels of GVA-63+	66
Table 4-6 5-tone model parameters for different drive levels of PMA-545G1+	66
Table 4-7 7-tone model parameters for different drive levels of GVA-63+	70
Table 4-8 7-tone model parameters for different drive levels of PMA-545G1+	70
Table 4-9 9-tone model parameters for different drive levels of GVA-63+	74
Table 4-10 9-tone model parameters for different drive levels of PMA-545G1+	75
Table 4-11 5-tone model parameters for different drive levels of GVA-63+	79
Table 4-12 CDMA signal parameters for different drive levels of GVA-63+	79
Table 4-13 5-tone model parameters for different drive levels of PMA-545G1+	80
Table 4-14 CDMA signal parameters for different drive levels of PMA-545G1+	81
Table 4-15 7-tone model parameters for different drive levels of GVA-63+	84
Table 4-16 7-tone model parameters for different drive levels of PMA-545G1+	85
Table 4-17 9-tone model parameters for different drive levels of GVA-63+	89
Table 4-18 9-tone model parameters for different drive levels of PMA-545G1+	89

Table 5- 1 EVM and BER results for CDMA signal for different power levels.....	96
Table 5-2 EVM and BER results for 5-tone model of CDMA signal.....	97
Table 5-3 EVM and BER results for 7-tone model of CDMA signal.....	97
Table 5-4 EVM and BER results for 9-tone model of CDMA signal.....	98
Table 5-5 EVM and BER results for WCDMA signal for different power levels...	101
Table 5-6 EVM and BER results for 3-tone model of WCDMA signal	101
Table 5-7 EVM and BER results for 5-tone model of WCDMA signal	102
Table 5-8 EVM and BER results for 7-tone model of WCDMA signal	102
Table 5-9 EVM and BER results for 9-tone model of WCDMA signal	103

LIST OF FIGURES

FIGURES

Figure 2-1 Output of a nonlinear amplifier under a two-tone input [6].....	8
Figure 2-2 Demonstration of intercept points of a typical amplifier [7].....	9
Figure 2-3 AM-AM characteristics of a typical amplifier [8].....	11
Figure 2-4 AM-PM distortion of a typical amplifier [9].....	11
Figure 2-5 Spectral regrowth in lower and upper adjacent channels [11]	12
Figure 2-6 Bandwidth definitions and locations for different types of signals [10]..	12
Figure 2-7 N^{th} order intercept point [17].....	16
Figure 2-8 AM-AM and AM-PM curves for Saleh model [18].....	19
Figure 2-9 Rapp model AM-AM conversion characteristics [16]	20
Figure 2-10 Ghorbani model AM-AM and AM-PM conversion characteristics [18]	21
Figure 3-1 RF envelope of a typical CDMA signal [25]	26
Figure 3-2 CCDF curve of the CDMA signal with corresponding power levels in	
Figure 3.1 [25].....	27
Figure 3-3 Comparison of CCDF curves of AWGN and different number of multi-	
tone signals [25]	28
Figure 3-4 Effect of phase variation on CCDF curve [25].....	29
Figure 3-5 Comparison of CCDF curves of a 4-tone signal and a 64-tone signal. [25]	
.....	30
Figure 3-6 Intermodulation products under 3- tone excitation with equal phases.....	31
Figure 3-7 Intermodulation products under 3-tone excitation with different phases	
(300, 90 and 40 degrees respectively).....	31
Figure 3-8 Effect of spacing between tones on periodic behavior of signal.....	33
Figure 3-9 Effect of tone spacing on CCDF curve	33
Figure 3-10 Output of 3rd order polynomial model amplifier under in-phase, equally	
spaced and -16 dBm equal amplitude 5-tones	34

Figure 3-11 Output of 3rd order polynomial model amplifier under in-phase, equally spaced and -11 dBm equal amplitude 5-tones.....	35
Figure 3-12 Effect of amplitude of tones on CCDF.....	36
Figure 3-13 CCDF curves of two 5-tone signal having very similar channel power and identical tone phases.....	37
Figure 3-14 Effect of number of tones on the peak to average ratio for equal amplitude and equi-spaced tones.....	38
Figure 3-15 AM-AM characteristics of the amplifier GVA-63+.....	42
Figure 3-16 AM-PM characteristics of the amplifier GVA-63+.....	43
Figure 3-17 3 rd order intermodulation products for different power levels of GVA-63+.....	45
Figure 3-18 5 th order intermodulation products for different power levels of GVA-63+.....	46
Figure 3-19 AM-AM characteristics of the amplifier PMA-545G1+.....	47
Figure 3-20 AM-PM characteristics of the amplifier PMA-545G1+.....	48
Figure 3-21 3 rd order intermodulation products for different power levels of PMA-545G1+.....	49
Figure 3-22 5 th order intermodulation products for different power levels of PMA-545G1+.....	50
Figure 3-23 RF carrier modulated by 3GPP uplink signal and its properties	51
Figure 3-24 Spectrum of the input (left) and output (right) carrier for 3GPP uplink signal	51
Figure 3-25 Magnitude (left) and phase (right) of the input carrier for 3GPP uplink signal.	52
Figure 3-26 Main, upper, lower channel band definitions and measurement equations for channel power calculations.....	52
Figure 3-27 Simulated band characteristics of WCDMA input signal	52
Figure 3-28 CCDF characteristics of WCDMA signal and WGN.....	53
Figure 3-29 RF carrier modulated by a CDMA signal and its properties	54
Figure 3-30 Spectrum of the input (left) and output (right) carrier for CDMA signal	54

Figure 3-31 Magnitude (left) and phase (right) of the input carrier for Fwd Link CDMA signal.	55
Figure 3-32 Main, upper, lower channel band definitions and measurement equations for channel power calculations.....	55
Figure 3-33 Simulated band characteristics of input CDMA signal	56
Figure 3-34 CCDF characteristics of CDMA signal and WGN	56
Figure 4-1 3-tone model schematic prepared in ADS.....	58
Figure 4-2 Baseband spectrum of 3-tone model (left) and amplified (with GVA-63+ amplifier) 3-tone model (right)	59
Figure 4-3 CCDF curves of 3-tone model and WCDMA signal	59
Figure 4-4 The distribution of instantaneous nonlinear power for WCDMA signal and its 3-tone model.....	60
Figure 4-5 5-tone model schematic prepared in ADS.....	63
Figure 4-6 Baseband spectrum of 5-tone model (left) and amplified (with GVA-63+ amplifier) 5-tone model (right)	64
Figure 4-7 CCDF curves of 5-tone model and WCDMA signal	64
Figure 4-8 The distribution of instantaneous nonlinear power of WCDMA signal and its 5-tone model.....	65
Figure 4-9 7-tone Model schematic prepared in ADS	67
Figure 4-10 Baseband spectrum of 7-tone signal (left) and amplified (with GVA-63+ amplifier) 7-tone signal (right).....	68
Figure 4-11 CCDF curves of 7-tone model and WCDMA signal	68
Figure 4-12 The distribution of instantaneous nonlinear power of WCDMA signal and its 7-tone model.....	69
Figure 4-13 9-tone model schematic prepared in ADS.....	71
Figure 4-14 Baseband spectrum of 9-tone model and amplified (with GVA-63+ amplifier) 9-tone signal	72
Figure 4-15 CCDF curves of 9-tone model and WCDMA signal	73
Figure 4-16 The distribution of instantaneous nonlinear power of WCDMA signal and its 9-tone model.....	73
Figure 4-17 5-tone model schematic prepared in ADS.....	76

Figure 4-18 Baseband spectrum of 5-tone model (left) and amplified (with GVA-63+ amplifier) 5-tone signal	77
Figure 4-19 CCDF curves of 5-tone model and CDMA signal	77
Figure 4-20 The distribution of instantaneous nonlinear power of CDMA signal and its 5-tone model.....	78
Figure 4-21 7-tone model schematic prepared in ADS.....	82
Figure 4-22 Baseband spectrum of 7-tone model (left) and amplified (with GVA-63+ amplifier) 7-tone model (right)	82
Figure 4-23 CCDF curves of 7-tone model and CDMA signal	83
Figure 4-24 The distribution of instantaneous nonlinear power of CDMA signal and its 7-tone model.....	83
Figure 4-25 9-tone model schematic prepared in ADS.....	86
Figure 4-26 Baseband spectrum of 9-tone model representing CDMA signal and amplified (with GVA-63+ amplifier) 9-tone signal	87
Figure 4-27 CCDF curves of 9-tone model and CDMA signal	87
Figure 4-28 The distribution of instantaneous nonlinear power of CDMA signal and its 9-tone model.....	88
Figure 5-1 Magnitude and phase error components of error vector [28].....	92
Figure 5-2 Block diagram representation for BER and EVM measurements.....	93
Figure 5-3 Comparison of the AM-AM characteristics of the GVA-63+ application board and model amplifier	94
Figure 5-4 Comparison of the AM-PM characteristics of the GVA-63+ application board and model amplifier	95
Figure 5-5 RMS EVM values of multi-tone signals and CDMA signal for different power levels.....	98
Figure 5-6 Max EVM values of multi-tone signals and CDMA signal for different power levels.....	99
Figure 5-7 Percentile EVM values of multi-tone signals and CDMA signal for different power levels.....	99
Figure 5-8 RMS EVM values of multi-tone signals and WCDMA signal for different power levels.....	103

Figure 5-9 Max EVM values of multi-tone signals and WCDMA signal for different power levels	104
Figure 5-10 Percentile EVM values of multi-tone signals and WCDMA signal for different power levels.....	104

LIST OF ABBREVIATIONS

ACPR	: Adjacent Channel Power Ratio
AM-AM	: Amplitude Dependent Amplitude Distortion
AM-PM	: Amplitude Dependent Phase Distortion
BER	: Bit Error Rate
CCDF	: Complementary Cumulative Distribution Function
CDMA	: Code Division Multiple Access
DPD	: Digital Predistortion
DSP	: Digital Signal Processing
EER	: Envelope Elimination and Restoration
EVM	: Error Vector Magnitude
FFT	: Fast Fourier Transform
FM	: Frequency Modulation
GaN	: Gallium Nitride
IIP_3	: Input Third Order Intercept Point
IIP_2	: Input Second Order Intercept Point
IMD	: Intermodulation Distortion
OFDM	: Orthogonal Frequency Division Multiplexing
OIP_2	: Output Second Order Intercept Point
OIP_3	: Output Third Order Intercept Point
PA	: Power Amplifier
PAPR	: Peak to Average Power Ratio
PSD	: Power Spectral Density
QAM	: Quadrature Amplitude Modulation
RF	: Radio Frequency
SER	: Symbol Error Rate
SNR	: Signal to Noise Ratio
WCMA	: Wideband Code Division Multiple Access

CHAPTER 1

INTRODUCTION

Today's communication systems use various types of modulation techniques. Spectral efficiency, i.e., highest possible transmission data rate for a given channel bandwidth, error detection capability, power efficiency, ease of demodulation are the critical parameters for modulation techniques. Modulation techniques can't satisfy all of the parameters above and usually choice of the appropriate modulation techniques is a tradeoff between these parameters.

In other words, "one technology fits all" approach is not sufficient in the present telecommunication markets, instead the most appropriate topology is chosen for a particular application.

These modulation techniques can be grouped in two parts. One of them is Constant Envelope Modulation Techniques, such as FSK, GFSK, MSK, GMSK, and CPM. Constant Envelope Modulations offer less Inter Symbol Interference (ISI), better BER (Bit Error Rate) performance, better immunity to random noise and fluctuations due to fading. They also enable the power amplifier in the transmitter side to operate at or near saturation levels, meaning better power efficiency and longer battery life. These properties make Constant Envelope Modulation techniques attractive for use in mobile communication systems. However, bandwidth efficiency is low when compared to the modulation techniques with fluctuating envelopes.

Examples to linear modulation are BPSK, QPSK, M-PSK, QAM, and M-QAM. In linear modulation, amplitude of the transmitted signal varies linearly with the modulating signal. Non-constant envelope modulation techniques require linear

amplification in order to preserve the signal shape. Both out-of-band (Adjacent channel) and in-band distortion are created due to nonlinearities. Adjacent channel power causes the expansion of the bandwidth occupancy of the signal. In-band distortion is like an additional noise in the system and it is very troublesome. Strict requirement of linear amplification is simply achieved by operating the amplifier in high back-off considering the peak to average ratio of the input signal. However energy efficiency of the amplifier drops with the increase in the back-off.

Considering the multi-carrier modulation techniques such as WCDMA, CDMA, OFDM and their derivations, in which very high peak to average ratio is obtained, backing of the input power as much as the peak to average ratio is not a very reasonable solution. At this point, linearization techniques are employed which lets the amplifier to operate close the compression points and at the same time presenting a good linearity behavior.

Frequently used linearization techniques are Feed-Forward, Envelope Elimination and Restoration (EER), Predistortion and Linearization with Nonlinear Components (LINC). Each linearization technique has its own advantages and drawbacks. Complexity, efficiency, bandwidth and distortion cancellation performance are critical parameters, which the designer should consider for a specific application. Furthermore, Doherty amplifier techniques allow large back-off for the input power of amplifier without significantly affecting the efficiency performance. With some form of correction and linearity enhancements such as digital predistortion, doherty amplifiers present significant advantages especially for the applications with high peak to average ratio input power.

For non-constant envelope communication signals (with high PAPR) like WCDMA and CDMA, it is almost impossible to analytically express the stimuli. To estimate final performance of efficiency enhancement and linearization techniques under multicarrier signals, which is arbitrary and noise like excitation, obtaining representative signals is crucial. It provides the designer understanding of the final performance of the system. In [1], arbitrary waveforms are modeled using multi-tones and estimation and analyze of final performance of the feedforward system under an arbitrary waveform is accomplished using simple multi-tone models. In [2],

ACPR performance of a nonlinear amplifier under pseudorandom digital modulation is compared with ACPR performance of the same amplifier driven by multi-tone signals. Under which circumstances better results are obtained is depicted.

In this thesis, response of a nonlinear system to an arbitrary input waveform is approximated by multi-tone modeling. Since the system is nonlinear, output of the arbitrary excitation can't be expressed as the superposition of elementary outputs. One can claim that once the characteristics of multi-tone model signal and arbitrary excitation are approximated better, the final regime of the system under arbitrary excitation is predicted better by replacing the arbitrary excitation with multi-tone model. Moreover, since it is easy to create, handle and express the multi-tone signals, making analytical derivations are easier.

The validity of the multi-tone modeling is tested by comparing responses of the same nonlinear amplifier to the arbitrary excitation (e.g. a sample of a multi user communication signal) and its multi-tone model. After the response to arbitrary excitation is approximated for a specific nonlinear amplifier configuration, it is shown that multi-tone model is amplifier independent and the model can be used under any nonlinear amplifier configuration. To prove this validity, multi-tone model and arbitrary waveform are investigated for different amplifier models in the simulation environment.

In Chapter 2, Amplifier characteristics will be discussed and typical nonlinear behaviors in an amplifier will be mentioned. Then popular amplifier models will be briefly discussed. In Chapter 3, multi-tone modeling concept will be introduced. Next, how multi-tone model parameters are chosen and how each parameter effects the results are explained in detail. In Chapter 4, different multi-tone models with different number of tones for a WCDMA signal and a CDMA signal is presented. Modeled multi-tone signals are applied to a single stage amplifier and results are compared with the amplified original signal results. Improvement in resemblance of the model signal with increasing number of tones is proved. In Chapter5, modulation performance of the multi-tone models and original signals are compared. BER (Bit Error Rate Analysis) and EVM (error vector magnitude) results for both original signal and modeled signal is given and resemblance between them is discussed.

CHAPTER 2

POWER AMPLIFIER CHARACTERISTICS AND MODELING

2.1 Power Amplifier Characteristics

An ideal, linear, power amplifier is characterized by a constant complex gain. The input-output relation of a linear amplifier is modeled as below;

$$V_{\text{out}} = G \cdot V_{\text{input}} \quad (2.1)$$

Where G is the complex gain including both voltage gain and linear phase relation. With the expression in (2.1), it is assumed that amplification characteristics is independent of input voltage level, however, this type of behavior is a conflicting fact for a real amplifier. That is why modeling of the RF Power Amplifier has become a quite interesting and intense research area. Different amplifier models were introduced in the past for both solid state and tube amplifiers. Several studies were published for behavioral modeling and equivalent circuit device modeling. In [3], time domain and frequency domain behavioral models are addressed for microwave transistors. In [4], semi-physical behavioral model to characterize a solid state high power amplifier is proposed. In [5], a behavioral model capturing both memory effects and nonlinear behavior of a PA is introduced.

In order to model an RF Power Amplifier, it is important to know certain parameters. These parameters include intermodulation products, intercept and compression points, Adjacent Channel Power Ratio, efficiency characteristics under typical input power levels and AM-AM, AM-PM relations.

2.1.1 Intermodulation Products

Input-output characteristics of a nonlinear amplifier could be expressed with a Taylor series

$$V_{\text{out}} = G_1 \cdot V_{\text{input}} + G_2 \cdot V_{\text{input}}^2 + G_3 \cdot V_{\text{input}}^3 + \dots + G_n \cdot V_{\text{input}}^n \quad (2.2)$$

Where $G_1, G_2, G_3, \dots, G_n$ are the complex gains. Main nonlinear contributions of the

PA can be extracted from (2.2). Assume a single-tone, $V_{\text{input}} = V \cdot \cos(\omega t)$ is

presented to the amplifier as an input.

$$V_{\text{out}} = G_1 \cdot V \cdot \cos(\omega t) + G_2 \cdot V^2 \cdot \cos^2(\omega t) + G_3 \cdot V^3 \cdot \cos^3(\omega t) + \dots + G_n \cdot V^n \cdot \cos^n(\omega t) \quad (2.3)$$

Now, examine the second and the third terms.

$$\cos^2(\omega t) = 0,5 \cdot (1 + \cos(2\omega t)) \text{ and } \cos^3(\omega t) = 0,25 \cdot (3 \cdot \cos(\omega t) + \cos(3\omega t))$$

Rearranging (2.3) up to the 3rd order term

$$V_{\text{out}} = G_1 \cdot V \cdot \cos(\omega t) + G_2 \cdot V^2 \cdot 0,5 \cdot (1 + \cos(2\omega t)) + G_3 \cdot V^3 \cdot 0,25 \cdot (3 \cdot \cos(\omega t) + \cos(3\omega t)) \quad (2.4)$$

$$V_{\text{out}} = G_2 \cdot V^2 \cdot 0,5 + \cos(\omega t) \cdot (G_1 \cdot V + 0,75 \cdot G_3 \cdot V^3) + \cos(2\omega t) \cdot (G_2 \cdot V^2 \cdot 0,5) + \cos(3\omega t) \cdot (G_3 \cdot V^3 \cdot 0,25) \quad (2.5)$$

As seen from (2.5), apart from the fundamental component, a DC component, a second harmonic component and a third harmonic component emerge at the output of a nonlinear amplifier. The DC, second harmonic and third harmonic components could be filtered out easily by placing a band-pass filter at the output of the amplifier since they are out of the band.

In the case of a two-tone signal, the output expression is more complicated. Now, assume $V_{\text{input}} = V_1 \cdot \cos(\omega_1 t) + V_2 \cdot \cos(\omega_2 t)$ is presented to the amplifier as an input.

The second term in (2.2) can be expressed in the case of a two-tone signal as follows,

$$\begin{aligned}
G_2 \cdot V_{\text{input}}^2 &= G_2 \cdot (V_1 \cdot \cos(\omega_1 t) + V_2 \cdot \cos(\omega_2 t))^2 \\
&= G_2 \cdot \left(V_1^2 \cdot \cos^2(\omega_1 t) + V_2^2 \cdot \cos^2(\omega_2 t) + \right. \\
&\quad \left. 2 \cdot V_1 \cdot V_2 \cdot \cos(\omega_1 t) \cdot \cos(\omega_2 t) \right) \\
&= G_2 \cdot (V_1^2 \cdot 0,5 \cdot (1 + 2 \cdot \cos(\omega_1 t)) + V_2^2 \cdot 0,5 \cdot (1 + 2 \cdot \cos(\omega_2 t))) + \\
&\quad V_1 \cdot V_2 \cdot (\cos((\omega_1 - \omega_2)t) + \cos((\omega_1 + \omega_2)t)) \\
&= G_2 \cdot (0,5 \cdot V_1^2 + 0,5 \cdot V_2^2) + G_2 \cdot V_1 \cdot V_2 \cdot \left(\begin{array}{l} \cos((\omega_1 - \omega_2)t) + \\ \cos((\omega_1 + \omega_2)t) \end{array} \right) + \\
&\quad G_2 \cdot 0,5 \cdot (V_1^2 \cdot \cos(2\omega_1 t) + V_2^2 \cdot \cos(2\omega_2 t))
\end{aligned} \tag{2.6}$$

From (2.6), the second term causes a DC term, a second harmonic component and intermodulation products. Since all of these products are far away from the fundamental component, these products could be filtered out easily. Hence in general, one can claim that the even terms in (2.2) are not troublesome, since they could be filtered out easily.

The third term in (2.2) is the problematic term and it could be expanded as below

$$\begin{aligned}
G_3 \cdot V_{\text{input}}^3 &= G_3 \cdot (V_1 \cdot \cos(\omega_1 t) + V_2 \cdot \cos(\omega_2 t))^3 \\
&= G_3 \cdot (V_1 \cdot \cos(\omega_1 t) + V_2 \cdot \cos(\omega_2 t)) \cdot \left[\begin{array}{l} (0,5 \cdot V_1^2 + 0,5 \cdot V_2^2) + \\ V_1 \cdot V_2 \cdot (\cos((\omega_1 - \omega_2)t) + \cos((\omega_1 + \omega_2)t)) + \\ 0,5 \cdot (V_1^2 \cdot \cos(2\omega_1 t) + V_2^2 \cdot \cos(2\omega_2 t)) \end{array} \right] \\
&= G_3 \cdot \left[\begin{array}{l} (0,5 \cdot V_1^3 \cdot \cos(\omega_1 t) + 0,5 \cdot V_2^2 \cdot V_1 \cdot \cos(\omega_1 t) + \\ V_1^2 \cdot V_2 \cdot 0,5 \cdot (\cos((2\omega_1 - \omega_2)t) + \cos\omega_2 t) + \\ V_1^2 \cdot V_2 \cdot 0,5 \cdot (\cos((2\omega_1 + \omega_2)t) + \cos\omega_2 t) + \\ 0,25 \cdot V_1^3 \cdot (\cos(3\omega_1 t) + \cos(\omega_1 t)) + \\ 0,25 \cdot V_1 \cdot V_2^2 \cdot (\cos(\omega_1 + 2\omega_2)t + \cos(2\omega_2 - \omega_1)t) \end{array} \right] + \\
&\quad G_3 \cdot \left[\begin{array}{l} (0,5 \cdot V_2^3 \cdot \cos(\omega_2 t) + 0,5 \cdot V_1^2 \cdot V_2 \cdot \cos(\omega_2 t) + \\ V_2^2 \cdot V_1 \cdot 0,5 \cdot (\cos((2\omega_2 - \omega_1)t) + \cos\omega_1 t) + \\ V_2^2 \cdot V_1 \cdot 0,5 \cdot (\cos((2\omega_2 + \omega_1)t) + \cos\omega_1 t) + \\ 0,25 \cdot V_2^3 \cdot (\cos(3\omega_2 t) + \cos(\omega_2 t)) + \\ 0,25 \cdot V_2 \cdot V_1^2 \cdot (\cos((\omega_2 + 2\omega_1)t) + \cos(2\omega_1 - \omega_2)t) \end{array} \right]
\end{aligned} \tag{2.7}$$

As seen from (2.7), the third order term produces $\cos((2\omega_1 - \omega_2)t)$, $\cos((2\omega_1 + \omega_2)t)$, $\cos((2\omega_2 - \omega_1)t)$, $\cos((2\omega_2 + \omega_1)t)$, $\cos(3\omega_2t)$, $\cos(3\omega_1t)$ and additional fundamental components $\cos(\omega_1t)$ and $\cos(\omega_2t)$.

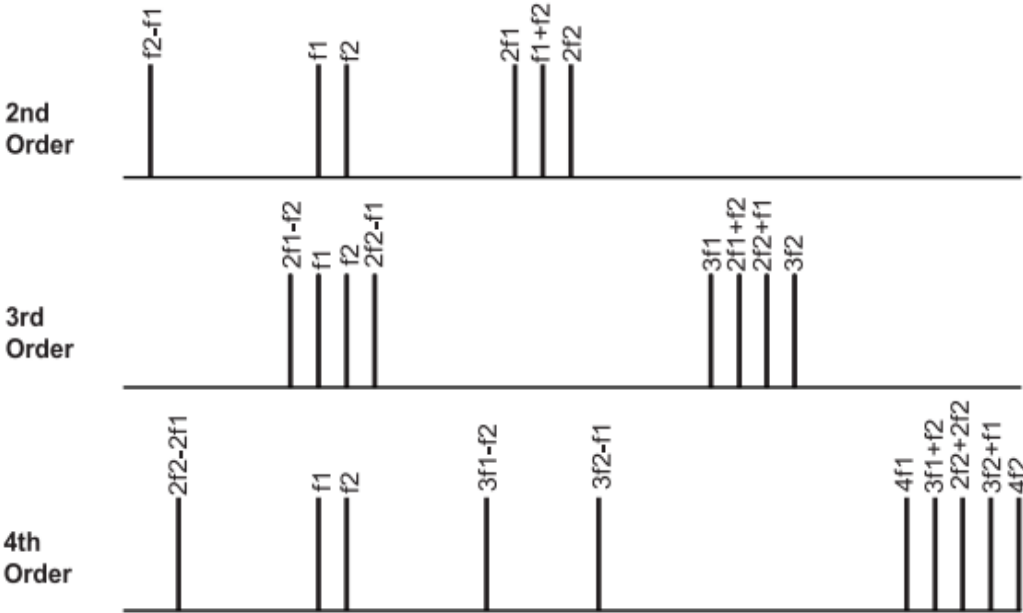


Figure 2-1 Output of a nonlinear amplifier under a two-tone input [6]

$\cos((2\omega_1 + \omega_2)t)$, $\cos((2\omega_2 + \omega_1)t)$, $\cos(3\omega_2t)$, $\cos(3\omega_1t)$ are out of band components and could be eliminated by a band pass filter as depicted previously. However, $\cos((2\omega_1 - \omega_2)t)$ and $\cos((2\omega_2 - \omega_1)t)$ terms are in band components and requires very sharp filter to eliminate, which is extremely difficult to realize. Moreover, some components at the exact frequencies with the fundamental tones but having different coefficients also appear in the spectrum and these are also included in to the in-band distortion. If (2.2) is expanded up to higher terms under two-tone input condition, $m \cdot f_1 \pm n \cdot f_2$ harmonic components are produced at the output of the amplifier.

2.1.2 Intercept Points

When considering multi-carrier modulation schemes like WCDMA, odd order distortion components will exist at the output of the amplifier and they will limit the

linearity of the amplifier. Among these odd order distortions, the 3rd order intermodulation products are the most troublesome since they are very closely placed to the fundamental components as seen in Figure 2-1. $2 \cdot f_1 - f_2$ and $2 \cdot f_2 - f_1$ components are usually characterized by the 3rd order intercept point either referred to the input (IIP3) or to the output (OIP3).

The most important fact with the 3rd order intermodulation products at $2 \cdot f_1 - f_2$ and $2 \cdot f_2 - f_1$ is that with the 1 dB increase in the input power in the linear zone of the amplifier, the power of the intermodulation products increase 3 dB. This is shown in Figure 2-2.

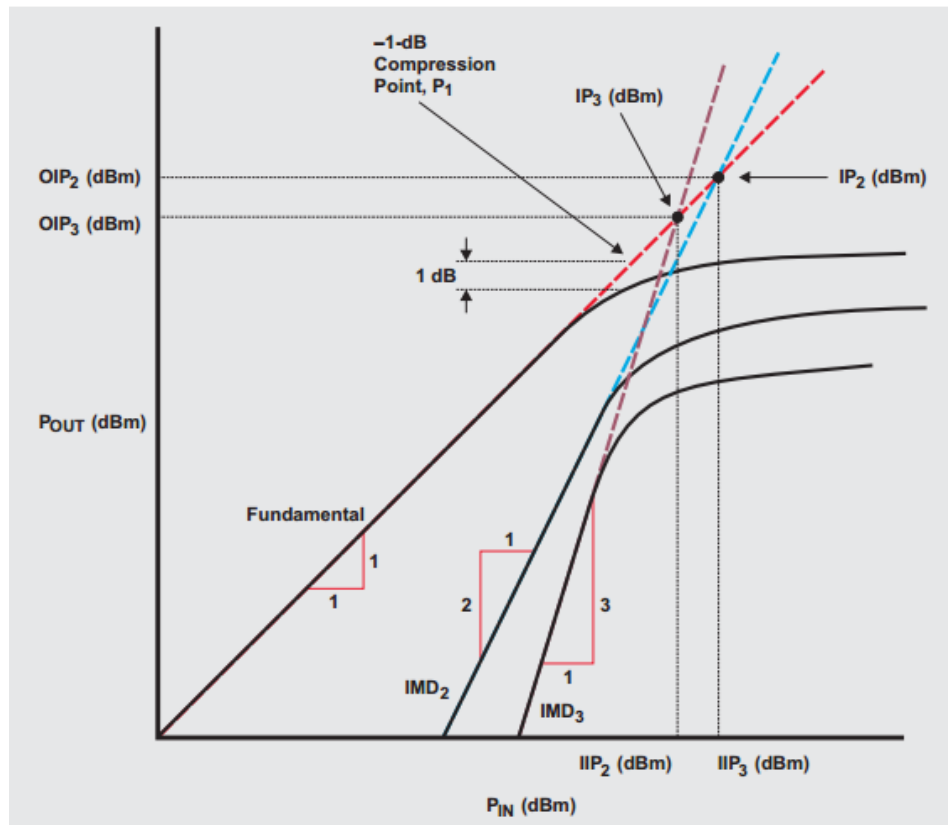


Figure 2-2 Demonstration of intercept points of a typical amplifier [7]

The point where the third order line intersects with the linear gain is called IP3 and the point where the second order line intersects with the linear gain is called IP2. Second order intercept points are not troublesome, since second order products could be filtered out without considerable effort.

2.1.3 Compression Points

Another figure of merit of amplifier nonlinearity is 1 dB compression point. It is defined as the point where the difference between linear gain and compressed gain is exactly 1 dB. In Figure 2-2, 1 dB compression point, P_{1dB} is clearly observed. Beyond the P_{1dB} point, linearity of the amplifier weakens very rapidly and this kind of operation is not recommended for applications requiring linearity. 3 dB compression point, P_{3dB} , is also defined by most of the amplifier manufacturers. Usually driving an amplifier beyond the P_{3dB} point could damage the amplifier in long term use.

2.1.4 AM-AM and AM-PM Conversion Rate

AM-AM and AM-PM conversion rates are also very critical parameters defining the nonlinear behavior of an amplifier. AM-AM conversion is widely known as the amplitude dependent amplitude distortion. AM-AM distortion is usually observed for the input power levels that will compress the output of the amplifier. AM-AM distortion is strongly dependent on the amplifier bias. For a hard biased amplifier, like class A, it is possible to avoid AM-AM distortion by backing off the amplifier from the compression points. However, for a soft biased or under biased amplifier like class-E, class-F and class-C, AM-AM distortion is also observed at several dBs below the compression point, since incoming RF signal also biases the amplifier up to a certain power level. Amplifier clipping effect is a result of AM-AM distortion. AM-PM conversion is a figure of merit for phase deviation caused by the amplitude variations. AM-PM conversion rate is usually defined as the change in the output phase with 1 dB power increment and it is expressed in degrees per dB, $^{\circ}/dB$. For an ideal power amplifier, output phase is independent of the input power level. AM-PM conversion rate is very critical for the systems that uses angular modulations, such as FM, QPSK. One of the main contributions of the Bit Error Rate (BER) in communication systems is undesired phase deviation caused by AM-PM conversion. Beyond the compression points of the amplifier, AM-PM conversion worsens rapidly, however several dBs below the compression point it could be still problematic depending on the amplifier bias type.

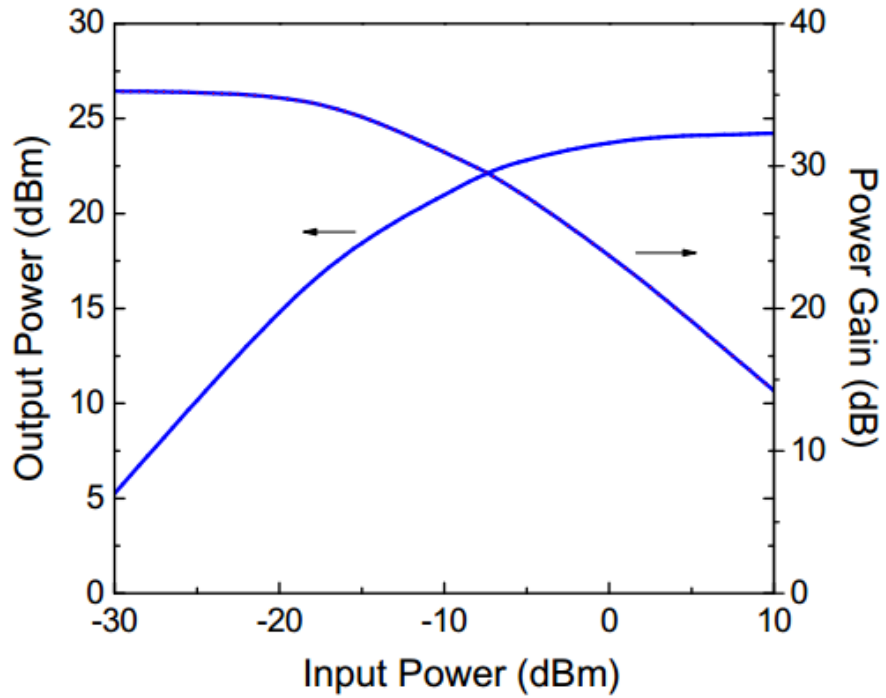


Figure 2-3 AM-AM characteristics of a typical amplifier [8]

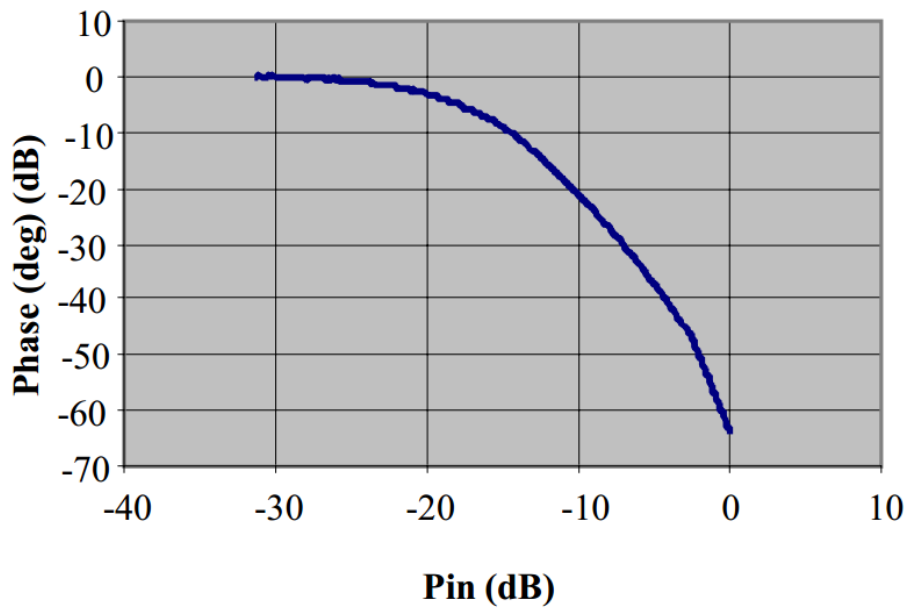


Figure 2-4 AM-PM distortion of a typical amplifier [9]

2.1.5 ACPR

Another figure of merit to characterize a PA is ACPR. Many power amplifier manufacturers give ACPR results to show the linearity performance of their products as a proof. “ACPR is the ratio of the power in a bandwidth away from the main

signal to the power in a bandwidth within the main signal” [10]. Figure 2-5, is a good illustration for ACPR measurements. Considering IMD measurements, ACPR may be related to the 3rd order products. However, IMD measurements cannot be used for complex multi-carrier modulation schemes. Therefore, ACPR measurements became inalterable. Bandwidth definitions and locations for ACPR measurements may differ for different signal types, which are shown in Figure 2-6.

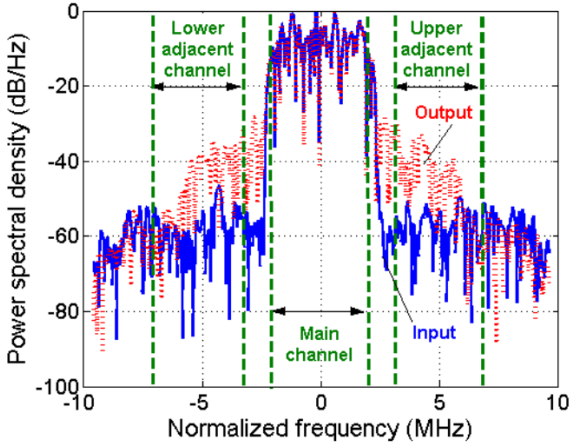


Figure 2-5 Spectral regrowth in lower and upper adjacent channels [11]

Type	NB CDMA IS-95 (rev link)	WB CDMA (one approach)
Main channel measurement BW	1.23 MHz or 30 kHz	3.84 MHz
Adj. channel location (from carrier)	± 885 kHz	± 5 MHz
Adj channel measurement BW	30 kHz	3.84 MHz
Alt channel location (from carrier)	± 1.98 MHz	± 10 MHz
Alt channel measurement BW	30 kHz	3.84 MHz

Figure 2-6 Bandwidth definitions and locations for different types of signals [10]

2.1.6 Efficiency

Efficiency is also a critical parameter to characterize a power amplifier. Efficiency is the ratio of the power delivered to the load to the power drawn from the supply. Power amplifiers are categorized into different classes according to their efficiency characteristics. Class A is the most linear but also least efficient one. Class A

amplifiers are highly biased amplifiers (full conduction angle) and maximum efficiency that could be obtained is 50%. Class B amplifiers show better efficiency but less linear characteristics when compared to Class A type. Class AB could be placed between class A and class B amplifiers in terms efficiency and linearity characteristics, and it is the most common amplifier topology. Maximum theoretical efficiency that a Class AB amplifier could reach is 78.5%. Switch mode amplifier types like class E and class F show superior efficiency characteristics to any amplifier topology but they suffer from linearity. Ideally they can present 100% efficiency. For the constant envelope schemes, driving the amplifier up to and maybe beyond the compression points is possible. This property of the constant envelope modulation techniques allow use of highly efficient but less linear amplifier types like class E and class F. For linear modulation techniques, using switch mode amplifiers are not possible and usually highly linear class A biased amplifiers are preferred. However, they are very inefficient especially at large back-off power. Recently some linearization techniques combined with a switch mode amplifiers have been a quite interesting research area. GaN Doherty amplifiers implemented with some linearity improvements has been researched in [12] and [13] and very promising results have been obtained. Moreover in the study [12] and [13], very good efficiency characteristics under a large back off power have been obtained.

For linear modulations having high peak to average input power ratio, to get rid of the clipping effect of the amplifier and to reduce the bit error rate, usually driving the amplifier at an output power level Peak to Average Power Ratio less than the maximum output power level is preferred. In other words, crest factor of the input signal affects the tolerable maximum output power level. Here, the word tolerable is used because how often the peaks are encountered is as important as crest factor. Depending on the encounter rate of the peaks, tolerable maximum output power level may be increased, which affects efficiency and heat dissipation. In [14] and [15], clipping effect of the amplifier on the performance of OFDM technique is investigated.

2.2 Power Amplifier Models

Modeling of an RF power amplifier could be accomplished either by equivalent circuit modeling or behavioral modeling. Equivalent circuit modeling requires a deep knowledge on the component side and hence it is very difficult. On the other hand, behavioral modeling is interested in the input output characteristics of the amplifier. In the behavioral model, characteristics of model amplifier are associated with the characteristics of real amplifier by mathematical functions of gain and phase. Behavioral modeling is also divided into two parts. These are frequency dependent and frequency independent modeling. In this thesis, frequency independent models are used. Frequency independent models are only interested in swept tone measurements for amplitude and phase. In other words, mathematical expressions for amplitude and phase for different power levels are searched. Most popular frequency independent amplifier models are Polynomial Model, Saleh Model, Rapp Model and Ghorbani Model. For the brief description of these models assume that input signal is represented by [16]

$$x(t) = r(t) \cdot \cos[\omega_0 t + \Psi(t)] \quad (2.8)$$

Where ω_0 is carrier frequency, $r(t)$ is modulated envelope and $\Psi(t)$ is modulated phase.

Output signal is represented by [16]

$$y(t) = A[r(t)] \cdot [\omega_0 t + \Psi(t) + \phi(r(t))] \quad (2.9)$$

$A(r)$ represent AM-AM relation and $\phi(r)$ represents AM-PM relation.

2.2.1 Polynomial Model

A finite order polynomial is fitted for both AM-AM and AM-PM relations. Amplitude conversion function $A(r)$ and phase conversion function $\phi(r)$ could be written as

$$A(r) = a_0 + a_1 \cdot r + a_2 \cdot r^2 + a_3 \cdot r^3 \dots \quad (2.10)$$

$$\phi(r) = b_0 + b_1 \cdot r + b_2 \cdot r^2 + b_3 \cdot r^3 \dots \quad (2.11)$$

Coefficients of $A(r)$ and $\phi(r)$ could be found by some approximation techniques such as least squares approximation. However, in this thesis, phase conversion function will be ignored and coefficients of the amplitude conversion function will be found from intercept points of RF power amplifiers. [17]

To achieve this, output of the amplifier is expressed as widely used Taylor series polynomial model.

$$y(t) = a_1 \cdot x(t) + a_3 \cdot x^3(t) + \dots + a_n \cdot x^n(t) \quad (2.12)$$

In (2.12), $x(t)$ is two-tone input in the form

$$x(t) = A \cdot (\cos\omega_1 t + \cos\omega_2 t) \quad (2.13)$$

When (2.13) is substituted in (2.12),

$$y(t) = a_1 \cdot A \cdot (\cos\omega_1 t + \cos\omega_2 t) + a_3 \cdot A^3 \cdot (\cos\omega_1 t + \cos\omega_2 t)^3 + \dots + a_n \cdot A^n \cdot (\cos\omega_1 t + \cos\omega_2 t)^n \quad (2.14)$$

is obtained, which consists of a dc term, fundamental tones, harmonic terms, intermodulation products that fall apart from the main tones and that fall in the vicinity of the main tones. By filtering, it is possible to get rid of the dc terms, harmonic terms and some of the intermodulation products. Hence the filtered signal $y'(t)$ could be expressed as [17]

$$\begin{aligned} y'(t) = & b_1 \cdot [\cos\omega_1 t + \cos\omega_2 t] + b_3 \cdot \left[\begin{array}{l} \cos(\omega_1 - 2\omega_2)t \\ + \cos(2\omega_1 - \omega_2)t \end{array} \right] + \dots \\ & + b_n \cdot \left[\cos\left(\left(\frac{n-1}{2}\omega_1\right) - \left(\frac{n+1}{2}\omega_2\right)\right)t \right] \\ & + b_n \cdot \left[\cos\left(\left(\frac{n+1}{2}\omega_1\right) - \left(\frac{n-1}{2}\omega_2\right)\right)t \right] \end{aligned} \quad (2.15)$$

In (2.15), b_n coefficients for odd n could be found as [17]

$$b_n = \frac{1}{2^{(n-1)}} \cdot \binom{n}{\frac{n+1}{2}} \cdot a_n \cdot A^n \quad (2.16)$$

$\binom{n}{\frac{n+1}{2}}$ gives number of different combinations for $(n+1)/2$ elements chosen from n

elements.

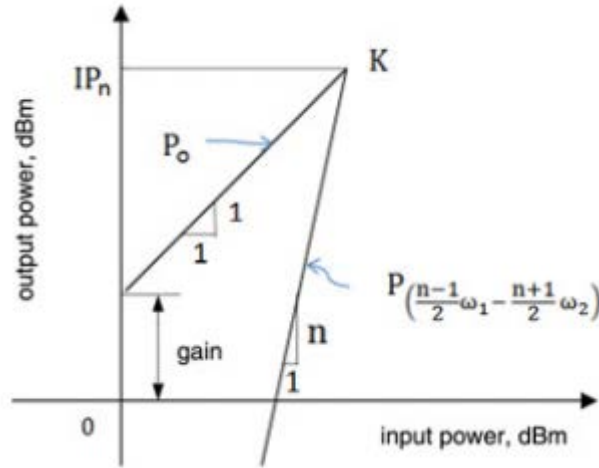


Figure 2-7 N^{th} order intercept point [17]

As shown in Figure 2-7, at the intercept point, power of the fundamental tone and N^{th} order term is equal. If the input and output impedance of the two port network are taken as $Z_{in} = Z_{out} = R$, then fundamental power and N^{th} order product power at the intercept point could be expressed as [17]

$$P_o = 10 \cdot \log \left[\left(\frac{a_1 \cdot A}{\sqrt{2}} \right)^2 \cdot \frac{10^3}{R} \right] \text{dBm} \quad (2.17)$$

$$P \left(\frac{n-1}{2} \omega_1 - \frac{n+1}{2} \omega_2 \right) = 10 \cdot \log \left[\left(\frac{b_n}{\sqrt{2}} \right)^2 \cdot \frac{10^3}{R} \right] \text{dBm} \quad (2.18)$$

When (2.16) is substituted in (2.18)

$$P \left(\frac{n-1}{2} \omega_1 - \frac{n+1}{2} \omega_2 \right) = 10 \cdot \log \left[\frac{\frac{1}{2^{n-1}} \cdot \binom{n}{\frac{n+1}{2}} \cdot a_n \cdot A^n}{\sqrt{2}} \cdot \frac{10^3}{R} \right] \text{dBm} \quad (2.19)$$

At the intercept point, intermodulation product power and fundamental power should be equal. When (2.19) and (2.17) are equated [17]

$$A^{(n-1)} = \left(\begin{array}{c} 2^{(n-1)} \\ \left(\begin{array}{c} n \\ \frac{n+1}{2} \end{array} \right) \end{array} \right) \cdot \left(\frac{a_1}{|a_n|} \right) \quad (2.20)$$

If scale is changed from dBm to dBw

$$\begin{aligned} P_o = IP_n &= 10 \cdot \log \left[\frac{a_1^2 \cdot A^2}{2R} \right] \\ &= \frac{2}{n-1} \cdot 10 \cdot \log \left[\frac{a_1^{n-1} \cdot A^{n-1}}{2R^{\frac{n-1}{2}}} \right] \end{aligned} \quad (2.21)$$

After substituting (2.20) into (2.21)

$$P_o = IP_n = \frac{20}{(n-1)} \cdot \log \left[\frac{a_1^n \cdot 2^{n-1}}{|a_n| \cdot \left(\begin{array}{c} n \\ \frac{n+1}{2} \end{array} \right) \cdot 2R^{\frac{n-1}{2}}} \right] \quad (2.22)$$

After substituting $a_1 = 10^{\frac{G}{20}}$ into (2.22), a_n can be obtained from (2.22) as [17]

$$|a_n| = \frac{10^{\frac{n \cdot G - (n-1) \cdot IP_n}{20}} \cdot 2^{n-1}}{\left(\begin{array}{c} n \\ \frac{n+1}{2} \end{array} \right) \cdot (2R)^{\frac{n-1}{2}}} \quad (2.23)$$

(2.23) is valid for odd n, for n>3. To realize the gain compression characteristics a_n values are considered negative. In (2.23), IP_n is the output intercept point in dBw, and G is the linear gain of the amplifier. If reference impedance is taken as R=50 ohm, then a_3 , a_5 , and a_7 could be found as

$$a_1 = 10^{\left(\frac{G}{20} \right)} \quad (2.24)$$

$$a_3 = \frac{-2}{3R} \cdot 10^{\left(\frac{3 \cdot G - 2 \cdot IP_3}{20} \right)} \quad (2.25)$$

$$a_5 = \frac{-2}{5 \cdot R^2} \cdot 10^{\left(\frac{5 \cdot G - 4 \cdot IP_5}{20}\right)} \quad (2.26)$$

$$a_7 = \frac{-8}{35 \cdot R^3} \cdot 10^{\left(\frac{7 \cdot G - 6 \cdot IP_7}{20}\right)} \quad (2.27)$$

Where intercept point IP_n could be found as [17]

$$IP_n = \frac{n \cdot Pt - IMP_n}{n - 1} \quad (2.28)$$

In (2.28), Pt is fundamental tone power at the output of the amplifier and IMP_n is the n^{th} order intermodulation product power. By including the terms up to 7th order, polynomial model could define the nonlinearity with good precision. Polynomial model with coefficients obtained from intercept points is simple but effective model to define the amplifier nonlinearity and this model is widely used in DPD. Drawback of this type of polynomial model is that it doesn't include phase distortion. Thus, this model can't reflect the AM-PM conversion characteristics of an amplifier. This model will be used during the analysis in Chapter 3 and Chapter 4.

2.2.2 Saleh Model

Saleh model was originally developed for travelling wave tube amplifiers, but it could be applied to solid state amplifiers as well. It's AM-AM and AM-PM conversion functions could be expressed as [19]

$$A(r) = \frac{\alpha_a \cdot r}{1 + \beta_a \cdot r^2} \quad (2.29)$$

$$\phi(r) = \frac{\alpha_\phi \cdot r^2}{1 + \beta_\phi \cdot r^2} \quad (2.30)$$

It uses parameters $\alpha_a, \beta_a, \alpha_\phi, \beta_\phi$ to fit the polynomial to the measured data.

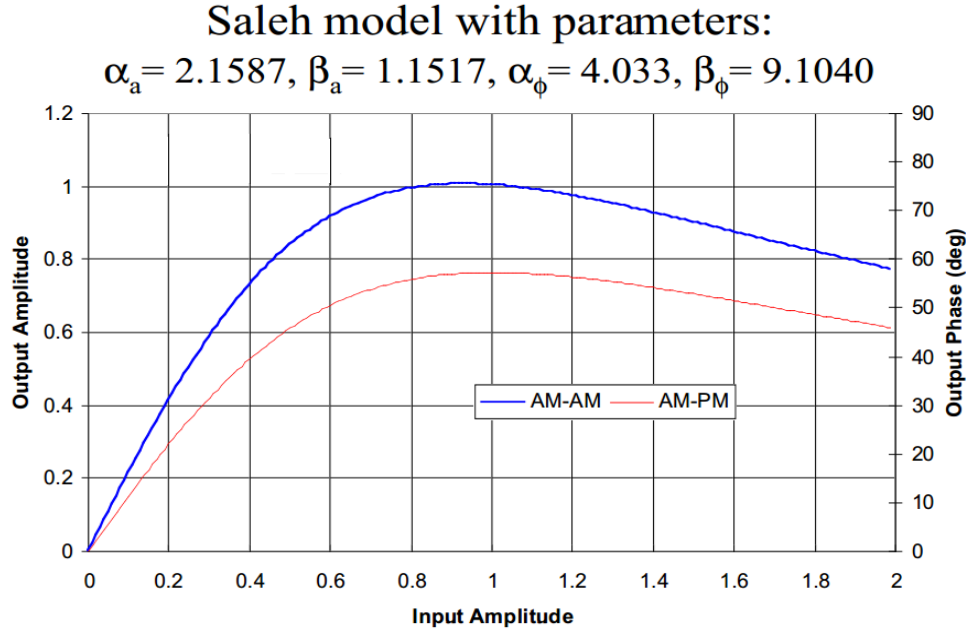


Figure 2-8 AM-AM and AM-PM curves for Saleh model [18]

2.2.3 Rapp Model

Rapp model approach is different from other frequency independent amplifier models since it assumes the phase distortion is negligibly small. Therefore, $\phi(r)$ is assumed to be 0. Its AM-AM conversion characteristics could be described as [19]

$$A(r) = s \cdot \frac{r}{\left[1 + \left(\frac{s \cdot r}{y}\right)^{2p}\right]^{1/2p}} \quad (2.31)$$

$$\phi(r) = 0 \text{ (neglected)} \quad (2.32)$$

In (2.31), s represents the small signal gain of the amplifier, y represents the limiting output amplitude and p controls the transition smoothness from the linear region to saturation region. With increased p , transition occurs faster as shown in Figure 2-9.

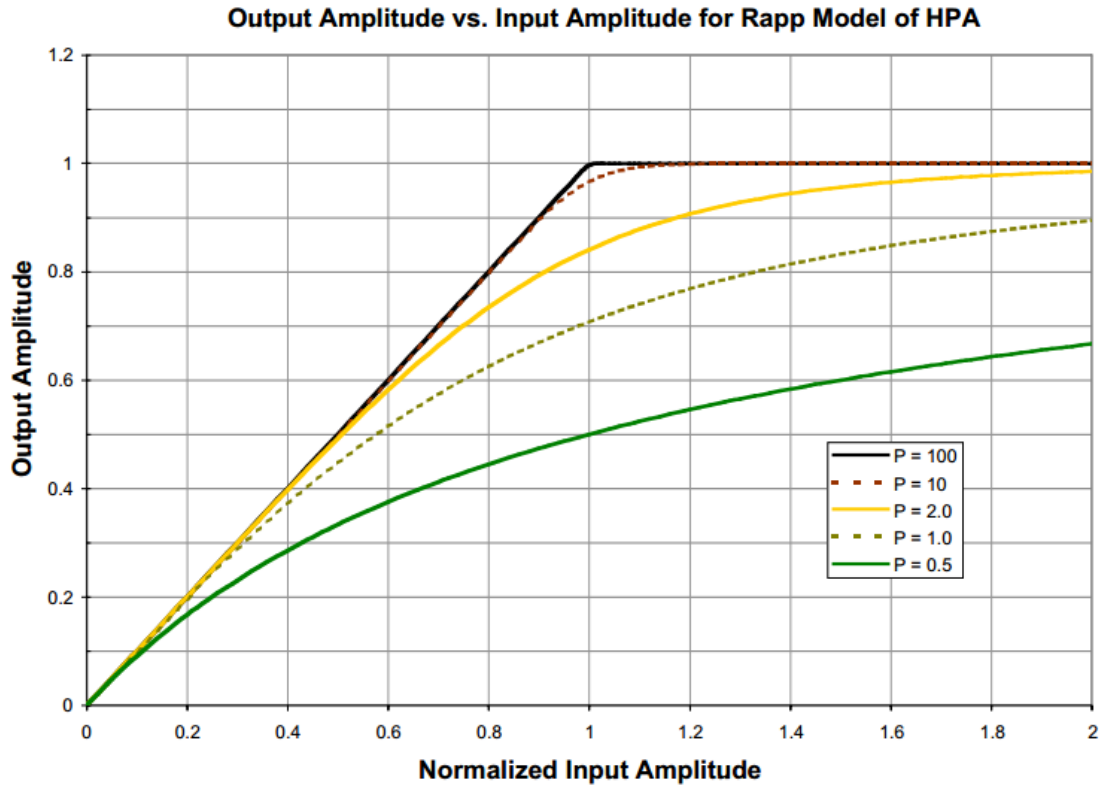


Figure 2-9 Rapp model AM-AM conversion characteristics [16]

2.2.4 Ghorbani Model

Ghorbani model uses similar approach with Saleh model but it is more suitable for solid state power amplifiers. Since solid state power amplifiers have smaller roll-off and phase distortion at saturation than TWTA. It uses four parameters to fit conversion characteristics of AM-AM and AM-PM to the measured data. Its AM-AM and AM-PM conversion characteristics could be described as [19]

$$A(r) = \frac{x1 \cdot r^{x2}}{(1 + x3 \cdot r^{x2})} + x4 \cdot r \quad (2.33)$$

$$\phi(r) = \frac{y1 \cdot r^{y2}}{(1 + y3 \cdot r^{y2})} + y4 \cdot r \quad (2.34)$$

$x1$, $x2$, $x3$, $x4$ and $y1$, $y2$, $y3$, $y4$ are unknown coefficients.

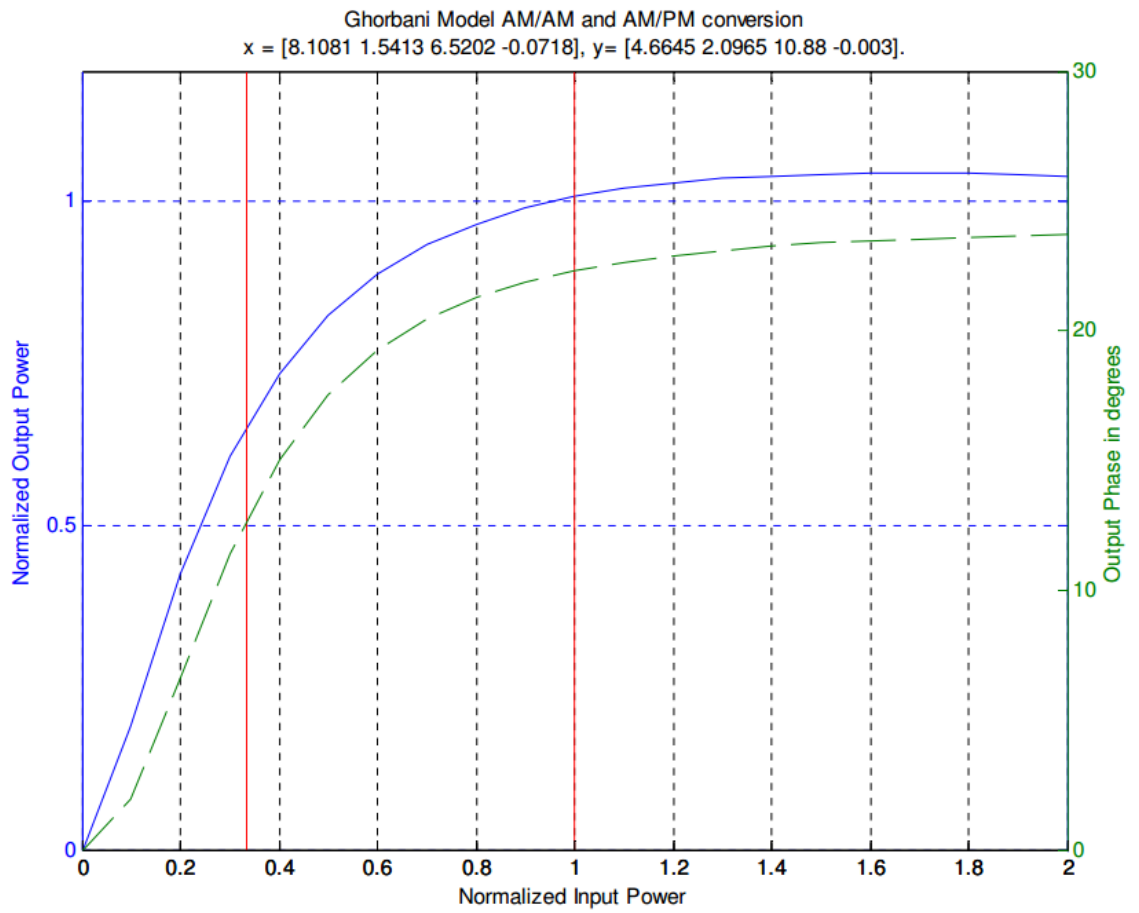


Figure 2-10 Ghorbani model AM-AM and AM-PM conversion characteristics [18]

Ghorbani model developed from AM-AM and AM-PM measurements of real amplifiers will be used for BER and EVM analysis in Chapter 5.

CHAPTER 3

MULTI-TONE MODELLING

In communication systems, complex modulation techniques evolved due to demand for high data rate and spectral efficiency. However, design and implementation of complex and random signals are challenging. Simulation tools like Advanced Design System and Microwave Office put more emphasis on the communication systems toolbox by involving examples of commonly used complex modulated signals. These simulation tools offer great flexibility to designers by including receiver and transmitter blocks of various types of modulated signals. However, to understand the effect of each component in transmitter or receiver block, designers may still need analytical tools and calculations.

Dealing with the complex modulated signals in analytical expressions is almost impossible. Therefore, designers need more practical signals that will sufficiently characterize the nonlinear behavior of the complex signals. By this way, the designer may have better understanding of the system and its requirements. In the past, characterization of the nonlinear RF systems was realized using single or two-tone measurements. However, limited data could be obtained by single and two-tone measurements. To sufficiently predict the nonlinear system behavior and final operation regime of the system, more involved analysis is needed. Therefore, representing the complex and digitally modulated communication signals by multi-tone signals for better nonlinear system characterization has become a quite important research area. Various studies have been done and promising results have been obtained. In [2], multi-sine excitations were used to approximate ACPR

performance of digitally modulated signals. In [2], it is depicted that better ACPR results could be obtained if PAPR of the multi-sine excitation and digital signal get closer. In [20], a complex enveloped signal is modeled by multi-tones. Then, model is used in feedforward circuit analysis to ease the analytical calculations. In [21], analytical expressions are developed for a 3rd order memoryless microwave circuit under constant amplitude, equally spaced tones with correlated or uncorrelated phases. In [21], it is also pointed out that a sufficiently large number of equally spaced but uncorrelated tones is similar to band limited white noise. In [22], linearity of high power amplifiers is investigated by intermodulation analysis. Load-pull characterization of microwave transistors under N-tone ($2 \leq N \leq 32$) excitation is studied. In [23], new closed form expressions are developed to predict the in-band and out-of-band intermodulation distortion of fifth order memoryless RF circuits excited by phase aligned or random phase multi-tones. In [23], an efficient algorithm is presented to calculate the steady state response of nonlinear circuit under multi-tone excitation.

In this part, first multi-tone concept is explained. Then, parameters and how the parameters are chosen for multi-tones are emphasized by showing the effect of each parameter. Next, amplifiers used throughout simulations will be introduced. Finally, characteristics of the communication signals that will be modeled are depicted.

3.1 Properties of Multi-Tone Stimuli

One of the main properties of the multi-tone signal is that it allows the user to obtain signals with different PAPR. Consider an in-phase, equal amplitude two-tone signal

$$V_{in}(t) = V \cdot \cos(\omega_1 t) + V \cdot \cos(\omega_2 t) = V_1(t) + V_2(t) \quad (3.1)$$

Peak power (P_p) and Average power (P_m) expressions are expressed for this two-tone signal as

$$P_p = \frac{(V_{1,rms} + V_{2,rms})^2}{R} = \frac{\left(\frac{V}{\sqrt{2}} + \frac{V}{\sqrt{2}}\right)^2}{R} = \frac{2 \cdot V^2}{R} \quad (3.2)$$

$$P_m = \frac{V_{1,rms}^2 + V_{2,rms}^2}{R} = \frac{V^2 + V^2}{2.R} = \frac{V^2}{R} \quad (3.3)$$

Where R is the reference circuit impedance and will be accepted as 50 ohm in this thesis.

Peak to average ratio for an in-phase, two-tone, equal amplitude signal is 3 dB, as expected. Now, consider an in-phase multi-tone signal with different amplitude coefficients. [1]

$$V_{in}(t) = V_1 \cdot \cos(\omega_1 t) + V_2 \cdot \cos(\omega_2 t) + V_3 \cdot \cos(\omega_3 t) + V_4 \cdot \cos(\omega_4 t) + \dots \quad (3.4)$$

Or it could be written as

$$V_{in}(t) = V \cdot \left[\sum_{n=1}^p M_n \cdot \cos(n \cdot \omega_m t) \right] \cdot \cos(\omega t) \quad (3.5)$$

Peak power for the signal in (3.5) is expressed as

$$P_p = \frac{V^2}{2 \cdot R} \cdot \left[\sum_{n=1}^p M_n \right]^2 \quad (3.6)$$

Mean power for the signal in (3.5) is expressed as

$$P_m = \frac{V^2}{4 \cdot R} \cdot \left[\sum_{n=1}^p M_n^2 \right] \quad (3.7)$$

Hence, peak to average ratio of an in-phase multi-tone signal has the following form.

$$\Psi = \frac{P_p}{P_m} = 2 \cdot \frac{\left[\sum_{n=1}^p M_n \right]^2}{\sum_{n=1}^p M_n^2} \quad (3.8)$$

By choosing different sets of M_n coefficients, signals having different PAPR could be obtained. In (3.8), p is the number of the tones forming the multi-tone signal. Maximum crest factor that could be obtained is $2p$. Different choices of the M_n coefficients may result in same crest factor, however, different intermodulation distortion and other nonlinear parameters may be produced by a nonlinear amplifier. In other words, modeling an arbitrary waveform by multi-tones may give unpredicted results if only crest factor is considered as a factor of resemblance.

Power complementary cumulative function provides very critical information about the signal. It also includes a quantitative value for the crest factor. CCDF curves define the power characteristics of the signal. Basically, a CCDF curve tells how much time the signal spends at or above a given power level. The lines 1, 2 and 3 on Figure 3-1, represent the power levels above the average power. The amount of time at or above given power level 1, 2 and 3 is related to the probability of encounter rate of that power level. Instead of time domain plot, probability vs peak to average ratio plot is used for CCDF.

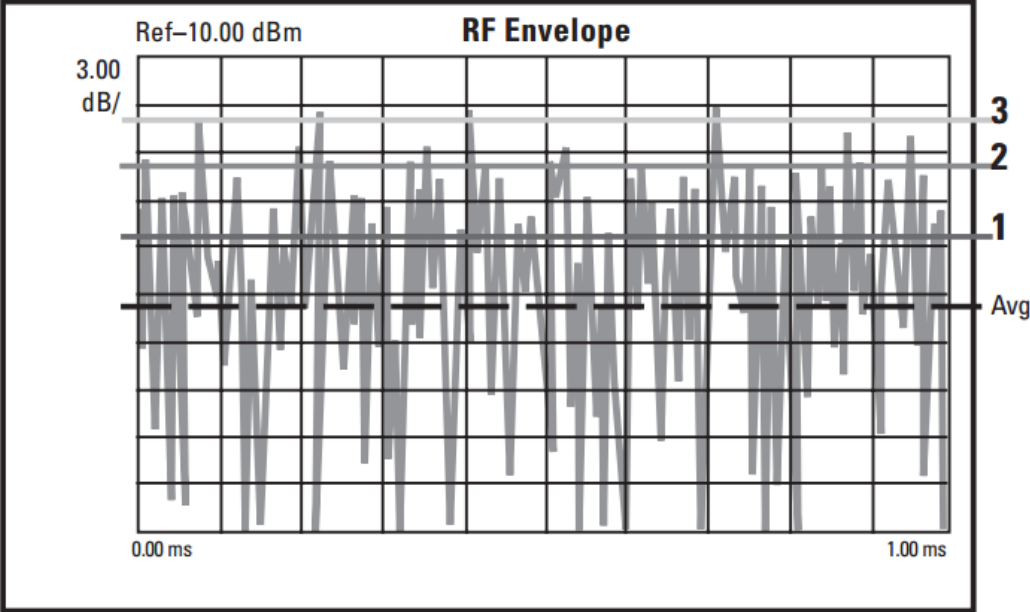


Figure 3-1 RF envelope of a typical CDMA signal [25]

The x-axis in Figure 3-2 is scaled to dB. By placing a vertical line on a desired point in x-axis, probability of having a sample at or above the corresponding power level could be read. For example, line 2 in Figure 3-2 refers to a power level of 7.5 dB above the average power level. By observing the Figure 3-2, one can conclude that for %1 of the envelope duration, the signal exceeds the average power level by at least 7.5 dB. Furthermore, interception of the CCDF curve with the x-axis is the crest factor of the input stimuli.

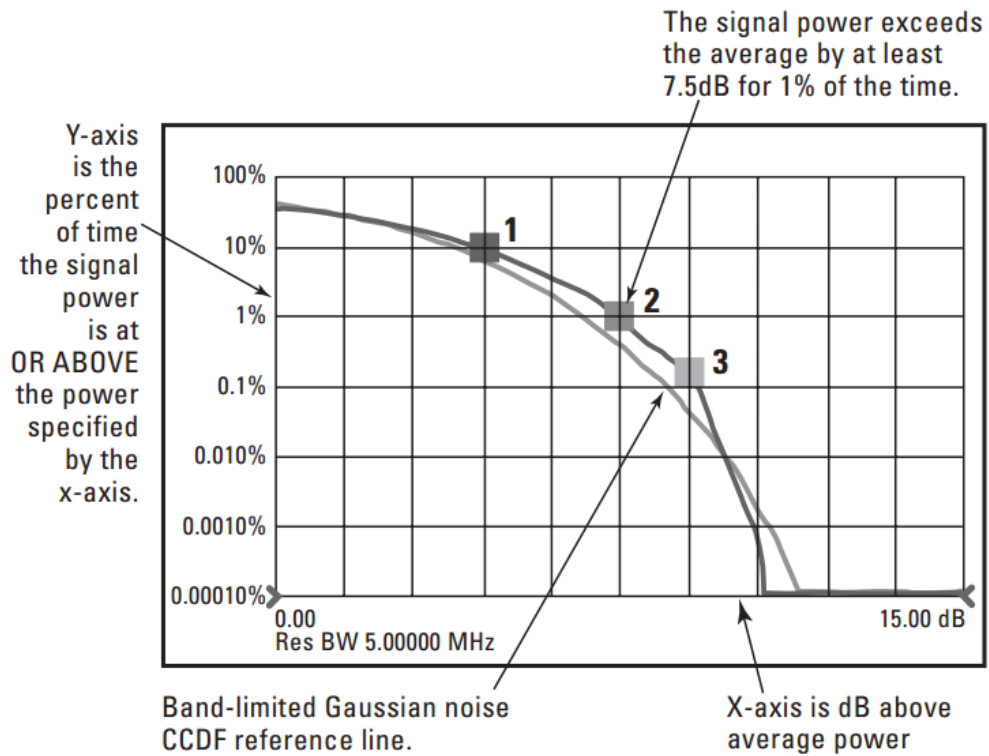


Figure 3-2 CCDF curve of the CDMA signal with corresponding power levels in Figure 3.1 [25]

CCDF curve gives statistical information about the input signal, and it is more reasonable to use CCDF curve instead of crest factor. Since, all the emphasis of the crest factor is placed on to the instantaneous peak value. Apart from the CCDF curve, a designer should also consider in-band distortion, out of band distortion, instantaneous nonlinear power distribution, channel power and bandwidth to have more accurate model.

3.2 Parameters of the Multi-Tone Model

To better represent the nonlinear behavior of an arbitrary waveform, multi-tone signals should be generated carefully. In telecommunication applications, multi carriers modulated with non-null information signals are used. Hence, these signals have finite bandwidth. One way to model these kind of signals is to use combination of various tones, i.e., multi-tone signals. According to the central limit theorem, when the number of tones is increased, and the phases of the tones are uncorrelated, resultant signal tends to a narrowband noise excitation. In other words, large number

of tones with uncorrelated phases resemble to a band limited noise as shown in Figure 3-3.

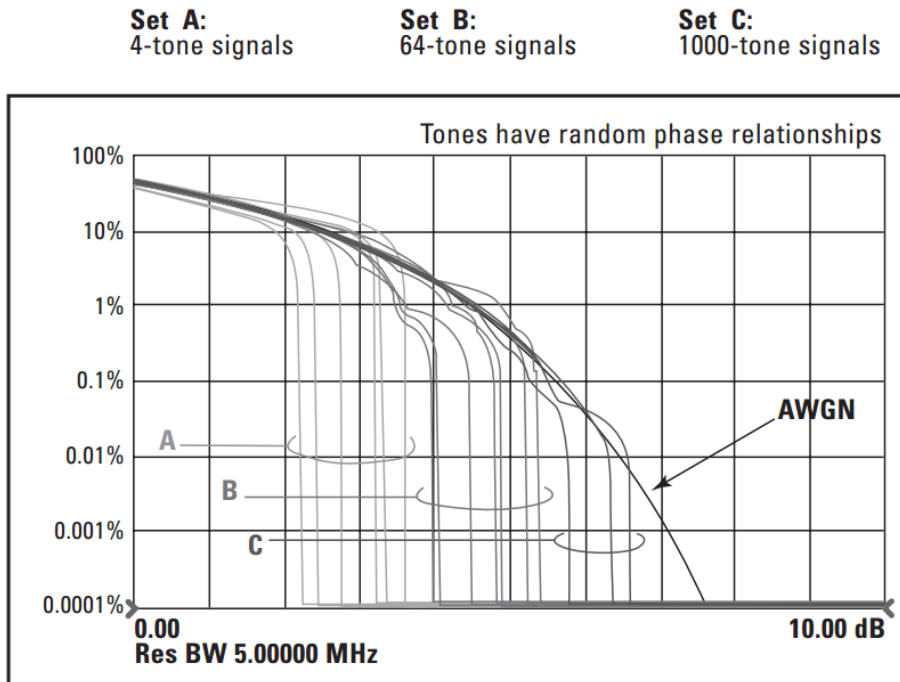


Figure 3-3 Comparison of CCDF curves of AWGN and different number of multi-tone signals [25]

In [24], large number of constant amplitude tones with correlated or uncorrelated phases is examined. Analytical expressions are given to predict the response of third order microwave circuits under the multi-tone signal. In the past, Noise Power Ratio measurements and Co-Channel distortion measurements used to be accomplished by creating this kind of multi-tone stimuli. In [1] and [20], in phase, equally spaced variable amplitude multi-tone signals were used to model an arbitrary waveform. Later, model input was used for analytical expressions of feed-forward linearizers. In [2], ACPR measurements of a nonlinear device excited with multi-sine signals are compared with ACPR measurements of digital modulation employing quadrature phase shift keying. It is concluded that when the crest factor of digitally modulated signal and multi-sine signal are comparable, better ACPR results are obtained.

In this thesis, to better represent an arbitrary waveform, multi-tones with variable tone spacing, phase and amplitude are used. Furthermore, for analytical expressions, amplifier nonlinearity is assumed to be third order. Before starting to model an

arbitrary waveform, effect of number of tones, amplitude variation of tones, spacing between tones and phases of the tones will be emphasized. Moreover, properties of the non-linear amplifiers used throughout characterization and modeling are given in this part of thesis.

3.2.1 Effect of Phase Variations of Tones

Phase relations of the tones strongly affect the CCDF curve. Resultant multi-tone is summation of each tone. Changing the phases of the tones affects whether they sum constructively, meaning increasing the crest factor, or destructively, meaning decreasing the crest factor. Furthermore, it is a common belief that increasing number of tones means increasing crest factor. However, it is possible to obtain higher crest factor with fewer number of tones by adjusting the phases as shown in Figure 3-5.

Signal A:
8 tones have phases all aligned

Signal B:
8-tones have phases offset by 45 degrees

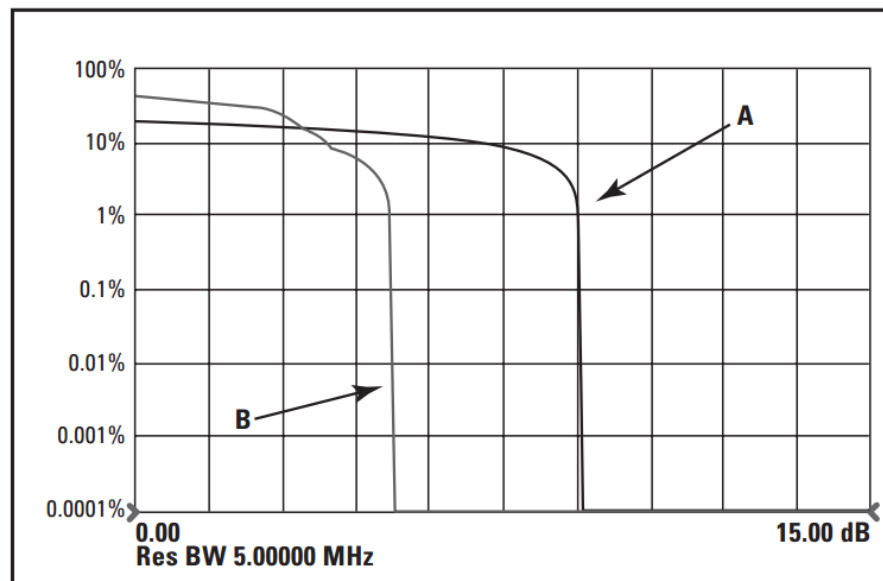


Figure 3-4 Effect of phase variation on CCDF curve [25]

To obtain the highest crest factor, phases of the tones should be aligned.

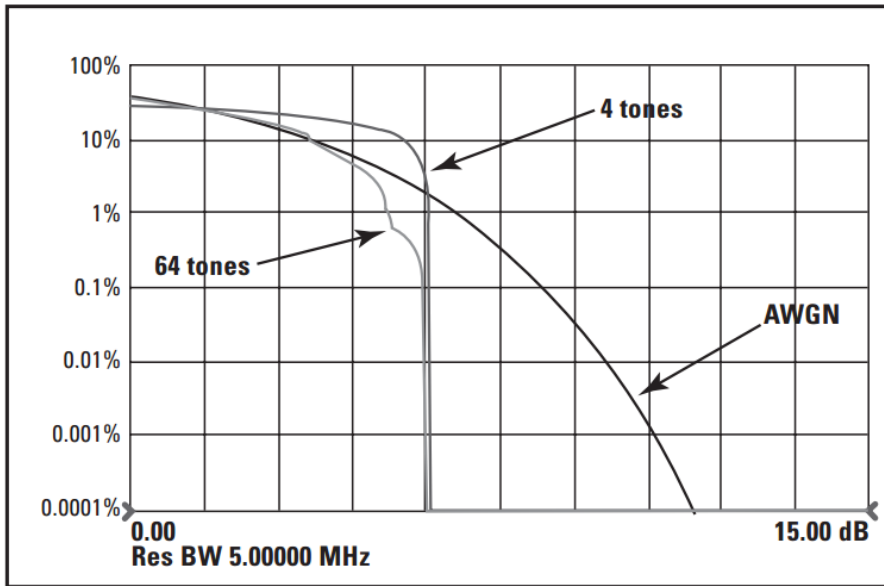


Figure 3-5 Comparison of CCDF curves of a 4-tone signal and a 64-tone signal. [25]

Phase distributions of the tones also affect the intermodulation products. Although IMD products depend heavily on the phase distributions of tones, IMD is not strongly correlated to phase relationships in statistical sense. In other words, by observing the IMD products of one phase set distribution, it is not possible to predict the IMD products of another phase set. Therefore, it is more reasonable to give average results of IMD products with different phase contributions.

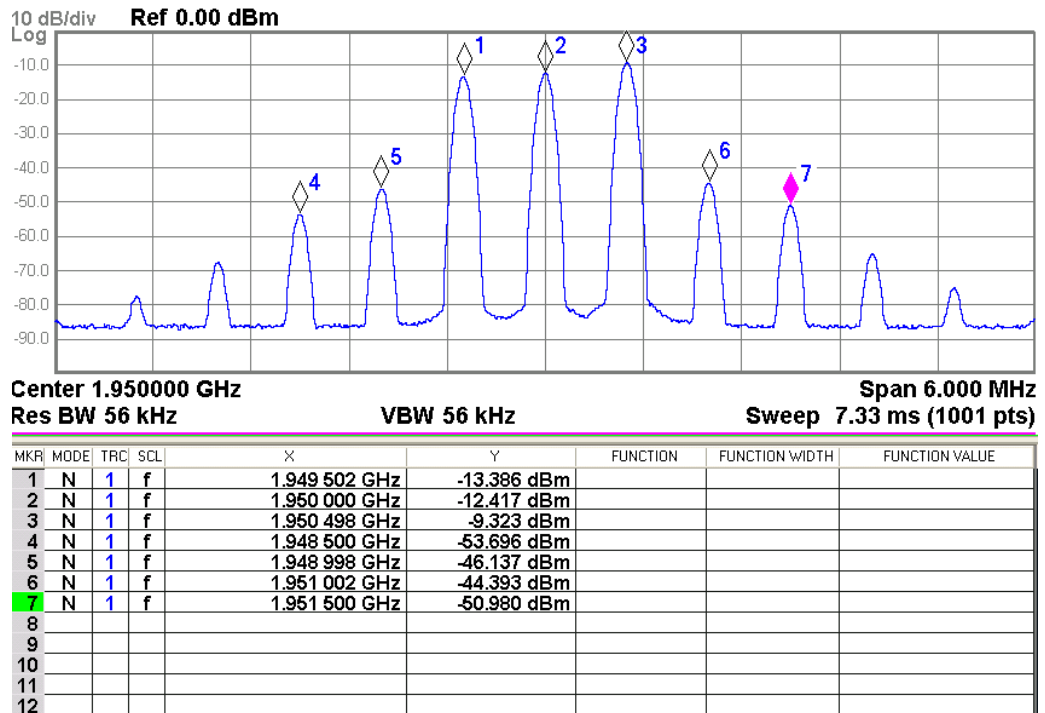


Figure 3-6 Intermodulation products under 3- tone excitation with equal phases

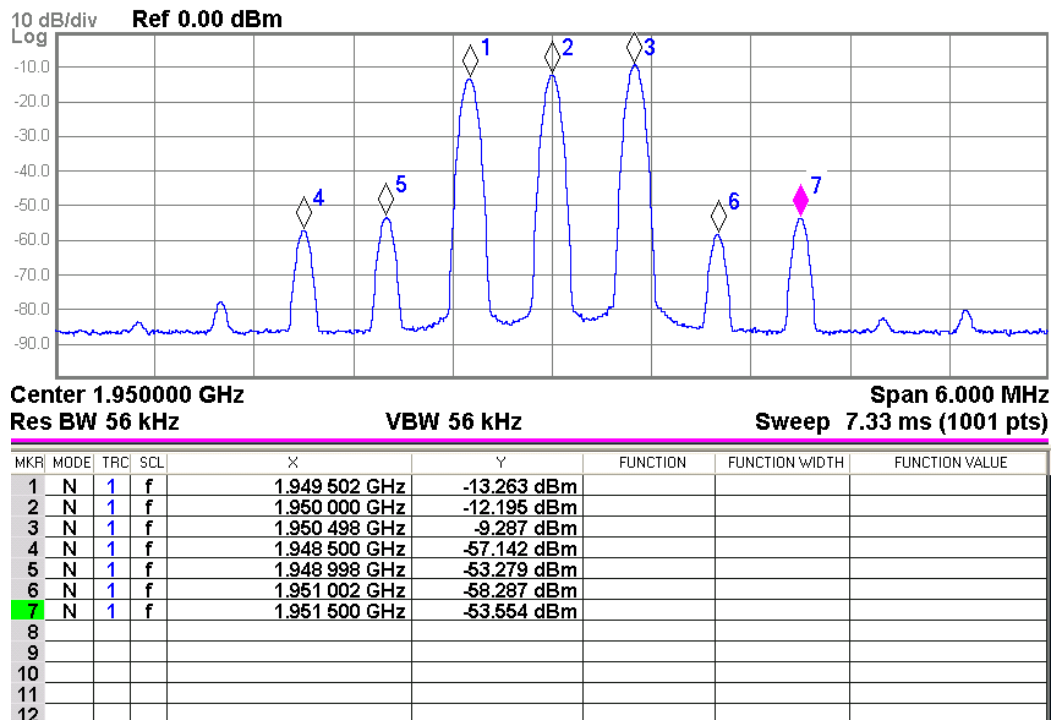


Figure 3-7 Intermodulation products under 3-tone excitation with different phases (300, 90 and 40 degrees respectively)

In Figure 3-6, intermodulation products under 3-tone equal phase excitation are shown. In Figure 3-7, spacing between tones and amplitude of tones are not changed but phases of the tones are adjusted to 300, 90 and 40 degrees. From Figure 3-6, it is clear that changing phases of the tones may significantly affect the IMD products. Marker 6 reading from Figure 3-6 and Figure 3-7 differ about 14 dB.

3.2.2 Effect of Spacing between Tones

First of all, spacing between tones affects the periodic behavior of the multi-tone signal. For p tones, there are $p-1$ tone spacing parameter. The period of the resultant signal is related to largest common denominator of the spacing between tones. For example, if 3 tones are used and spacing between tones are made $\Delta_1=\Delta_2=0.5$ MHz, then period of the multi-tone signal is 2 μ s. If spacing between tones are chosen as $\Delta_1=0.2$ MHz and $\Delta_2=0.4$ MHz, then period of the multi-tone signal is 5 μ s. Effect on the period is also seen at peak occurrence rate. When period is decreased, peaks are encountered more for a given specific time interval. Spacing between tones also affects the crest factor and CCDF curve of the input signal. With equally spaced tones, higher crest factor is obtained. Another effect of the tone spacing is position of both fundamental and IMD products in frequency axis. To model a signal with known center frequency and bandwidth more precisely, tone spacing may be arranged in such a way that, all fundamental tones drop in bandwidth limits of the modeled signal.

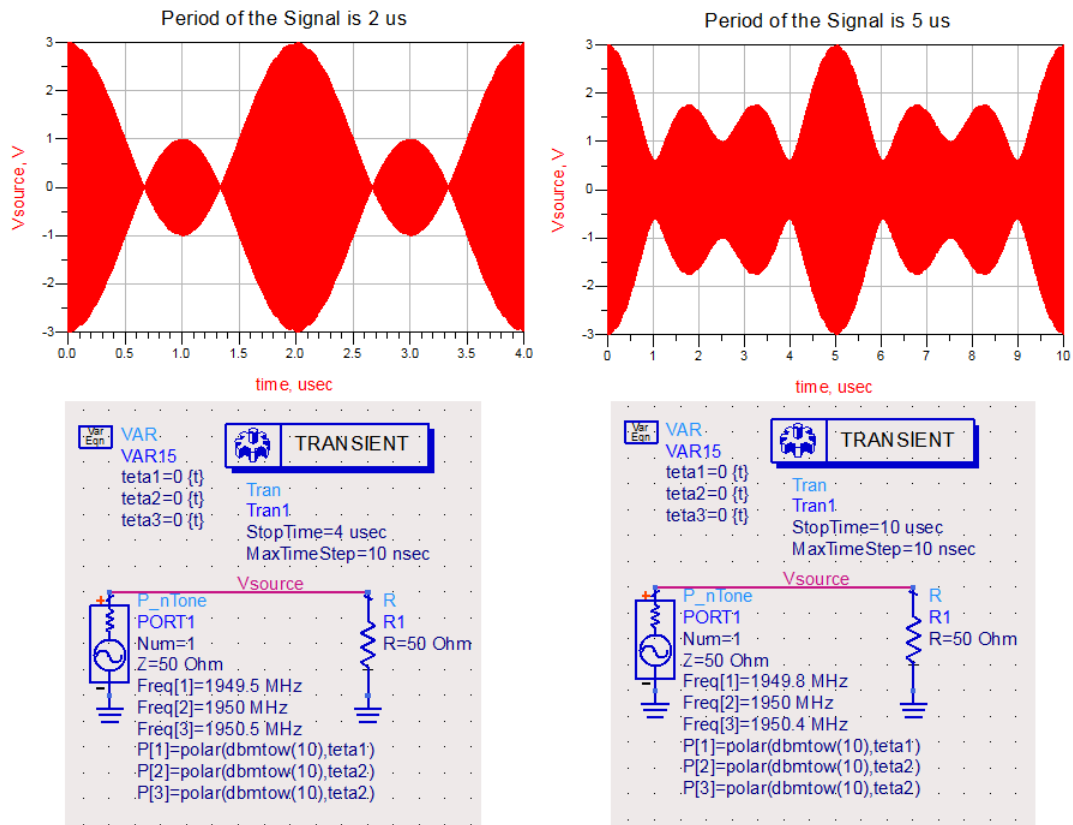


Figure 3-8 Effect of spacing between tones on periodic behavior of signal

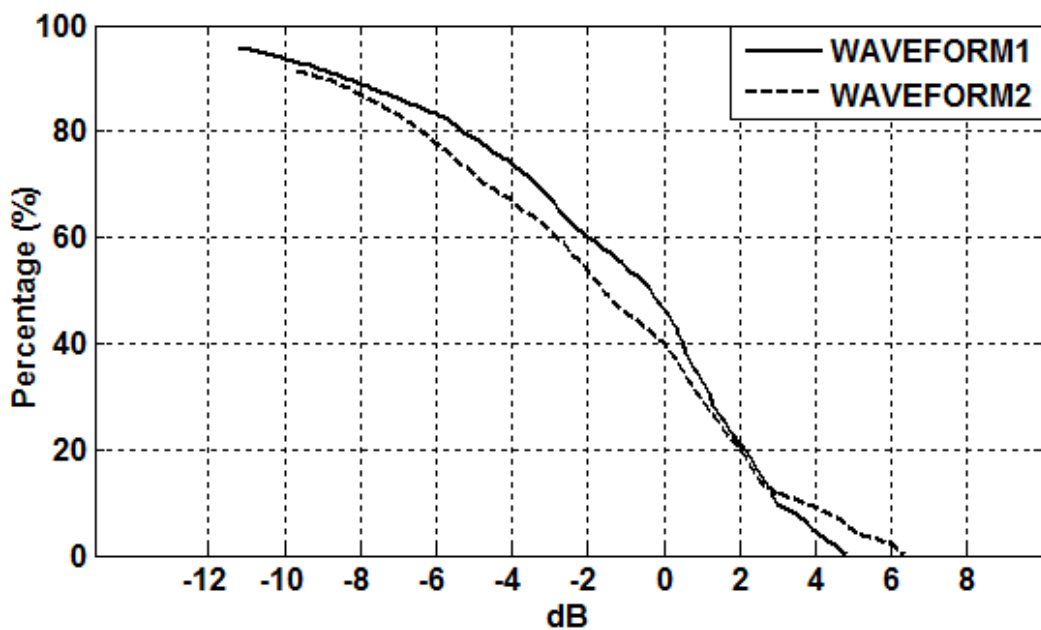


Figure 3-9 Effect of tone spacing on CCDF curve

In Figure 3-9, two 5-tone signals are examined. Magnitude and phase of the tones for WAVEFORM1 and WAVEFORM2 are made equal. Only difference between

WAVEFORM1 and WAVEFORM2 is that one of the tones in WAVEFORM2 is shifted 0.05 MHz to the left. Effect of this shifting on CCDF curve is clearly observed, which proves that tone spacing is a very strong parameter.

3.2.3 Effect of Amplitudes of Tones

Modeling an arbitrary waveform starts with a specific input power level of that signal. Amplitude coefficients of the multi-tone signals are arranged in such a way that, channel power of the original signal and multi-tone signal resembles each other. Once the modeling is achieved in a specific power level, it is expected that resemblance between multi-tone model and the arbitrary waveform continues with equal amount of power increase in both signals. Furthermore, change in the amplitude of the tones also causes change in in-band and out-of band components.

m3 freq=1.950GHz Pspec_dBm=-34.414	m1 freq=1.951GHz Pspec_dBm=5.781	m2 freq=1.952GHz Pspec_dBm=-36.801
--	--	--

Output of 3rd Order Polynomial Model Amplifier Under 5-Tone Excitation

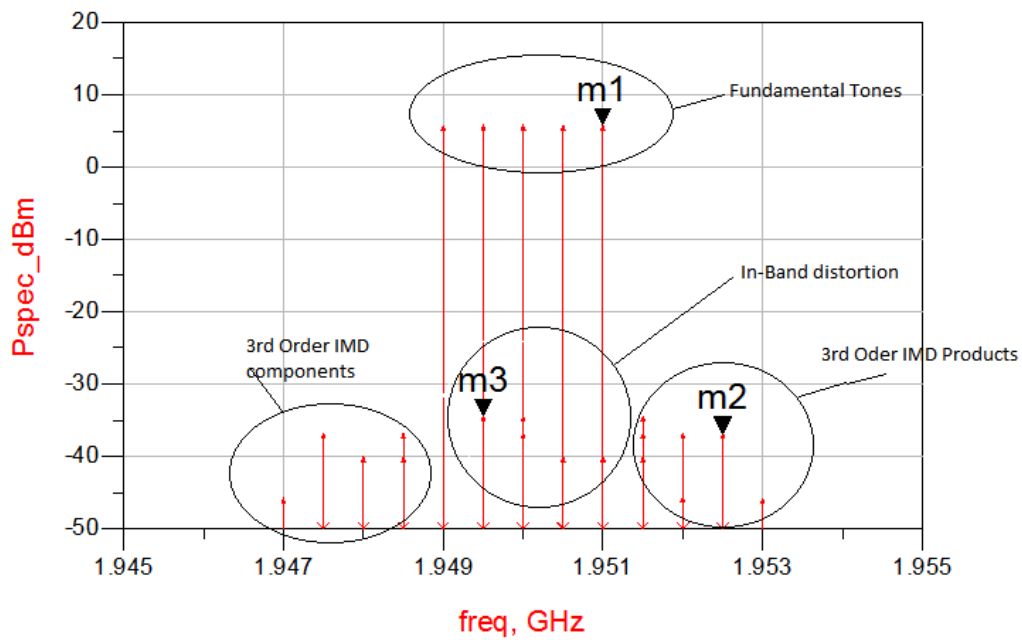


Figure 3-10 Output of 3rd order polynomial model amplifier under in-phase, equally spaced and -16 dBm equal amplitude 5-tones

m3 freq=1.950GHz Pspec_dBm=-16.851	m1 freq=1.951GHz Pspec_dBm=10.103	m2 freq=1.952GHz Pspec_dBm=-19.104
--	---	--

Output of 3rd Order Polynomial Model Amplifier Under 5-Tone Excitation

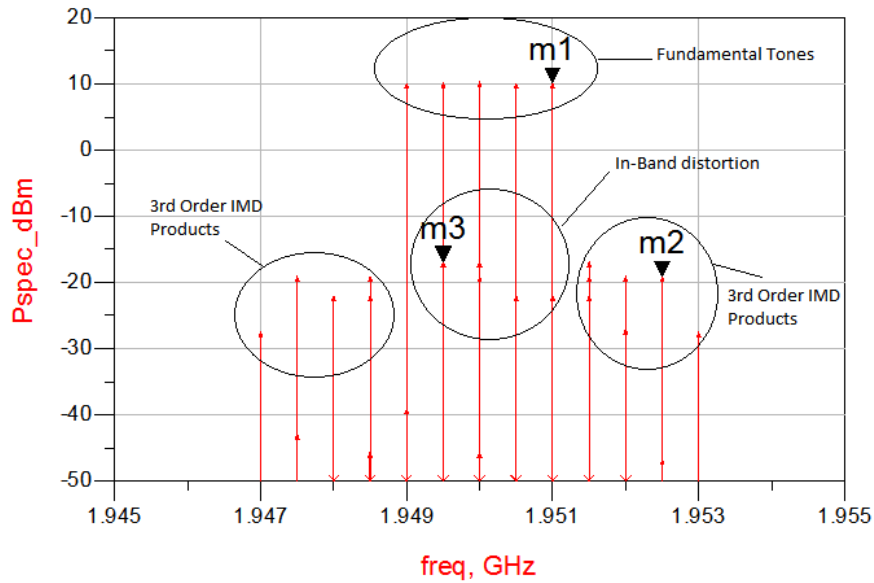


Figure 3-11 Output of 3rd order polynomial model amplifier under in-phase, equally spaced and -11 dBm equal amplitude 5-tones

By examining Figure 3-10 and Figure 3-11, it is observed that when tone amplitudes are increased 5 dB, fundamental tones at the output increase approximately 5 dB. In-band distortion power levels and 3rd order IMD component power levels increase approximately 15 dB, as expected.

In Figure 3-12, two 5-tone signals with same channel power, tone phases and spacings are obtained. These 5-tone signals have different characteristics as shown in Table 3-1 and Figure 3-13.

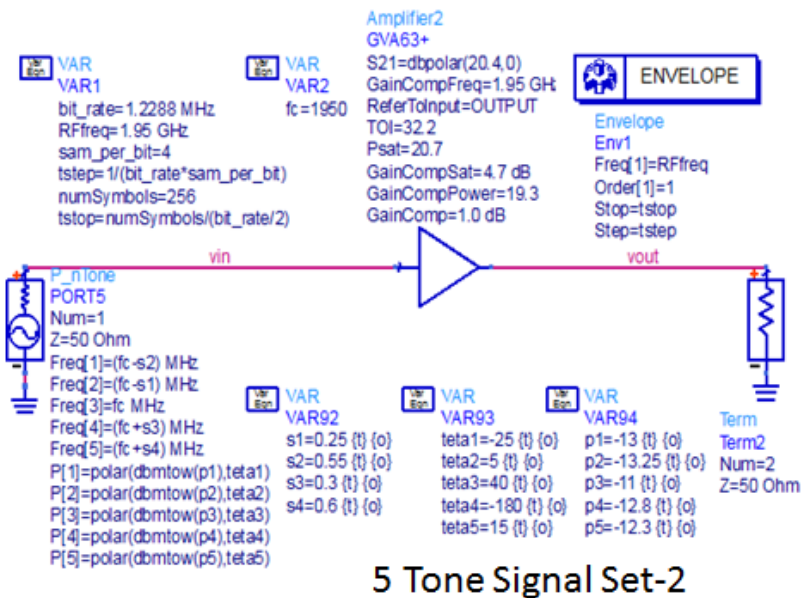
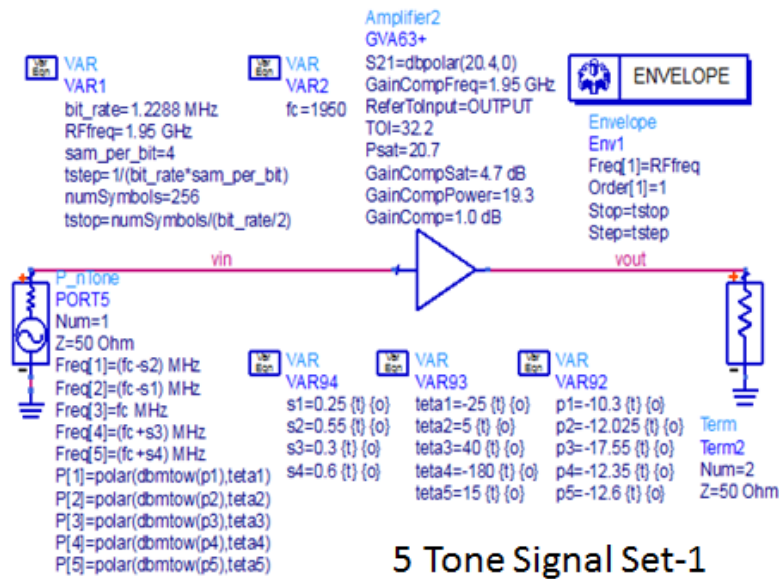


Figure 3-12 Effect of amplitude of tones on CCDF

Table 3-1 Characteristics of two 5-tone signal with same channel power, tone phases and spacings

	5-Tone Signal Set-1	5-Tone Signal Set-2
Channel Power	-5.424 dBm	-5.403 dBm
Crest Factor	4.182	4.806
Out of Band Power (F)	9918.730	13891.793
Total Nonlinear Power	161.916	189.436

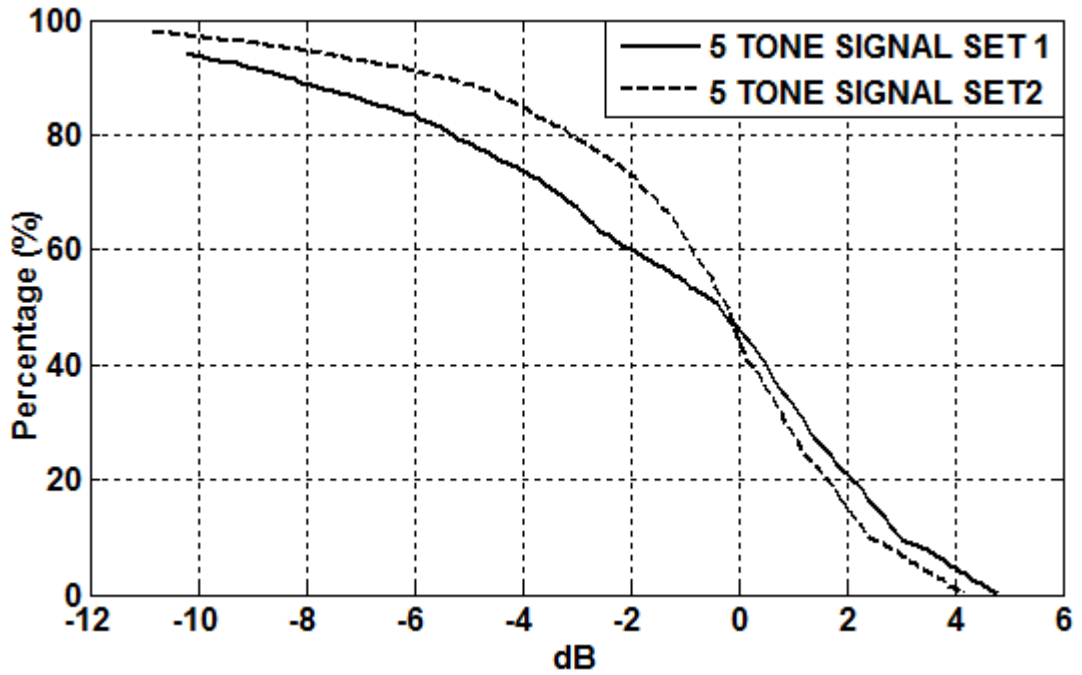


Figure 3-13 CCDF curves of two 5-tone signal having very similar channel power and identical tone phases

3.2.4 Effect of Number of Tones

To determine the adequate number of tones, crest factor of the arbitrary waveform is considered. It is known that by using p tones, maximum crest factor of $2p$ (or $10 \times \log[2p]$ in dB) could be obtained. For example, to model an arbitrary waveform with 7 dB crest factor, at least 3 tones should be used ($10 \log[6] = 7.78 > 7$). Increasing the number of tones provide more choices and more accurate results for multi-tone solution. It is important to note that while modeling a random excitation, several solutions with different number of tones, phase settings and tone spacings may exist. In Figure 3-14, it is shown that a 4-tone signal could have maximum PAR of 9 dB with equal amplitude, phase and tone spacing settings, whereas a 2-tone signal with same settings could have maximum PAR of 6 dB.

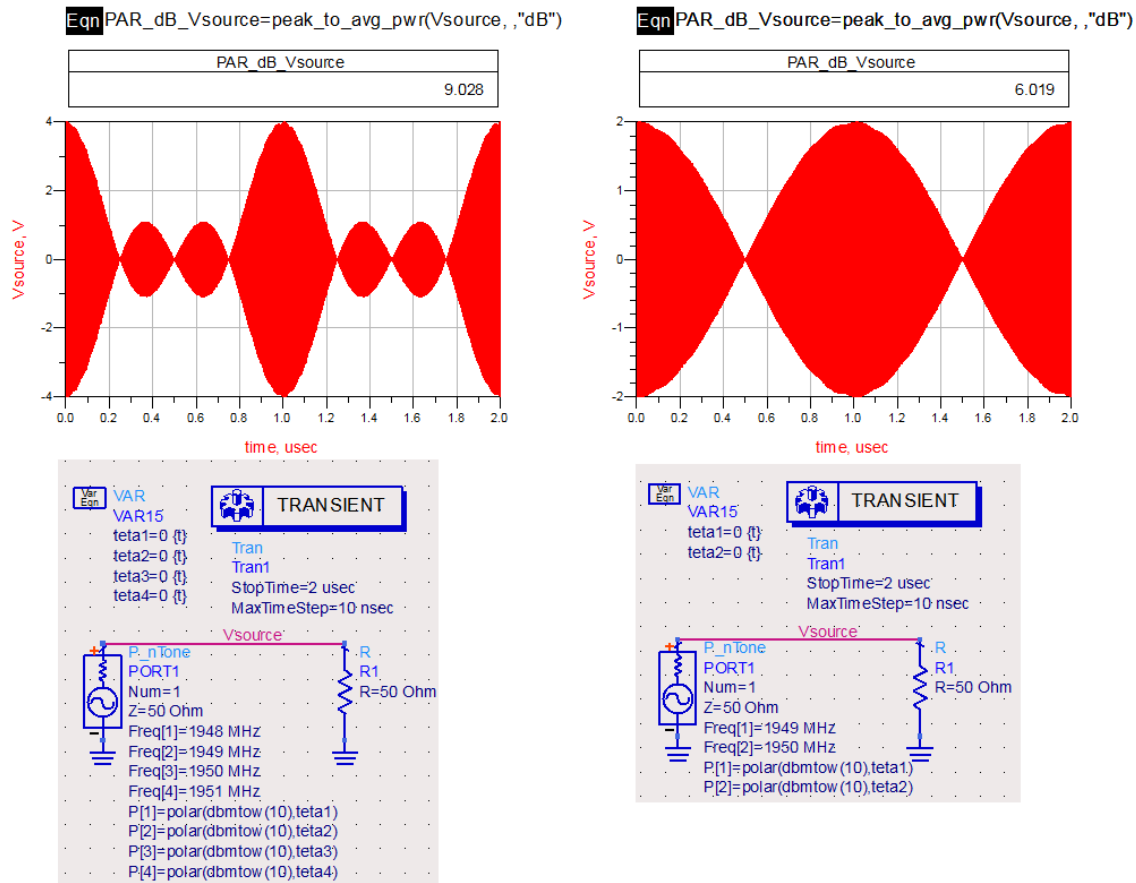


Figure 3-14 Effect of number of tones on the peak to average ratio for equal amplitude and equi-spaced tones.

3.3 Parameter Selection Criteria

In previous part, parameters of multi-tone signal are mentioned. In this thesis, none of the multi-tone parameters will be restricted. To better represent final regime of a nonlinear system operating under an arbitrary stimuli, multi-tone modeling should be given utmost importance. While choosing multi-tone parameters, there are some critical design parameters that should be considered carefully.

CCDF is one of these design parameters. CCDF curve tells designers the probability of encounter rate for a specific power level and also presents the PAPR. However, this parameter is not enough to correctly mimic the nonlinear behavior of arbitrary signal.

Other design parameter to decide the multi-tone signal arguments is distribution of instantaneous nonlinear power at the output of a nonlinear amplifier [1]. Assume the amplifier nonlinearity is restricted to third order.

$$V_{out} = a_1 \cdot V_{in} + a_3 \cdot V_{in}^3 \quad (3.9)$$

Where a_1 and a_3 are expressed as

$$a_1 = 10^{\left(\frac{G}{20}\right)} \quad (3.10)$$

$$a_3 = \frac{-2}{3R} \cdot 10^{\left(\frac{3G-2 \cdot IP_3}{20}\right)} \quad (3.11)$$

Where G is the linear power gain, IP_3 is the third order intercept point referred to the output of the amplifier and R is the reference circuit impedance.

Power relation at the output of an amplifier could be written for 1 ohm reference impedance as [1]

$$P_{out} = \frac{V_{out}^2}{2} = \frac{(a_1 \cdot V_{in} + a_3 \cdot V_{in}^3)^2}{2} \quad (3.12)$$

$$P_{out} = \frac{1}{2} \cdot a_1^2 \cdot V_1^2 + \frac{3}{4} a_1 \cdot a_3 \cdot V_1^4 + \frac{9}{32} \cdot a_3^2 \cdot V_1^6 \quad (3.13)$$

Where V_1 is the instantaneous envelope voltage of V_{in} .

In (3.13), the term $\frac{1}{2} \cdot a_1^2 \cdot V_1^2$ is referred as instantaneous linear power, whereas the

term $\frac{3}{4} \cdot a_1 \cdot a_3 \cdot V_1^4 + \frac{9}{32} \cdot a_3^2 \cdot V_1^6$ is referred as instantaneous nonlinear power.

Throughout this thesis, instantaneous nonlinear power will be referred as S .

$$S = \text{abs} \left(\frac{3}{4} a_1 \cdot a_3 \cdot V_1^4 + \frac{9}{32} \cdot a_3^2 \cdot V_1^6 \right) \quad (3.14)$$

Expression S , includes both in-band and out-of band distortion. Term $\frac{3}{4} \cdot a_1 \cdot a_3 \cdot V_1^4$

is responsible for in-band products and term $\frac{9}{32} \cdot a_3^2 \cdot V_1^6$ is responsible for out-of

band products. Now, consider that samples are taken from the envelope voltage with

specific time intervals. When the instantaneous envelope voltage increases, instantaneous nonlinear power also increases. In other words, samples close to the peak value of the envelope signal are troublesome. These samples drive the amplifier into nonlinearity. When the power of the input signal is increased, S values for all of the samples start to become more significant. Hence, although modeling an arbitrary waveform starts with a certain power level, modeled multi-tone signal should be valid for any power level.

Another design parameter is K, which represents the overall distortion power. [1]

$$K = \sum_i S_i \cdot N_i \quad (3.15)$$

Where S is instantaneous nonlinear power, and N_i is the corresponding number of samples. Since instantaneous nonlinear power includes both in-band and out-of band products, so does parameter K. To calculate K, first S values are quantized for a specific number of levels. Each sample of S drops in to certain level and by this way N_i values for each level are calculated.

Average of calculated S values could be other design parameter. M, can be expressed as [1]

$$M = \frac{1}{N} \cdot \sum_i S_i \quad (3.16)$$

In expression (3.16), N is the total number of samples. Similar to the parameter K, M also includes in-band and out of band products.

Comparing adjacent channel power results of multi-tone signal and original signal also tells designers resemblance between multi-tone signal and original stimuli. Since ACP measurements includes only out-of band products, parameter K and M are not useful while calculating ACP values. Only, the term $\frac{9}{32} \cdot a_3^2 \cdot V_1^6$ is considered while calculating out of band products. This calculation is closely related to ACP calculation. In this thesis, instead of ACPR measurements, an alternative parameter F will be defined. [1]

$$F = \sum_{\text{OUT-OF-BAND}} \left| \text{FFT} \left(\frac{3}{4} \cdot a_3 \cdot V_1^3, N \right) \right|^2 \quad (3.17)$$

Throughout this thesis, design parameters K , M , F , CCDF curve and distribution of S will be used to select the parameters of multi-tone stimuli.

3.4 Properties of the Amplifiers Used in Simulations

Communication signals are unpredictable. They can't be expressed in terms of elementary outputs easily. Therefore, expressing response of a non-linear system to those arbitrary inputs is very challenging task. For those kinds of nonlinear systems, it would be very useful to be able to predict the final response. Here, the importance of multi-tone modeling comes out. It makes possible to express the output of the nonlinear system in terms of the tones forming the input excitation. Therefore, it is possible to say that once an appropriate multi-tone model is obtained for a telecommunication signal, which is unpredictable and arbitrary in practice, then final response of the system could be estimated. Here, unpredictable and arbitrary excitation is emphasized, because it is important to show multi-tone model could be employed to represent any kind of waveform.

In this thesis, nonlinear amplifiers are employed as nonlinear systems. To verify the multi-tone modeling, nonlinear amplifier is excited by the communication signal and its multi-tone model. Nonlinear parameters S , K , F , M , CCDF curve, channel bandwidth and channel power are compared. To prove that multi-tone model is valid under any nonlinear system, amplifiers with different AM-AM, and AM-PM characteristics are used. As communication signal, first digitally modulated RF signal which has the modulation characteristics of 3GPP (WCDMA) signal is used. To prove that modeling could be accomplished for any kind of input, a digitally modulated RF signal which has the modulation characteristics of base-station CDMA signal is also modeled and verified. Frequency for both of the communication signals is set to 1.95 GHz and amplifiers are characterized for 1.95 GHz. Nonlinear amplifiers used for verification are GVA-63+ and PMA-545G1+ from Mini-Circuits.

The GVA-63+ is a wideband amplifier operating from 0.01 GHz to 6 GHz. It is fabricated using InGap HBT technology. This amplifier offers high gain and dynamic range over a broad frequency range. GVA-63+ has about 20 dB small signal gain, 18.6 dBm P_{1dB} and 32.2 dBm OIP_3 at 2 GHz as stated in manufacturer's

datasheet. The amplifier works with 5 volt supply voltage. Gain, P_{1dB} and OIP₃ are obtained for the board designed for GVA-63+. Intermodulation distortion products are measured for different power levels and from these measurements OIP₃ is calculated using (3.18).

$$OIP_3 \text{ (dBm)} = \frac{IMD \left(\frac{\text{dBm}}{\text{Tone}} \right)}{2} + P_{out} \left(\frac{\text{dBm}}{\text{Tone}} \right) \tag{3.18}$$

Moreover, P_{1dB} and linear gain is calculated from AM-AM measurement.



Figure 3-15 AM-AM characteristics of the amplifier GVA-63+

From Figure 3-15, it is observed that 1 dB decrease from linear gain, which is 20.4, occurs for input power of about -0.1 dBm. At this point gain is found as 19.41 dB. Therefore P_{1dB} point for the amplifier GVA63+ is calculated as 19.31 dBm at 1.95 GHz. Moreover, for the same frequency under overdrive conditions, maximum power of the amplifier is found as approximately 20.7 dBm. As depicted before, for linear modulation schemes, operating an amplifier beyond the 1 dB compression point may result in corrupted signal at the output.

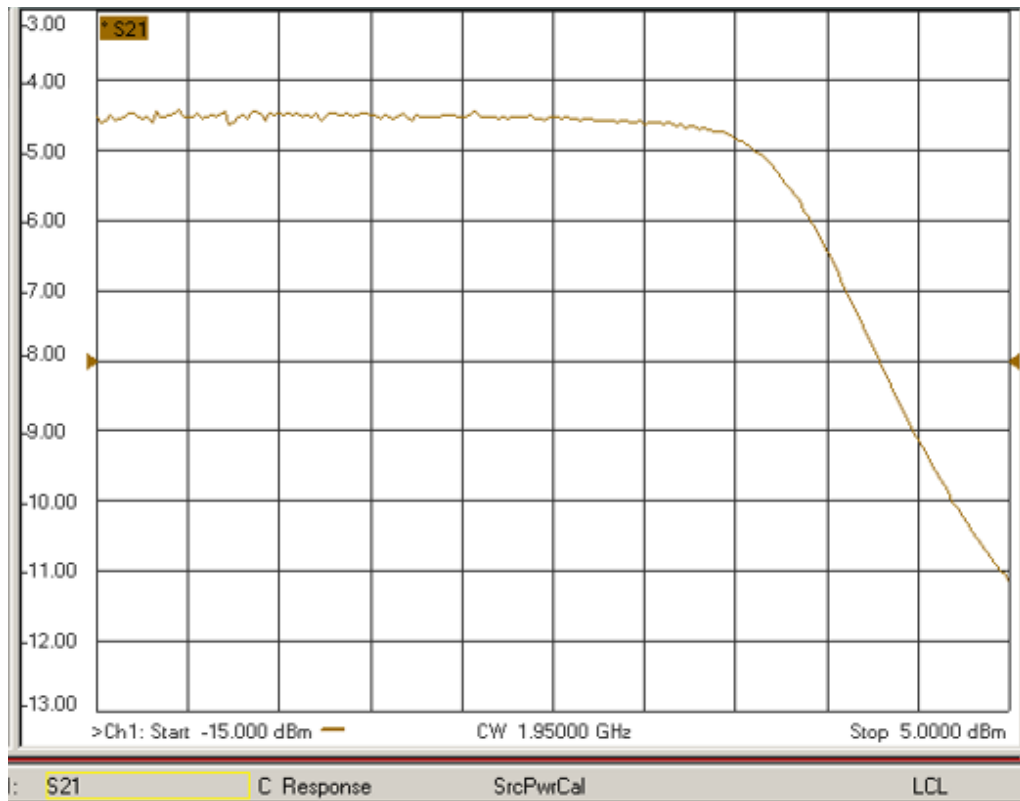


Figure 3-16 AM-PM characteristics of the amplifier GVA-63+

AM-PM conversion characteristics of the amplifier GVA-63+ shows an excellent performance up to 1 dB compression point, almost no phase corruption at all. However, beyond the 1 dB compression point, output phase changes more than 1 degree for 1 dB increase in the input power. If constellation diagram is observed for the M-QAM input signal and amplified output signal under over drive conditions, significant deviation is observed from the desired diagram, which results in undesired BER.

Intermodulation products are calculated for different power levels, from linear zone to beyond compression points. Intermodulation distortion test is run at 1.95 GHz carrier frequency with a 2-tone signal. Tones are separated by 1MHz. To have symmetrical distortion products, amplitude of the tones are made equal. By using (3.18) for the input power level of -10 dBm,

$$OIP_3 \text{ (dBm)} = \frac{\text{IMD} \left(\frac{\text{dBm}}{\text{Tone}} \right)}{2} + P_{\text{out}} \left(\frac{\text{dBm}}{\text{Tone}} \right) = \frac{49.23}{2} + 7.58 = 32.195 \text{ dBm}$$

OIP3 value specified by the manufacturer's datasheet is 32.2 dBm for 2 GHz operating frequency, which is very close to calculated value.

Table 3-2 Intermodulation distortion products under two equal amplitude tone with 1 MHz tone spacing for the amplifier board GVA-63+

Input Power (dBm/Tone)	Output Power (dBm/tone)	3rd order left (dBc)	3rd order right (dBc)	5rd order left (dBc)	5rd order right (dBc)
-16	4.64	-55.78	-56.96	---	---
-15	5.63	-53.65	-54.80	---	---
-14	6.61	-51.42	-52.52	---	---
-13	7.58	-49.23	-50.14	-75.02	-75.60
-12	8.58	-46.85	-47.57	-73.62	-73.44
-11	9.59	-44.36	-45.07	-70.22	-70.89
-10	10.43	-41.13	-41.54	-65.61	-65.05
-9	11.38	-38.34	-38.71	-60.47	-60.27
-8	12.30	-35.18	-35.39	-54.41	-54.38
-7	13.15	-31.28	-31.50	-47.46	-47.46
-6	13.88	-26.82	-26.97	-40.97	-41.00
-5	14.49	-22.64	-22.76	-37.90	-38.02
-4	14.96	-19.51	-19.64	-39.82	-40.12
-3	15.33	-17.3	-17.44	-47.15	-45.60
-2	15.62	-15.66	-15.82	-35.59	-34.94
-1	15.77	-14.89	-15.05	-31.38	-31.0

For the simulations, amplifier nonlinearity is assumed be third order. After finding OIP₃ and linear gain, amplifier polynomial coefficients a₁ and a₃ could be found using (3.10) and (3.11).

$$a_1 = 10^{\left(\frac{G}{20}\right)} = 10^{\left(\frac{20.4}{20}\right)} = 10.47$$

$$a_3 = \frac{-2}{3 \cdot R} \cdot 10^{\left(\frac{3G-2IP_3}{20}\right)} = \frac{-2}{3 \cdot 50} \cdot 10^{\left(\frac{3 \cdot 20.4 - 2 \cdot (32.195 - 30)}{20}\right)} = -9.224$$

Throughout the simulations, calculated a_1 and a_3 values will be used to compare the K, M and F values of modeled multi-tone signal and original signal.

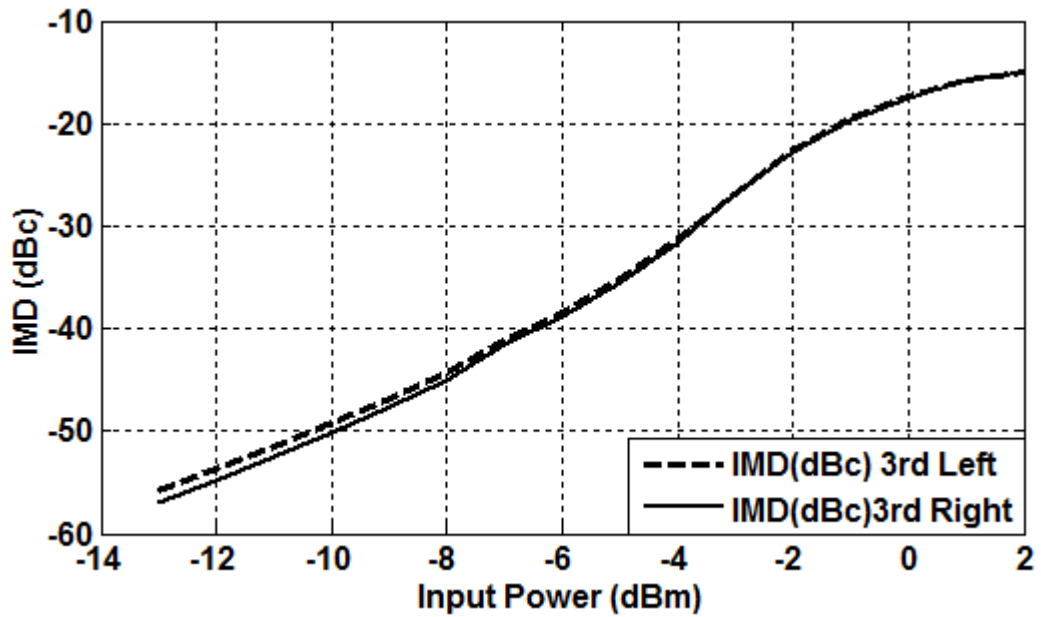


Figure 3-17 3rd order intermodulation products for different power levels of GVA-63+

Ideally, when 3rd order Intermodulation components are observed, 3rd order IMD (in dBc) should increase 2 dB for 1 dB increase in the input power. However, in a real amplifier condition, increase in 3rd order IMD (in dBc) may reach to 4 dB for 1 dB increase in the input power at specific power levels.

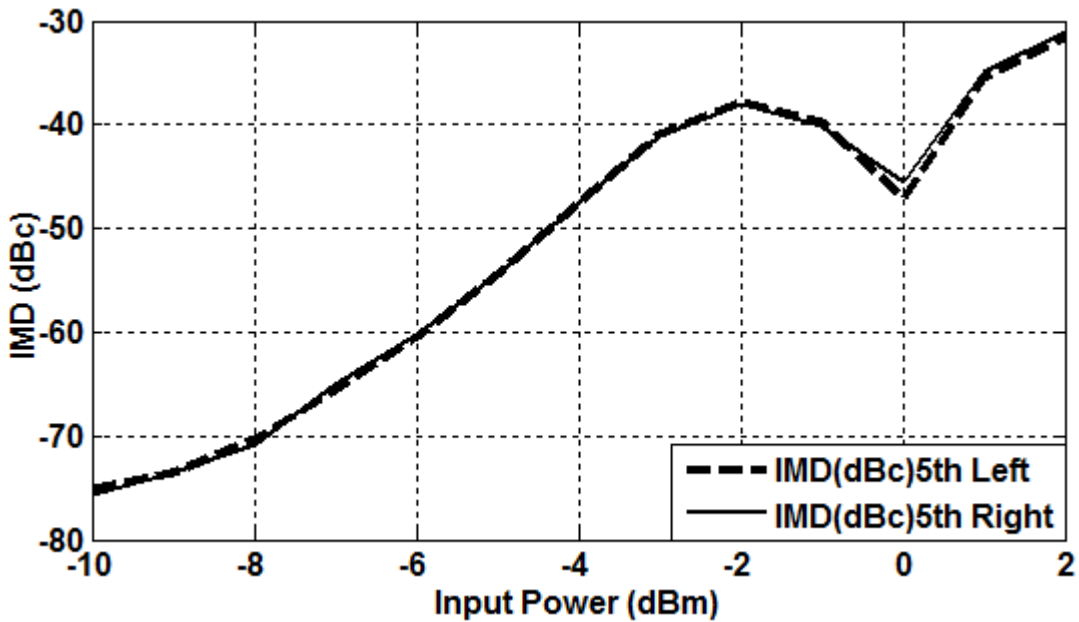


Figure 3-18 5th order intermodulation products for different power levels of GVA-63+

From Figure 3-18, a notch for the 5th order products are clearly observed. For specific power levels, increasing the input power level may decrease the IMD products. These operating points are called as sweet spot. Ideally, the slope of the curve in Figure 3-18 should be 5, however, for GVA-63+ at certain power levels, 5th order IMD increase may reach to 7 dB for 1 dB input power increase.

Another amplifier used for verification of multi-tone modeling is PMA-545G1+ from Mini-Circuits. PMA-545G1+ is E-PHEMT based low noise MMIC amplifier operating from 0.4 to 2.2 GHz. According to the manufacturer's datasheet, amplifier has 26.1 dB small signal gain, 22.6 dBm P_{1dB} and 33.6 dBm OIP₃ around 2.2 GHz. The amplifier works with 5 volt supply voltage. Gain, P_{1dB} and OIP₃ are obtained from the board designed for PMA-545G1+. Intermodulation distortion products are measured for different power levels. From these measurements, OIP₃ is calculated using (3.18). Moreover P_{1dB} and linear gain is calculated from AM-AM measurement given in Figure 3-19.

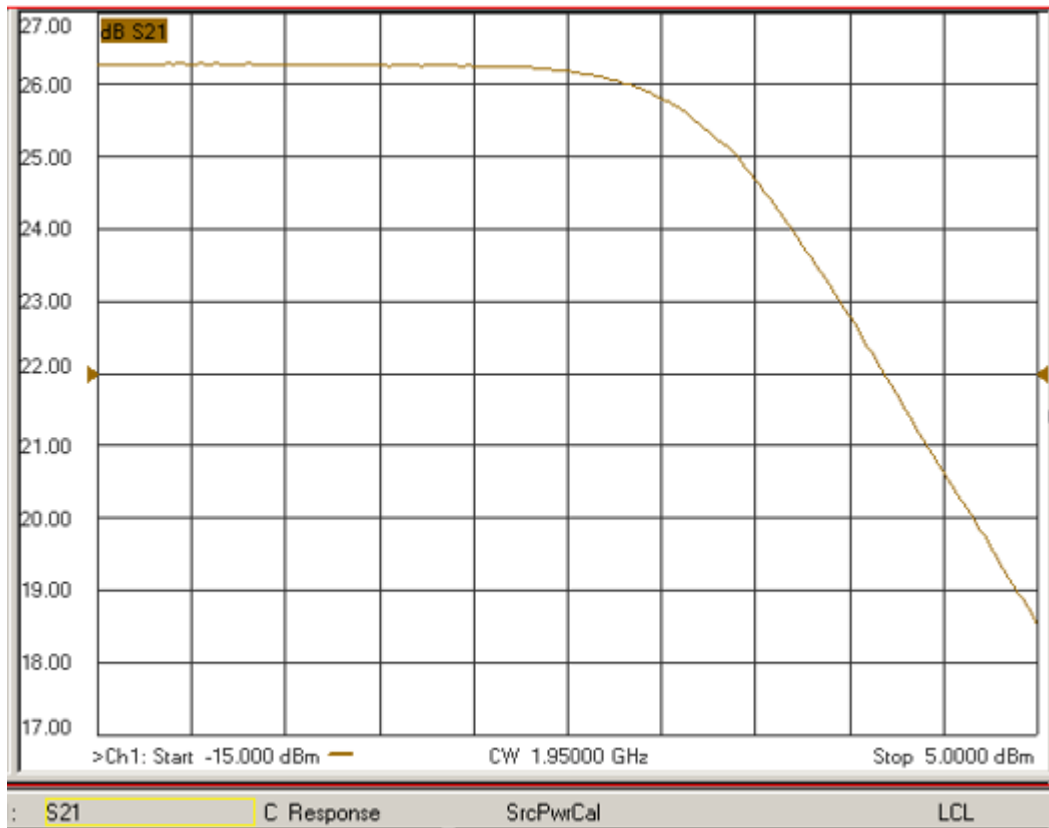


Figure 3-19 AM-AM characteristics of the amplifier PMA-545G1+

1 dB gain decrease from linear gain, which is 26.3, occurs for input power level of -2 dBm. For this input power level, gain is measured as 25.3 dB. Thus, P_{1dB} point is calculated as 23.3 dBm. When amplifier is driven beyond the 1 dB compression point, saturated output power is calculated as 23.6 dBm.

PMA-545G1+ exhibits adequate phase distortion characteristics up to P_{1dB} operating point. After this point, output phase increases more than 2 degrees for 1 dB input power increase. It could be concluded that although PMA-545G1+ exhibits adequate phase performance below the compression points, under over drive conditions it performs worse than GVA-63+ amplifier in terms of output phase characteristics. Thus, amplifier PMA-545G1+ is expected to have more corrupted constellation diagram than GVA-63+ for the power levels close to the compression points.

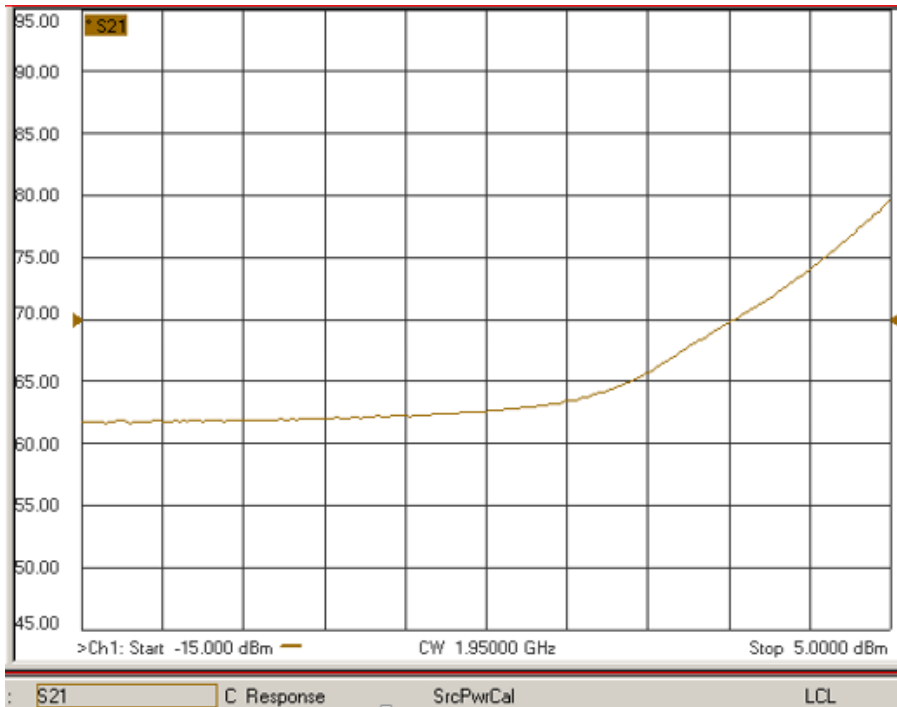


Figure 3-20 AM-PM characteristics of the amplifier PMA-545G1+

Table 3-3 Intermodulation distortion products under two equal amplitude tone with 1 MHz tone spacing for the amplifier board PMA-545G1+

Input Power (dBm/Tone)	Output Power (dBm/ tone)	3rd order left IMD (dBc)	3rd order right IMD (dBc)	5rd order left IMD (dBc)	5rd order right IMD (dBc)
-18	8.3	-64.509	-67.428	---	---
-17	9.3	-62.173	-63.972	---	---
-16	10.24	-60.221	-61.39	---	---
-15	11.23	-57.693	-58.176	---	---
-14	12.24	-55.085	-55.229	---	---
-13	13.2	-52.73	-52.553	---	---
-12	14.182	-50.565	-50.243	---	---
-11	15.17	-47.981	-47.542	-64.3	-63.45
-10	16.213	-42.579	-42.048	-52.263	-52.073
-9	17.088	-35.919	-35.797	-44.808	-44.738
-8	17.869	-29.575	-29.624	-39.049	-39.009
-7	18.478	-24.335	-24.426	-35.388	-35.388
-6	18.907	-20.242	-20.347	-34.427	-34.407
-5	19.185	-17.2	-17.325	-37.585	-37.385
-4	19.348	-15.017	-15.174	-45.608	-41.478
-3	19.443	-13.446	-13.621	-33.123	-32.553
-2	19.472	-12.209	-12.379	-27.052	-27.102

Intermodulation products are calculated for different power levels, from linear zone to beyond compression points. Intermodulation distortion test is run at 1.95 GHz carrier frequency with a 2-tone signal having 1MHz tone spacing. To have symmetrical distortion products, amplitude of the tones are made equal. By using (3.18) for the input power level of -5 dBm,

$$OIP_3 \text{ (dBm)} = \frac{\text{IMD} \left(\frac{\text{dBm}}{\text{Tone}} \right)}{2} + P_{\text{out}} \left(\frac{\text{dBm}}{\text{Tone}} \right) = \frac{29.575}{2} + 17.86 = 32.66$$

OIP3 value specified by the manufacturer's datasheet is 33.6 dBm for 2.2 GHz operating frequency, which is close to the calculated value. After finding OIP₃ and linear gain, amplifier polynomial coefficients a_1 and a_3 could be found using (3.10) and (3.11).

$$a_1 = 10^{\left(\frac{G}{20} \right)} = 10^{\left(\frac{26.3}{20} \right)} = 20.65$$

$$a_3 = \frac{-2}{3 \cdot R} \cdot 10^{\left(\frac{3G - 2 \cdot IP_3}{20} \right)} = \frac{-2}{3 \cdot 50} \cdot 10^{\left(\frac{3 \cdot 26.3 - 2 \cdot (32.66 - 30)}{20} \right)} = -63.67$$

Throughout the simulations, calculated a_1 and a_3 value will be used to compare the K, M and F values of multi-tone signal and original signal.

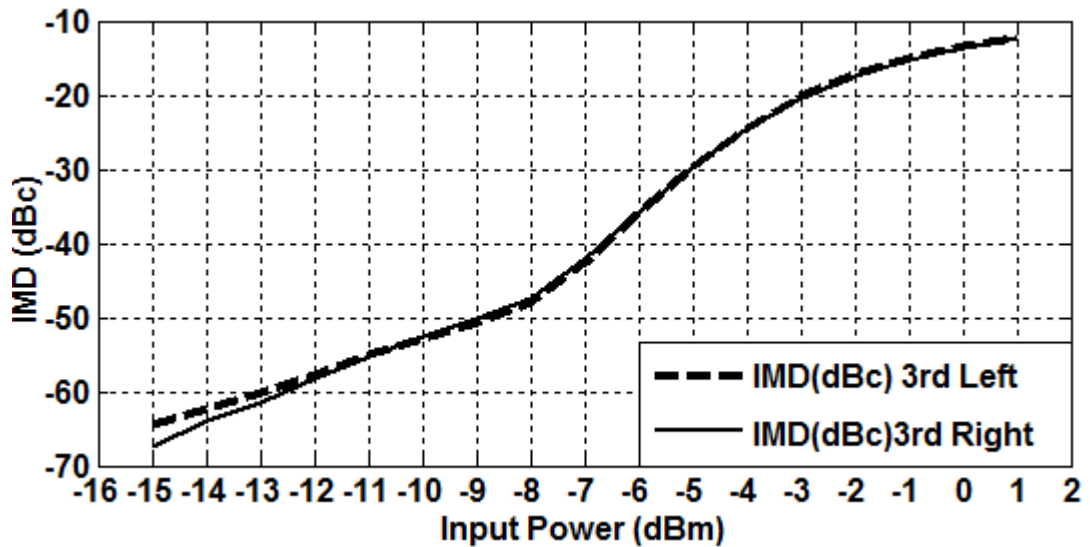


Figure 3-21 3rd order intermodulation products for different power levels of

PMA-545G1+

From Table 3-3 and Figure 3-21, it is observed that IMD increase with 1 dB input power increase is not always 2 dB. IMD curve slope is not constant. Furthermore, from Figure 3-22 effect of sweet spot is clearly observed.

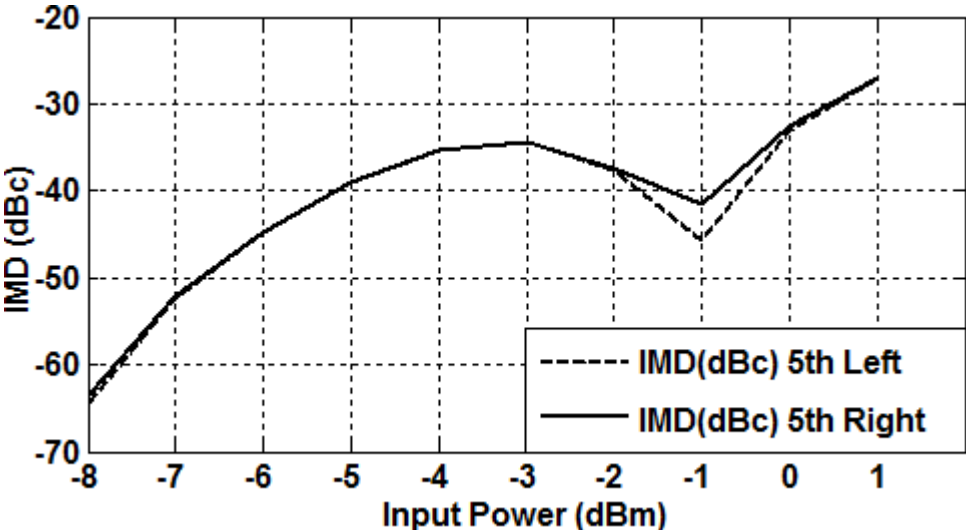


Figure 3-22 5th order intermodulation products for different power levels of PMA-545G1+

3.5 Properties of Waveforms Used in Simulations

Throughout this part, the arbitrary waveform that is being modeled is called as original waveform and multi-tone signal that represents the original signal is called as model signal. Original signals are available in Agilent Advanced Design Systems library. Two signals from ADS library will be used. These signals have different bandwidth, peak to average ratio and CCDF characteristics. Purpose of modeling different types of signals is to show that any arbitrary waveform could be modeled by using multi-tone signals.

The first signal that will be modeled is RF carrier modulated by 3GPP uplink signal. This signal generates a digitally modulated RF signal that has the modulation characteristics of WCDMA signal. This source is implemented by interpolating data from a stored data file instead of recalculating the source for every simulation. The data file consists of 1 frame of 3GPP data (38400 chips at 1/3.84 us per chip). Frame length is 10 ms. Each frame is divided into 15 slots with each slot having 2560 chips at the chip rate of 3.84Mcps. To simulate the source properly, there are critical points

that should be taken into account during envelope simulation. To prevent the data interpolation between data samples, simulation time step should be set to $1/3.84/4$ us, in other words, taking four samples per chip. Recommended controller setup provided by Agilent and WCDMA signal properties are shown in Figure 3-23.

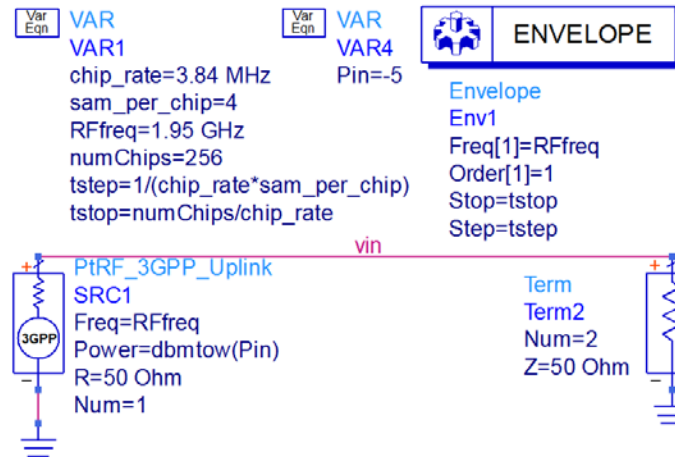


Figure 3-23 RF carrier modulated by 3GPP uplink signal and its properties

After arranging the envelope simulation settings, baseband spectrum of the input carrier and output carrier are obtained as in Figure 3-24. Spectral regrowth in adjacent and alternate channels are clearly observed. Channel bandwidth is 3.84 MHz as specified in the settings. Magnitude of carrier is also shown in Figure 3-25.

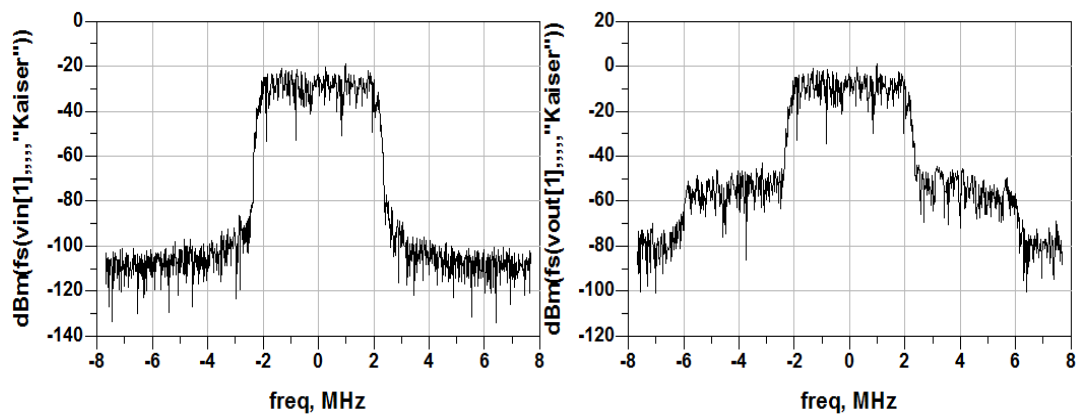


Figure 3-24 Spectrum of the input (left) and output (right) carrier for 3GPP uplink signal

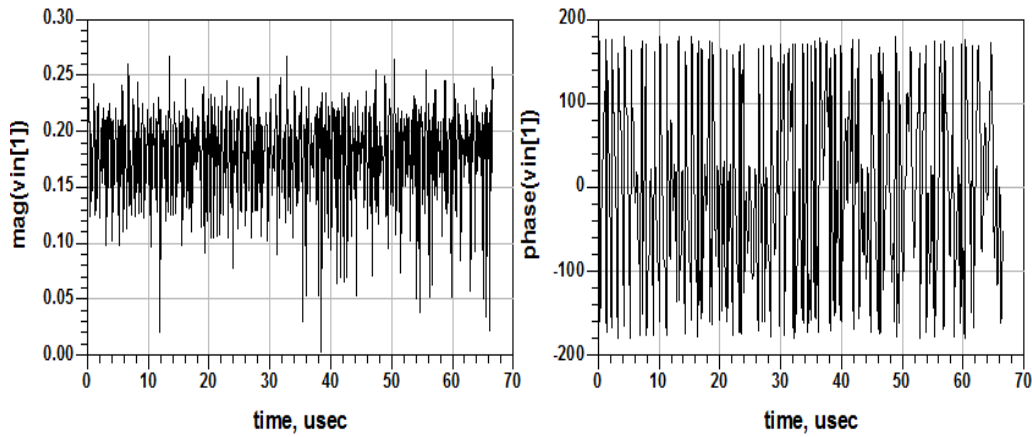


Figure 3-25 Magnitude (left) and phase (right) of the input carrier for 3GPP uplink signal.

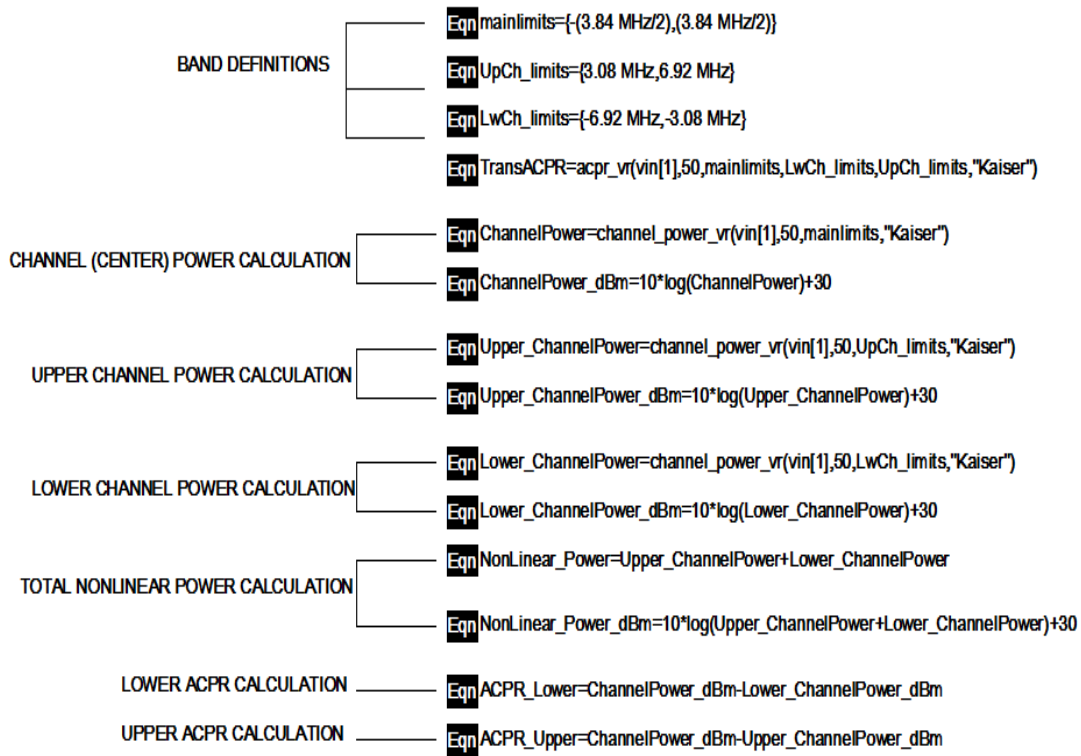


Figure 3-26 Main, upper, lower channel band definitions and measurement equations for channel power calculations

ChannelPower_dBm	Upper_ChannelPower_dBm	Lower_ChannelPower_dBm
-5.231	-82.298	-81.731
ACPR_Lower	ACPR_Upper	NonLinear_Power_dBm
76.500	77.068	-78.995

Figure 3-27 Simulated band characteristics of WCDMA input signal

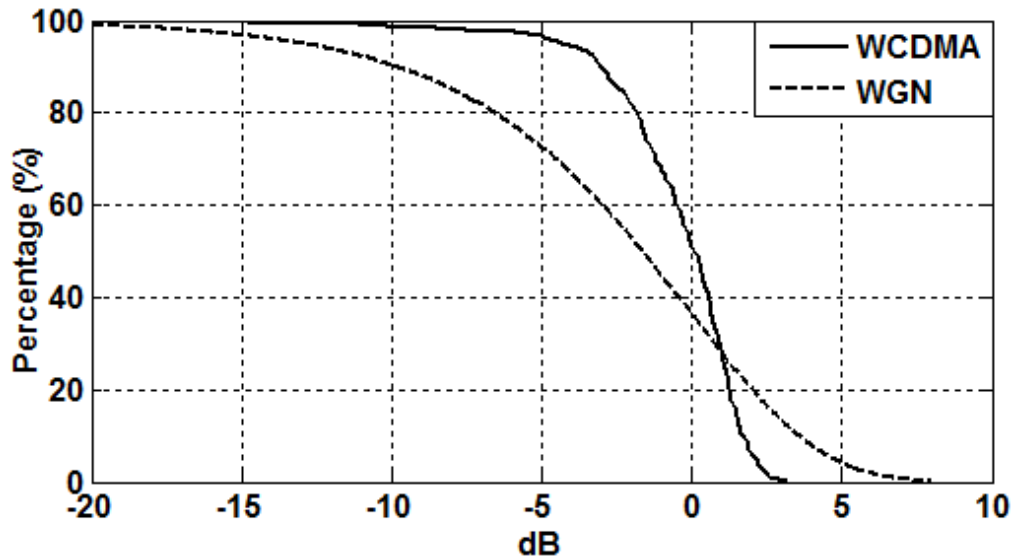


Figure 3-28 CCDF characteristics of WCDMA signal and WGN

Envelope peak to average power ratio of WCDMA signal is 3.228 dB. This value is considerably low when compared to the crest factor of WGN, which is approximately 8 dB. CCDF of WGN performs a smooth characteristics, on the other hand, CCDF of WCDMA signal is very steep. When CCDF of WCDMA signal is examined, it is seen that encounter rate of samples with more than 0 dB PAPR is 50%. Furthermore, encounter rate of samples with more than 2 dB PAPR is 5.5%. This steep characteristic of WCDMA signal indicates that although PAPR is low, it will not be possible to represent the CCDF characteristics of WCDMA with few tones, which will be discussed in detail later.

Second signal that will be modeled is a digitally modulated RF signal. It has the modulation characteristics of a base station CDMA signal. CDMA technique permits several users communicate simultaneously over the same bandwidth. To achieve this, a pseudo random code (orthogonal spreading factor) is assigned to each user and information data modulates the pseudo random code. After modulation of the resulting signal with a carrier, it is broadcasted. During the reception, same despreading factors are applied to received sum signal. By this way, signal from all other participants in the system appears as noise for the relevant user's receiver. One of the most important properties of the CDMA signal is that it has high peak to average ratio. CDMA signal that will be used during the envelope simulations is implemented by interpolating data from a stored data file which is generated by

Agilent ESG series signal generator. This CDMA signal has 1.2288 MHz channel bandwidth. To simulate the source properly and to prevent data interpolation between data samples, it is important to make simulation time step equal to $0.25/1.2288$ MHz, in other words, taking four samples per bit. Recommended controller setup provided by Agilent is shown in Figure 3-29.

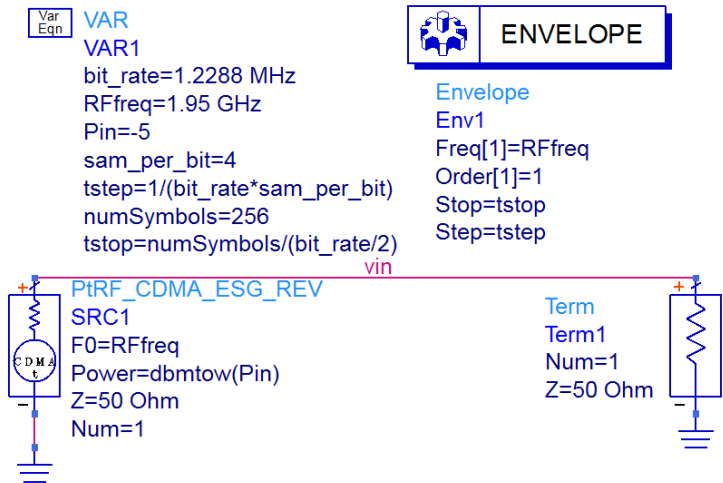


Figure 3-29 RF carrier modulated by a CDMA signal and its properties

After arranging the envelope simulation settings, spectrum of the input and output carrier are obtained as in Figure 3-30. Spectral regrowth in adjacent and alternate channels are clearly observed. Channel bandwidth is 1.2288 MHz as specified in the settings.

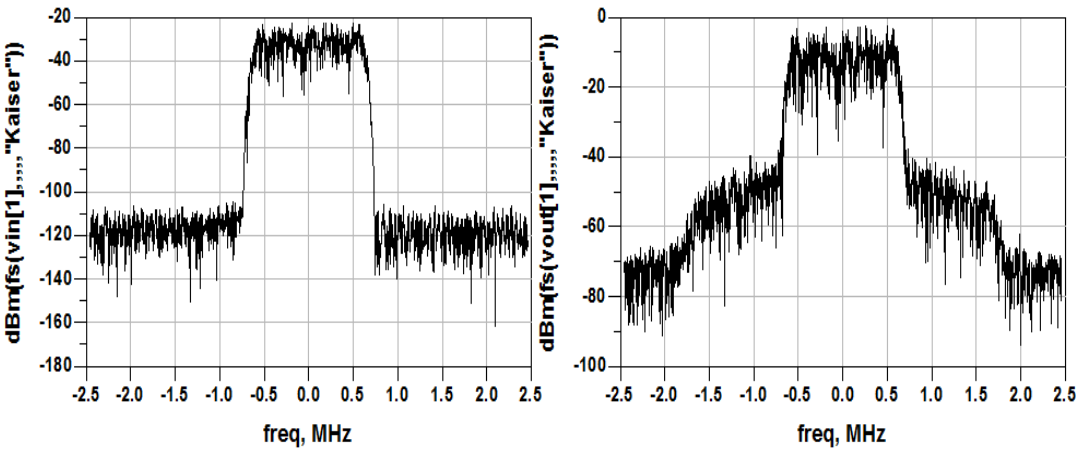


Figure 3-30 Spectrum of the input (left) and output (right) carrier for CDMA signal

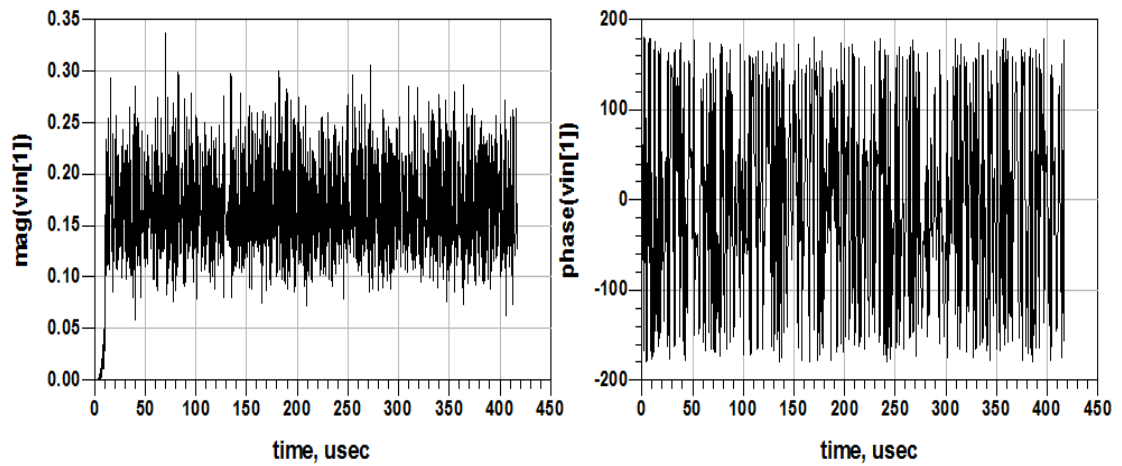


Figure 3-31 Magnitude (left) and phase (right) of the input carrier for Fwd Link CDMA signal.

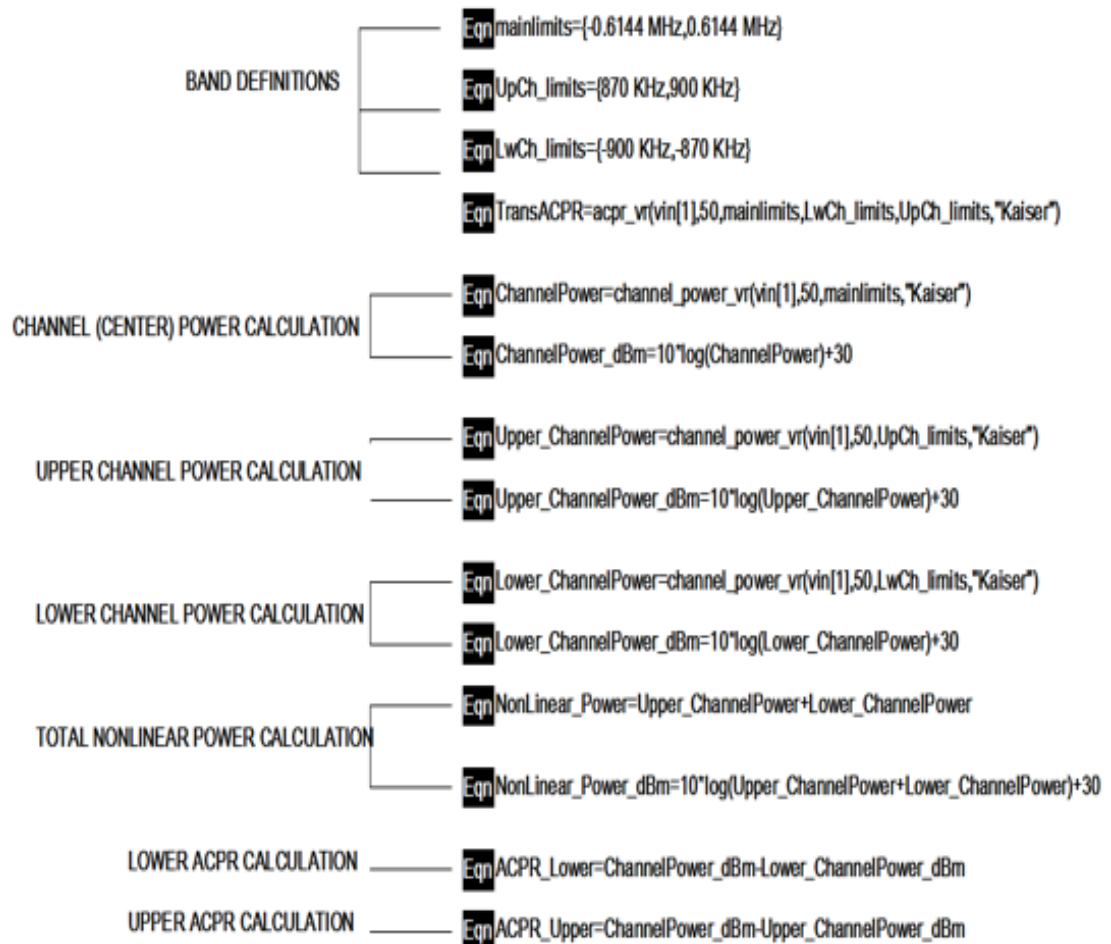


Figure 3-32 Main, upper, lower channel band definitions and measurement equations for channel power calculations

ChannelPower_dBm	Upper_ChannelPower_dBm	Lower_ChannelPower_dBm
-5.027	-111.875	-104.264
ACPR_Lower	ACPR_Upper	NonLinear_Power_dBm
99.237	106.848	-103.569

Figure 3-33 Simulated band characteristics of input CDMA signal

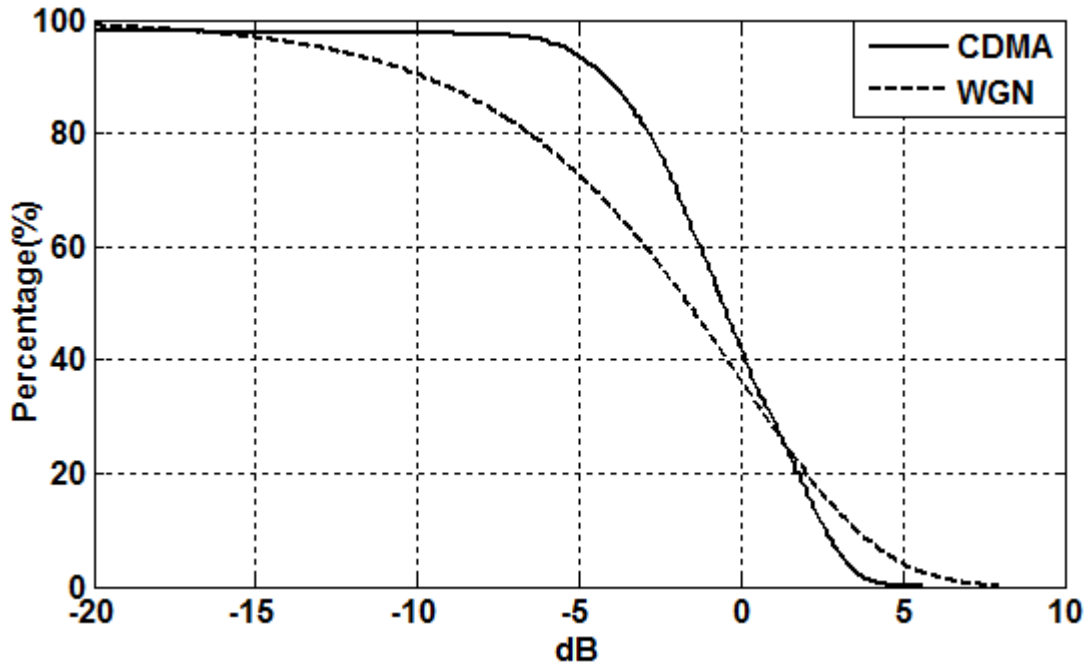


Figure 3-34 CCDF characteristics of CDMA signal and WGN

Envelope peak to average power ratio of CDMA signal is 5.628 dB, which is lower than the peak to average ratio of WGN (8 dB). However CCDF curve of CDMA signal exhibits steeper characteristics than that of WGN. The CCDF curve in Figure 3-34 implies that encounter rate of samples with more than 4 dB PAPR is about 0.9% and encounter rate of samples with more than 5 dB PAPR is 0.05%, which is very rare. Hence, it could be deduced that although peak to average ratio is high, peak occurrence rate is rare for the CDMA signal.

CHAPTER 4

VERIFICATION OF MULTI-TONE MODELS WITH AMPLIFIERS

In this part of the thesis, multi-tone models will be presented for the communication signals introduced in previous part. First signal that will be modeled is WCDMA signal. It has a bandwidth of 3.84 MHz. This signal has maximum envelope peak to average ratio of 3.228 dB, which is not very high for a multi user communication signal. To model this signal 3-tone, 5-tone, 7-tone and 9-tone models with variable tone spacing, amplitude and phase will be used. The purpose of using 3, 5, 7 and 9 tones signals is to show that with increasing number of tones better representations could be obtained. Here, using odd number of tones doesn't have a specific meaning. To emphasize the effect of number of tones on modeling clearly, number of tones is increased by two. Then, WCDMA signal and multi-tone signal are applied to a nonlinear power amplifier model in ADS, whose parameters are obtained from measurements of Mini-Circuits GVA-63+ demo board. Results are discussed in detail. Next, WCDMA signal and multi-tone models are applied to second amplifier whose parameters are obtained from Mini-Circuits PMA-545G1+ demo board. Purpose is to show that validity of the model signals are independent of the amplifier properties. Second signal that will be modeled is a CDMA signal. Its crest factor is 5.628 dB. CDMA signal is modeled with 5-tone, 7-tone and 9-tone signals. Using odd number of tones for models doesn't have a specific meaning. It is just to emphasize the effect of number of tones on modeling more clearly. Next, multi-tone signals and CDMA signal are applied to a nonlinear amplifier. Strong sides of each model are depicted. Similar to WCDMA case, CDMA signal and its models are also applied to a second amplifier to show that validity of the model signals doesn't depend on amplifier properties.

4.1 Multi-Tone Models for WCDMA Signal

In this part, a 3-tone, 5-tone, 7-tone and 9-tone models are developed to characterize a WCDMA signal with certain statistical and channel properties. To find the coefficients of the tones, channel power, channel bandwidth, CCDF curve and nonlinear parameters K, F, M are considered. Results for each model are discussed, compared and strong sides of the different models are expressed with reasoning.

4.1.1 3-Tone Model for WCDMA signal

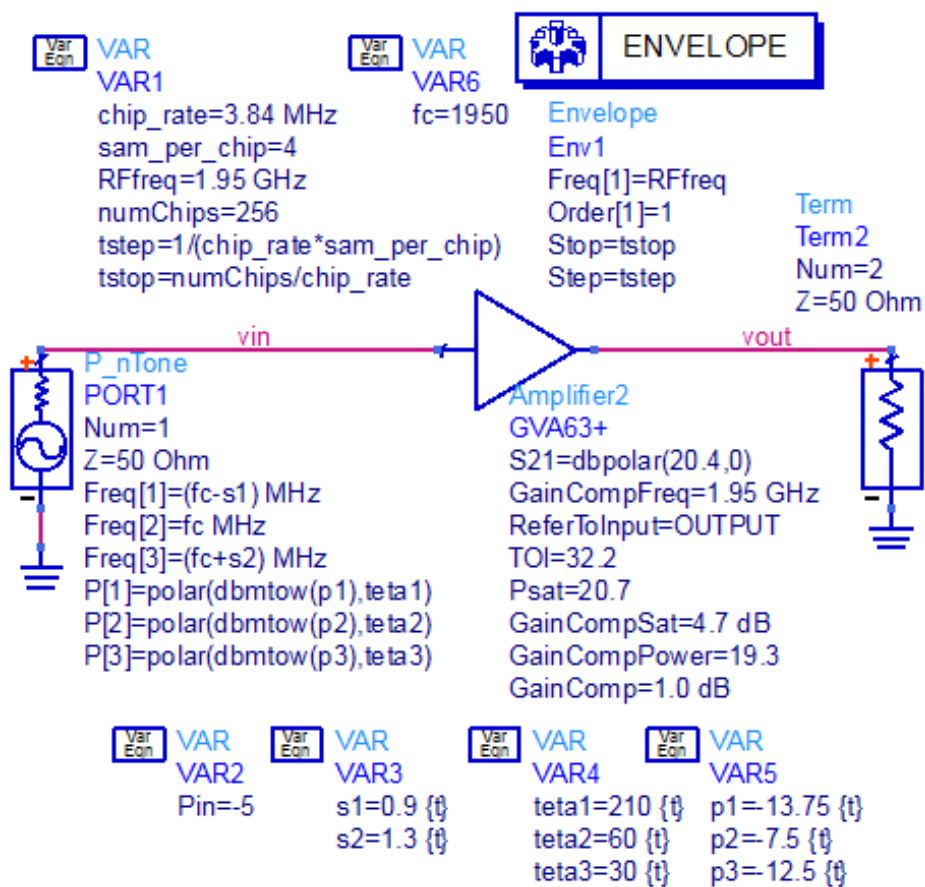


Figure 4-1 3-tone model schematic prepared in ADS

As seen in Figure 4-1, power of the tones are -13.75, -7.5, -12.5 dBm and phase coefficients are 210, 60, 30 degrees. One tone is placed 0.9 MHz left of the center tone and the other is placed 1.3 MHz right of the center tone.

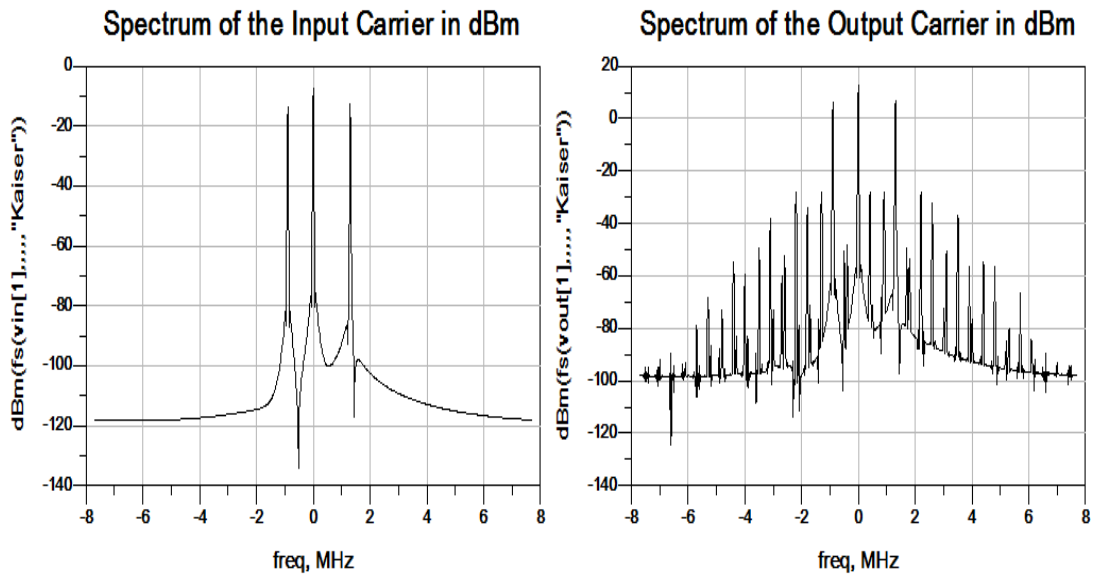


Figure 4-2 Baseband spectrum of 3-tone model (left) and amplified (with GVA-63+ amplifier) 3-tone model (right)

From Figure 4-2, it is possible to observe distorted output signal with in-band and out of band components. As the input drive level increases, in-band and out of band products become more significant at the output.

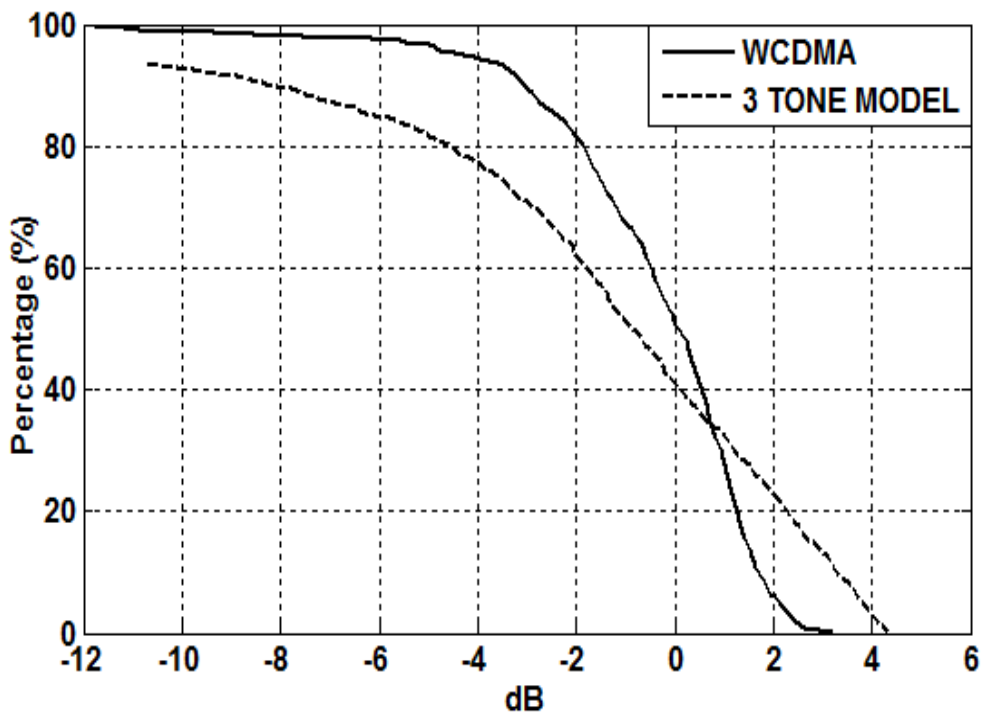


Figure 4-3 CCDF curves of 3-tone model and WCDMA signal

From Figure 4-3, 3-tone model has crest factor of 4.309 dB, whereas WCDMA signal has crest factor of 3.228 dB. Moreover CCDF curve of 3-tone model does not

approach the CCDF curve of WCDMA signal. This implies that number of samples specific amount above the average power level is different for two signals. From Table 4-1 and Table 4-2, it could be concluded that although 3-tone model represents WCDMA signal in terms of channel power, K and M parameters correctly, parameter F, which is related to the out of band products, is higher for the 3-tone model. Moreover, channel bandwidth of 3-tone model is narrower than channel bandwidth of WCDMA signal. Table 4-1 and Table 4-2 also show that 3-tone Model is valid in terms of channel power, K and M parameters for different input power levels. Figure 4-4 is a histogram showing the distribution of instantaneous nonlinear power for WCDMA signal and its 3-tone model. Histogram shows that number of samples for low level and high level of S are different for two signals.

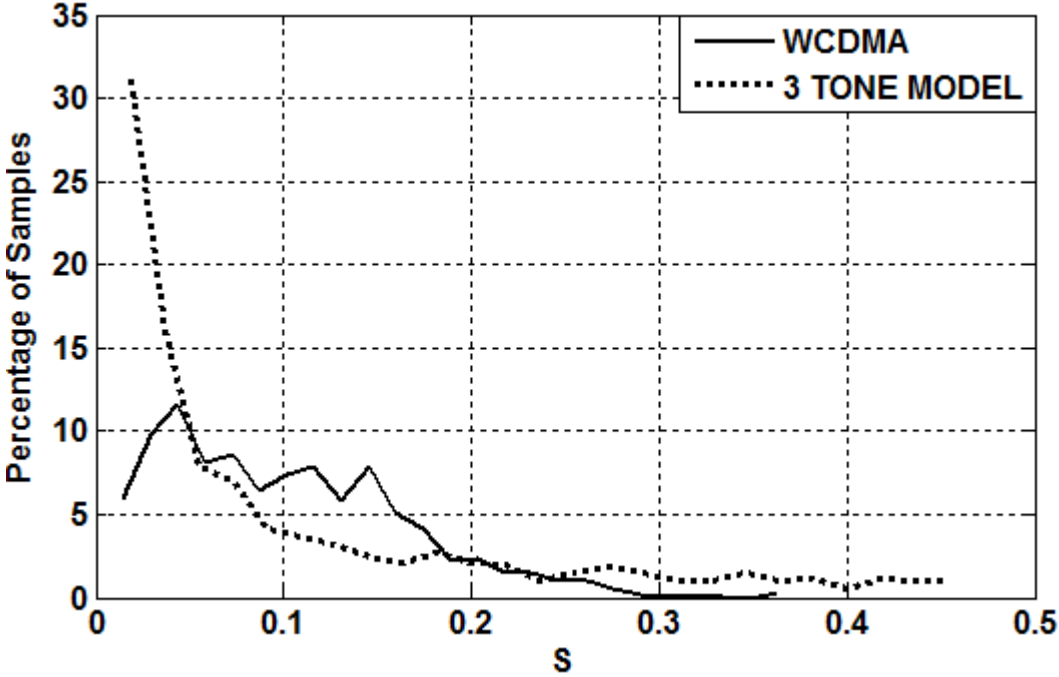


Figure 4-4 The distribution of instantaneous nonlinear power for WCDMA signal and its 3-tone model

Table 4-1 WCDMA parameters for different drive levels of GVA-63+

Pin		INPUT_ChannelPower_dBm	OUTPUT_ChannelPower_dBm			
	-10.000	-9.960				10.100
	-9.000	-8.960				11.081
	-8.000	-7.960				12.056
	-7.000	-6.960				13.023
	-6.000	-5.960				13.978
	-5.000	-4.960				14.916
	-4.000	-3.960				15.828
	-3.000	-2.960				16.699
	-2.000	-1.960				17.495
	-1.000	-0.960				18.169
	0.000	0.040				18.693
	1.000	1.040				19.074
	2.000	2.040				19.358
	3.000	3.040				19.577
	4.000	4.040				19.752
	5.000	5.040				19.894
Pin	M	K	F	Input_Crest_Factor	Output_Crest_Factor	
-10.000	0.009	9.695	88.072	3.228	3.166	
-9.000	0.015	15.365	175.727	3.228	3.146	
-8.000	0.024	24.352	350.621	3.228	3.119	
-7.000	0.038	38.595	699.580	3.228	3.079	
-6.000	0.060	61.167	1.396E3	3.228	3.019	
-5.000	0.095	96.942	2.785E3	3.228	2.927	
-4.000	0.150	153.638	5.557E3	3.228	2.784	
-3.000	0.238	243.492	1.109E4	3.228	2.426	
-2.000	0.377	385.893	2.212E4	3.228	2.049	
-1.000	0.597	611.568	4.414E4	3.228	1.734	
0.000	0.946	969.208	8.807E4	3.228	1.285	
1.000	1.500	1535.968	1.757E5	3.228	0.928	
2.000	2.377	2434.102	3.506E5	3.228	0.690	
3.000	3.767	3857.310	6.996E5	3.228	0.604	
4.000	5.969	6112.474	1.396E6	3.228	0.597	
5.000	9.459	9685.749	2.785E6	3.228	0.640	

Table 4-2 3-tone model parameters for different drive levels of GVA-63+

Pin		INPUT_ChannelPower_dBm	OUTPUT_ChannelPower_dBm			
	-10.000	-10.317				9.732
	-9.000	-9.317				10.709
	-8.000	-8.317				11.679
	-7.000	-7.317				12.638
	-6.000	-6.317				13.581
	-5.000	-5.317				14.500
	-4.000	-4.317				15.383
	-3.000	-3.317				16.188
	-2.000	-2.317				16.889
	-1.000	-1.317				17.498
	0.000	-0.317				18.020
	1.000	0.683				18.457
	2.000	1.683				18.818
	3.000	2.683				19.113
	4.000	3.683				19.355
	5.000	4.683				19.553
Pin	M	K	F	Input_Crest_Factor	Output_Crest_Factor	
-10.000	0.010	9.731	112.696	4.309	4.242	
-9.000	0.015	15.422	224.858	4.309	4.220	
-8.000	0.024	24.440	448.650	4.309	4.189	
-7.000	0.038	38.732	895.174	4.309	4.144	
-6.000	0.060	61.378	1.786E3	4.309	4.076	
-5.000	0.095	97.263	3.564E3	4.309	3.970	
-4.000	0.151	154.122	7.111E3	4.309	3.798	
-3.000	0.238	244.208	1.419E4	4.309	3.397	
-2.000	0.378	386.927	2.831E4	4.309	3.016	
-1.000	0.599	613.004	5.648E4	4.309	2.650	
0.000	0.948	971.082	1.127E5	4.309	2.203	
1.000	1.502	1538.136	2.249E5	4.309	1.859	
2.000	2.379	2435.941	4.486E5	4.309	1.639	
3.000	3.767	3857.050	8.952E5	4.309	1.528	
4.000	5.963	6105.757	1.786E6	4.309	1.435	
5.000	9.436	9662.590	3.564E6	4.309	1.268	

Table 4-3 WCDMA parameters for different drive levels of PMA-545G1+

Pin		INPUT_ChannelPower_dBm			OUTPUT_ChannelPower_dBm	
	-15.000			-14.960		11.006
	-14.000			-13.960		11.993
	-13.000			-12.960		12.978
	-12.000			-11.960		13.960
	-11.000			-10.960		14.942
	-10.000			-9.960		15.921
	-9.000			-8.960		16.900
	-8.000			-7.960		17.875
	-7.000			-6.960		18.841
	-6.000			-5.960		19.777
	-5.000			-4.960		20.622
	-4.000			-3.960		21.311
	-3.000			-2.960		21.824
	-2.000			-1.960		22.193
	-1.000			-0.960		22.469
	0.000			0.040		22.685
Pin	M	K	F	Input_Crest_Factor	Output_Crest_Factor	
-15.000	0.013	13.199	132.690	3.228	3.186	
-14.000	0.020	20.919	264.751	3.228	3.181	
-13.000	0.032	33.155	528.248	3.228	3.175	
-12.000	0.051	52.547	1.054E3	3.228	3.171	
-11.000	0.081	83.281	2.103E3	3.228	3.166	
-10.000	0.129	131.992	4.196E3	3.228	3.160	
-9.000	0.204	209.192	8.372E3	3.228	3.146	
-8.000	0.324	331.545	1.670E4	3.228	3.109	
-7.000	0.513	525.460	3.333E4	3.228	2.917	
-6.000	0.813	832.790	6.650E4	3.228	2.486	
-5.000	1.289	1319.870	1.327E5	3.228	2.137	
-4.000	2.043	2091.826	2.648E5	3.228	1.777	
-3.000	3.238	3315.265	5.282E5	3.228	1.253	
-2.000	5.131	5254.233	1.054E6	3.228	0.905	
-1.000	8.132	8327.180	2.103E6	3.228	0.725	
0.000	12.888	13197.260	4.196E6	3.228	0.583	

Table 4-4 3-tone model parameters for different drive levels of PMA-545G1+

Pin		INPUT_ChannelPower_dBm			OUTPUT_ChannelPower_dBm	
	-15.000			-15.317		10.643
	-14.000			-14.317		11.629
	-13.000			-13.317		12.613
	-12.000			-12.317		13.596
	-11.000			-11.317		14.577
	-10.000			-10.317		15.557
	-9.000			-9.317		16.533
	-8.000			-8.317		17.500
	-7.000			-7.317		18.433
	-6.000			-6.317		19.256
	-5.000			-5.317		19.978
	-4.000			-4.317		20.600
	-3.000			-3.317		21.128
	-2.000			-2.317		21.570
	-1.000			-1.317		21.931
	0.000			-0.317		22.223
Pin	M	K	F	Input_Crest_Factor	Output_Crest_Factor	
-15.000	0.013	13.251	169.788	4.309	4.266	
-14.000	0.021	21.001	338.772	4.309	4.260	
-13.000	0.033	33.285	675.939	4.309	4.255	
-12.000	0.052	52.752	1.349E3	4.309	4.250	
-11.000	0.082	83.604	2.691E3	4.309	4.246	
-10.000	0.129	132.501	5.369E3	4.309	4.239	
-9.000	0.205	209.993	1.071E4	4.309	4.221	
-8.000	0.325	332.804	2.138E4	4.309	4.174	
-7.000	0.515	527.432	4.265E4	4.309	4.014	
-6.000	0.816	835.873	8.510E4	4.309	3.473	
-5.000	1.294	1324.666	1.698E5	4.309	3.144	
-4.000	2.050	2099.251	3.388E5	4.309	2.719	
-3.000	3.249	3326.681	6.759E5	4.309	2.204	
-2.000	5.148	5271.623	1.349E6	4.309	1.874	
-1.000	8.158	8353.343	2.691E6	4.309	1.653	
0.000	12.926	13235.932	5.369E6	4.309	1.580	

Table 4-3 and Table 4-4 are obtained for the same signals applied to a different amplifier. From the tables, it is clear that output channel power, K and M parameters are still comparable for WCDMA and its 3-tone model for different input drive levels. This shows that model validity doesn't depend on the amplifier characteristics. In short, 3-tone model represents the WCDMA well enough in terms channel power, parameter K and M. When CCDF, distribution of instantaneous nonlinear power, channel bandwidth and parameter F are taken account, it could be said that better representative multi-tones could be found with increasing number of tones. Furthermore, it is important to emphasize that this is not the only 3-tone model for WCDMA signal. There could be other 3-tone models with different amplitude, phase and tone spacing that represent the WCDMA signal closely, maybe better than the presented 3-tone model in terms of some of the parameters mentioned above.

4.1.2 5-Tone Model for WCDMA signal

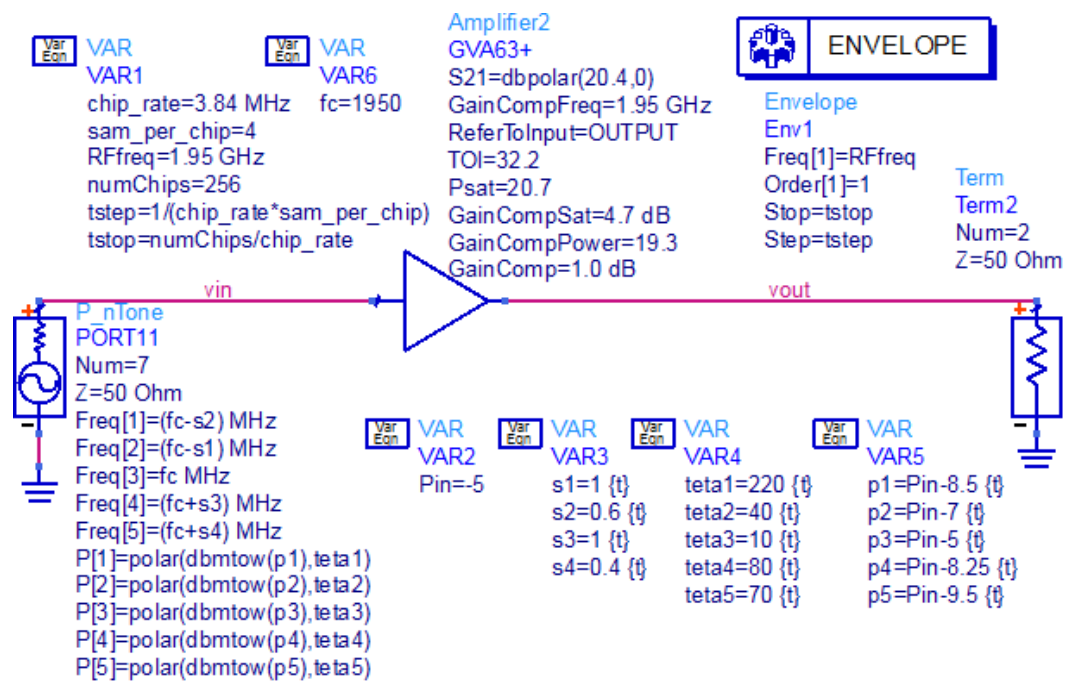


Figure 4-5 5-tone model schematic prepared in ADS

From Figure 4-5, power of the tones are -13.5 dBm, -12 dBm, -10 dBm, -13.25 dBm, -14.5 dBm, and phase coefficients are 220, 40, 10, 80, 70 degrees. Two of the tones are placed 0.6 and 1 MHz left of the center tone and other two tones are placed 0.4

and 1 MHz right of the center tone. Tones are placed in such a way that all of the tones fall in to the 3.84 MHz channel bandwidth.

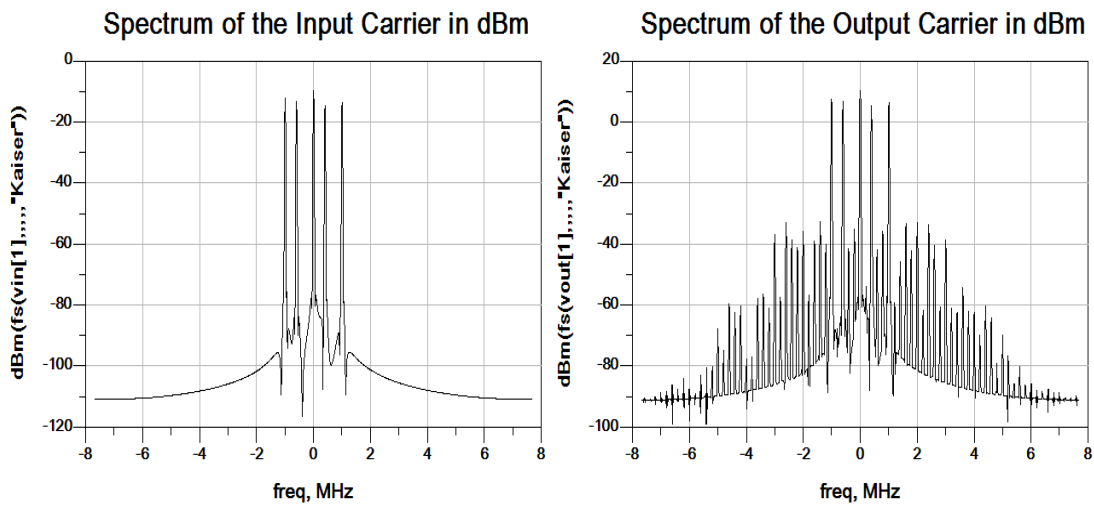


Figure 4-6 Baseband spectrum of 5-tone model (left) and amplified (with GVA-63+ amplifier) 5-tone model (right)

From Figure 4-6, it is clear that channel bandwidth of the 5-tone model is narrower than channel bandwidth of WCDMA signal. From Figure 4-6, it is also possible to observe distorted output signal with in-band and out-of-band components. As the input drive level increases, in-band and out of band products become more significant at the output.

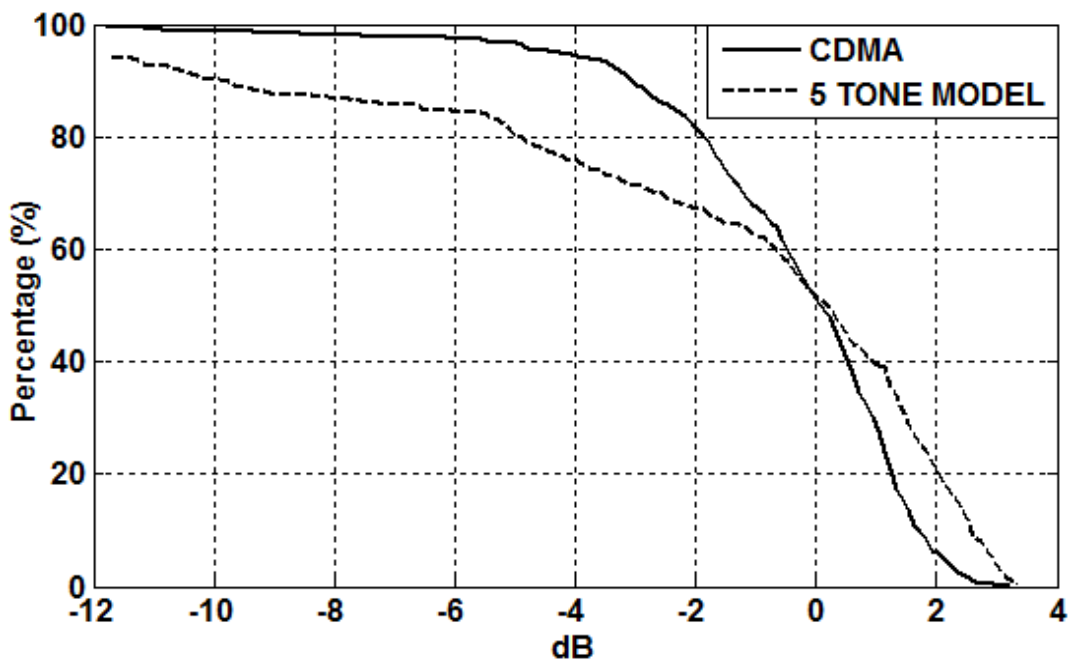


Figure 4-7 CCDF curves of 5-tone model and WCDMA signal

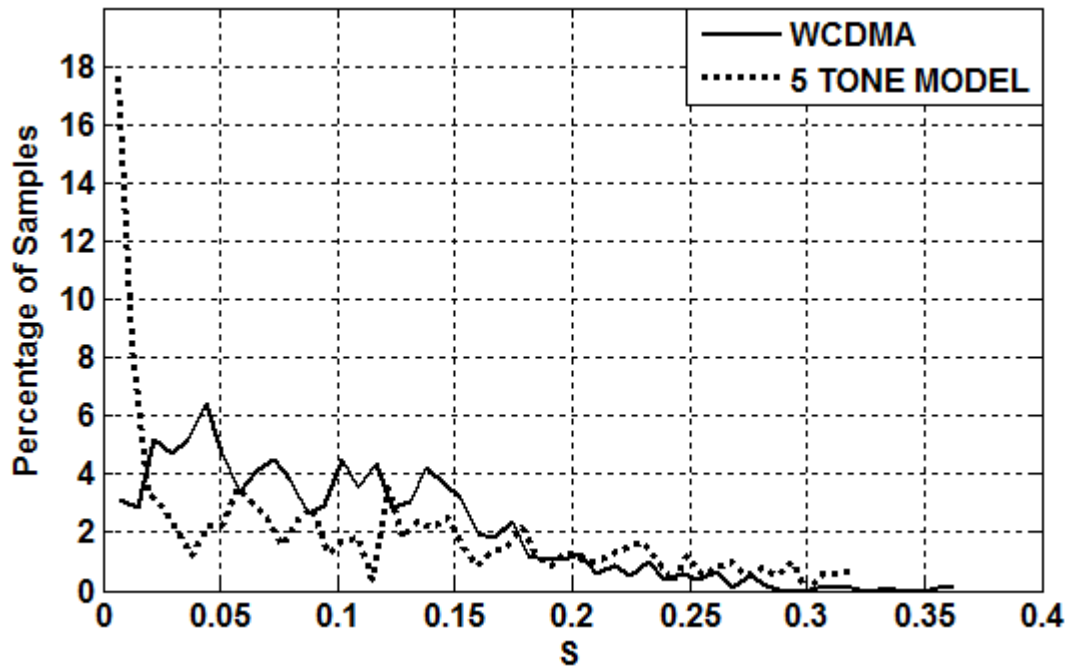


Figure 4-8 The distribution of instantaneous nonlinear power of WCDMA signal and its 5-tone model

From Figure 4-7, crest factor of 5-tone model (3.326 dB) and crest factor of WCDMA signal (3.228 dB) are very close to each other. Moreover, CCDF curve of 5-tone model shows better characteristic than that of the 3-tone model, however CCDF curves are still not close enough to each other. In Figure 4-8, distribution of nonlinear term S is plotted for WCDMA and 5-tone model. Distribution of term S for 5-tone model shows better characteristic than that of the 3-tone model. However for very low values of S, WCDMA and 5-tone model nonlinear term distribution are still different.

Table 4-5 5-tone model parameters for different drive levels of GVA-63+

Pin		INPUT_ChannelPower_dBm	OUTPUT_ChannelPower_dBm			
	-10.000	-10.097				9.956
	-9.000	-9.097				10.935
	-8.000	-8.097				11.907
	-7.000	-7.097				12.870
	-6.000	-6.097				13.818
	-5.000	-5.097				14.747
	-4.000	-4.097				15.644
	-3.000	-3.097				16.489
	-2.000	-2.097				17.227
	-1.000	-1.097				17.840
	0.000	-0.097				18.337
	1.000	0.903				18.718
	2.000	1.903				19.000
	3.000	2.903				19.220
	4.000	3.903				19.404
	5.000	4.903				19.560
Pin	M	K	F	Input_Crest_Factor	Output_Crest_Factor	
-10.000	0.010	9.731	99.238	3.326		3.280
-9.000	0.015	15.423	198.006	3.326		3.266
-8.000	0.024	24.444	395.074	3.326		3.246
-7.000	0.038	38.742	788.277	3.326		3.218
-6.000	0.060	61.404	1.573E3	3.326		3.175
-5.000	0.095	97.322	3.138E3	3.326		3.110
-4.000	0.151	154.250	6.262E3	3.326		3.008
-3.000	0.239	244.482	1.249E4	3.326		2.791
-2.000	0.378	387.502	2.493E4	3.326		2.452
-1.000	0.600	614.197	4.974E4	3.326		2.136
0.000	0.951	973.534	9.924E4	3.326		1.892
1.000	1.507	1543.142	1.980E5	3.326		1.546
2.000	2.389	2446.110	3.951E5	3.326		1.355
3.000	3.787	3877.623	7.883E5	3.326		1.258
4.000	6.003	6147.246	1.573E6	3.326		1.227
5.000	9.518	9746.062	3.138E6	3.326		1.212

Similar to 3-tone model, 5-tone model also has very close channel power, K and M values as shown in Table 4-5. Moreover, parameter F shows an improvement when compared to that of the 3-tone model. When Table 4-5 is compared with Table 4-1, it is clear that modeling is valid for all input drive levels.

Table 4-6 5-tone model parameters for different drive levels of PMA-545G1+

Pin		INPUT_ChannelPower_dBm	OUTPUT_ChannelPower_dBm			
	-15.000	-15.097				10.864
	-14.000	-14.097				11.850
	-13.000	-13.097				12.835
	-12.000	-12.097				13.817
	-11.000	-11.097				14.798
	-10.000	-10.097				15.777
	-9.000	-9.097				16.754
	-8.000	-8.097				17.727
	-7.000	-7.097				18.687
	-6.000	-6.097				19.581
	-5.000	-5.097				20.340
	-4.000	-4.097				20.974
	-3.000	-3.097				21.469
	-2.000	-2.097				21.839
	-1.000	-1.097				22.107
	0.000	-0.097				22.325
Pin	M	K	F	Input_Crest_Factor	Output_Crest_Factor	
-15.000	0.013	13.248	149.513	3.326		3.295
-14.000	0.021	20.997	298.318	3.326		3.290
-13.000	0.032	33.277	595.222	3.326		3.286
-12.000	0.052	52.741	1.188E3	3.326		3.282
-11.000	0.082	83.590	2.370E3	3.326		3.279
-10.000	0.129	132.482	4.728E3	3.326		3.276
-9.000	0.205	209.970	9.434E3	3.326		3.269
-8.000	0.325	332.783	1.882E4	3.326		3.248
-7.000	0.515	527.431	3.756E4	3.326		3.194
-6.000	0.816	835.932	7.493E4	3.326		2.855
-5.000	1.294	1324.884	1.495E5	3.326		2.509
-4.000	2.051	2099.840	2.983E5	3.326		2.262
-3.000	3.250	3328.103	5.952E5	3.326		1.863
-2.000	5.151	5274.850	1.188E6	3.326		1.568
-1.000	8.164	8360.400	2.370E6	3.326		1.372
0.000	12.940	13250.995	4.728E6	3.326		1.282

When Table 4-6 is compared with Table 4-3, it is observed that for all input drive levels, channel power, crest factor, K and M parameters have very similar values, which shows modeling is independent of the amplifier properties. It could be concluded that 5-tone model is superior to the 3-tone model when peak to average ratio, parameter F and distribution of instantaneous nonlinear power are considered. Furthermore, presented 5-tone model is not unique. Different 5-tone models presenting similar performance or better representative 5-tone models for some of the parameters mentioned above could be found.

4.1.3 7-Tone Model for WCDMA signal

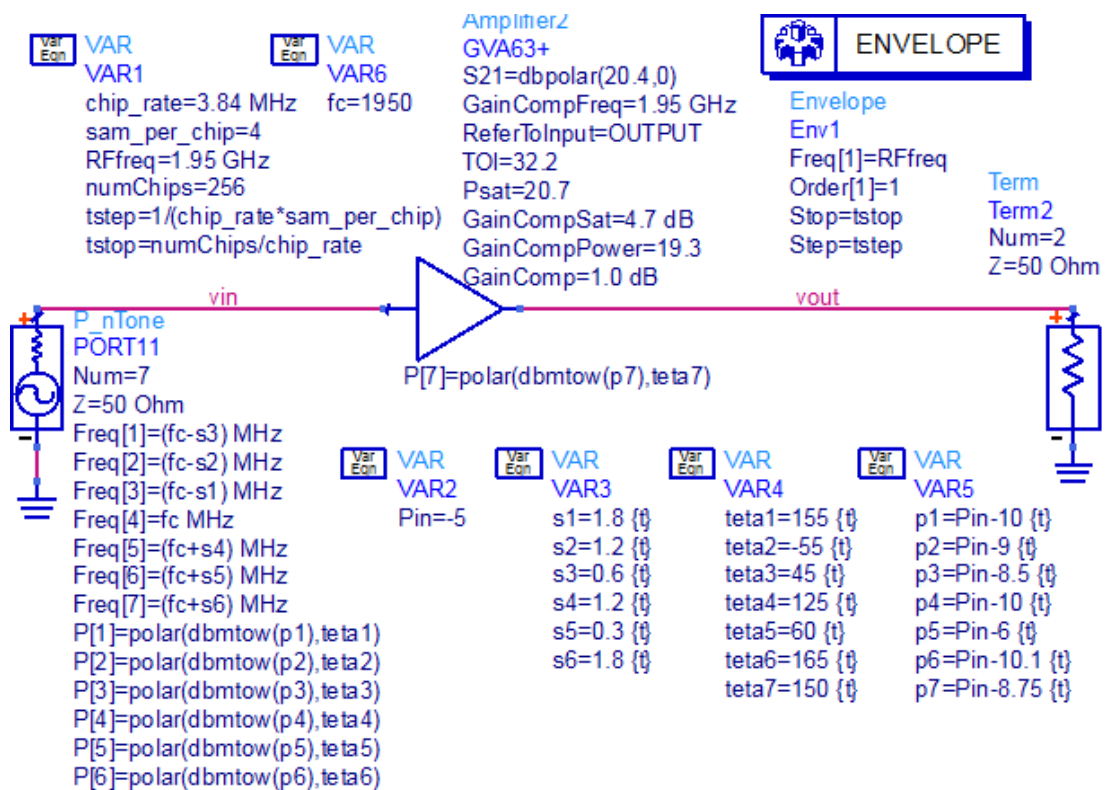


Figure 4-9 7-tone Model schematic prepared in ADS

From Figure 4-9, power of the tones are -15 dBm, -14 dBm, -13.5 dBm, -15 dBm, -11 dBm, -15.1 dBm, -13.75 dBm and phase coefficients are 155, -55, 45, 125, 60, 165 and 150 degrees. Three of the tones are placed 1.8, 1.2 and 0.6 MHz left of the center tone and other three tones are placed 0.3, 1.2 and 1.8 MHz right of the center tone. Tones are placed in such a way that all of the tones fall in to the 3.84 MHz channel bandwidth.

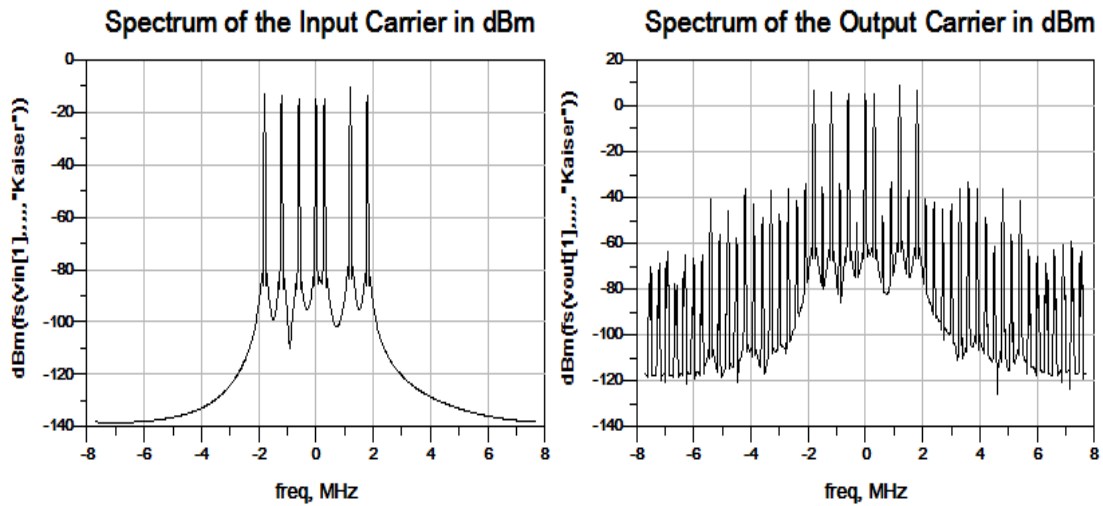


Figure 4-10 Baseband spectrum of 7-tone signal (left) and amplified (with GVA-63+ amplifier) 7-tone signal (right)

From Figure 4-10, it is possible to observe distorted output signal with in-band and out of band components. As the input drive level increases, in-band and out of band products become more significant at the output. It is also important to note that 7-tone model represents the channel bandwidth of WCDMA signal better. 7-tone model presented here has a channel bandwidth of 3.6 MHz which is close to 3.84 MHz.

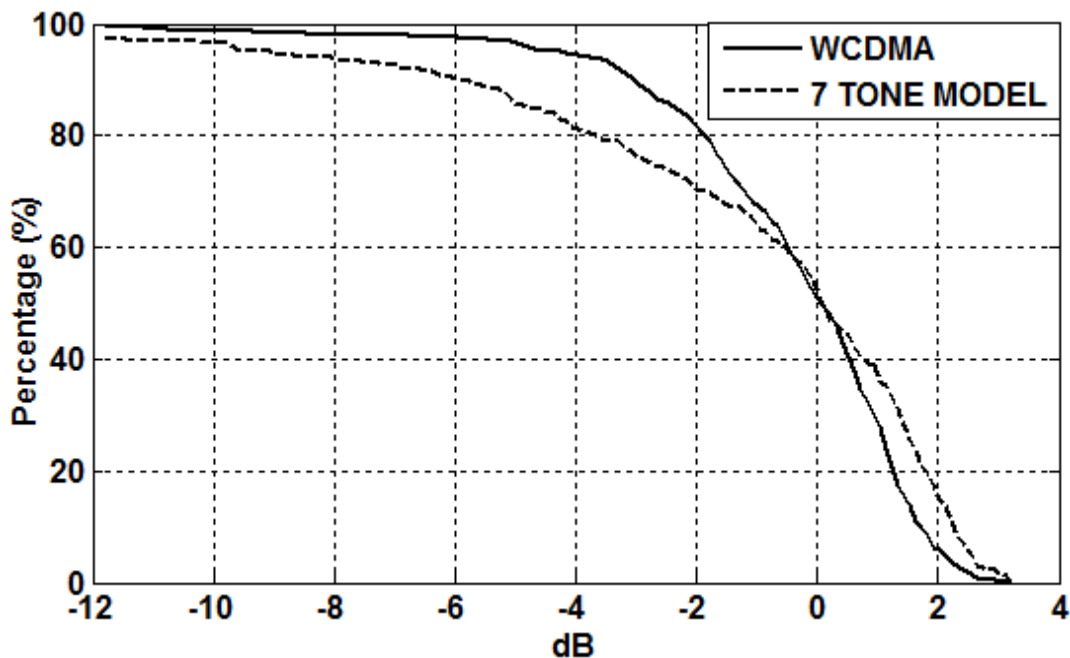


Figure 4-11 CCDF curves of 7-tone model and WCDMA signal

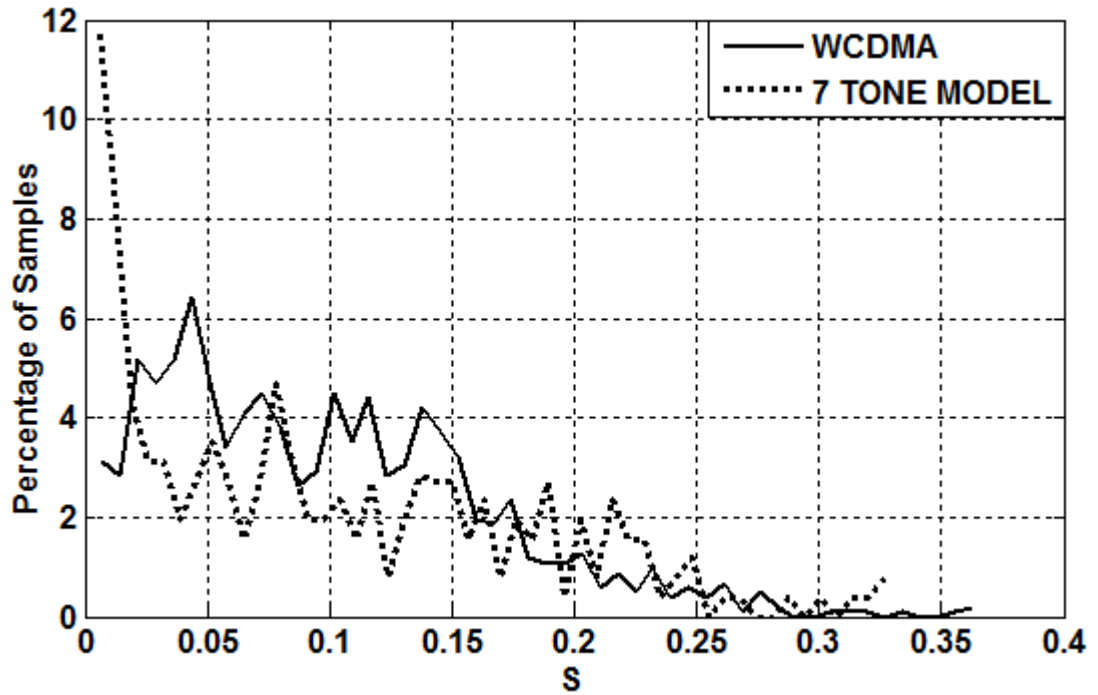


Figure 4-12 The distribution of instantaneous nonlinear power of WCDMA signal and its 7-tone model

As shown in the figure, crest factor of 7-tone model (3.224 dB) and crest factor of WCDMA signal (3.228 dB) are very close to each other. Moreover, CCDF curve of 7-tone model shows better characteristic than that of the 5-tone model. 7-tone model and WCDMA CCDF curves come closer to each other, but curves are still distinct. In Figure 4-12, distribution of nonlinear term S is plotted for WCDMA and 7-tone model. Distribution of term S for 7-tone model shows better characteristic than that of the 5-tone model. For very low values of S , there is clearly an improvement with respect to 5-tone model.

Table 4-7 7-tone model parameters for different drive levels of GVA-63+

Pin		INPUT_ChannelPower_dBm			OUTPUT_ChannelPower_dBm	
	-10.000			-9.955		10.101
	-9.000			-8.955		11.081
	-8.000			-7.955		12.054
	-7.000			-6.955		13.018
	-6.000			-5.955		13.970
	-5.000			-4.955		14.902
	-4.000			-3.955		15.805
	-3.000			-2.955		16.660
	-2.000			-1.955		17.425
	-1.000			-0.955		18.057
	0.000			0.045		18.553
	1.000			1.045		18.930
	2.000			2.045		19.226
	3.000			3.045		19.463
	4.000			4.045		19.654
	5.000			5.045		19.810
Pin	M	K	F	Input_Crest_Factor	Output_Crest_Factor	
-10.000	0.010	9.729	95.300	3.224	3.174	
-9.000	0.015	15.420	190.148	3.224	3.158	
-8.000	0.024	24.439	379.396	3.224	3.136	
-7.000	0.038	38.734	756.994	3.224	3.104	
-6.000	0.060	61.391	1.510E3	3.224	3.057	
-5.000	0.095	97.300	3.014E3	3.224	2.985	
-4.000	0.151	154.215	6.013E3	3.224	2.872	
-3.000	0.239	244.423	1.200E4	3.224	2.597	
-2.000	0.378	387.403	2.394E4	3.224	2.261	
-1.000	0.600	614.027	4.776E4	3.224	2.005	
0.000	0.950	973.238	9.530E4	3.224	1.665	
1.000	1.506	1542.621	1.901E5	3.224	1.298	
2.000	2.388	2445.177	3.794E5	3.224	1.043	
3.000	3.785	3875.926	7.570E5	3.224	0.900	
4.000	6.000	6144.107	1.510E6	3.224	0.865	
5.000	9.512	9740.152	3.014E6	3.224	0.874	

Similar to 3-tone and 5-tone model, 7-tone model also has very close channel power, K and M values as shown in Table 4-7. Moreover, Parameter F shows an improvement and gets closer to F values calculated for WCDMA signal. When Table 4-7 is compared with Table 4-1, it is clear that modeling is valid for all input drive levels, as expected.

Table 4-8 7-tone model parameters for different drive levels of PMA-545G1+

Pin		INPUT_ChannelPower_dBm			OUTPUT_ChannelPower_dBm	
	-15.000			-14.955		11.009
	-14.000			-13.955		11.995
	-13.000			-12.955		12.979
	-12.000			-11.955		13.962
	-11.000			-10.955		14.943
	-10.000			-9.955		15.922
	-9.000			-8.955		16.900
	-8.000			-7.955		17.874
	-7.000			-6.955		18.837
	-6.000			-5.955		19.752
	-5.000			-4.955		20.547
	-4.000			-3.955		21.188
	-3.000			-2.955		21.675
	-2.000			-1.955		22.043
	-1.000			-0.955		22.338
	0.000			0.045		22.571
Pin	M	K	F	Input_Crest_Factor	Output_Crest_Factor	
-15.000	0.013	13.246	143.579	3.224	3.190	
-14.000	0.021	20.993	286.479	3.224	3.185	
-13.000	0.032	33.271	571.600	3.224	3.180	
-12.000	0.051	52.732	1.140E3	3.224	3.176	
-11.000	0.082	83.574	2.276E3	3.224	3.172	
-10.000	0.129	132.457	4.540E3	3.224	3.167	
-9.000	0.205	209.931	9.059E3	3.224	3.156	
-8.000	0.325	332.721	1.808E4	3.224	3.129	
-7.000	0.515	527.330	3.607E4	3.224	3.041	
-6.000	0.816	835.770	7.196E4	3.224	2.627	
-5.000	1.294	1324.621	1.436E5	3.224	2.334	
-4.000	2.050	2099.413	2.865E5	3.224	2.135	
-3.000	3.249	3327.405	5.716E5	3.224	1.645	
-2.000	5.150	5273.702	1.140E6	3.224	1.321	
-1.000	8.163	8358.494	2.276E6	3.224	1.083	
0.000	12.937	13247.802	4.540E6	3.224	0.916	

When Table 4-8 is compared with Table 4-3, it is observed that for all input drive levels, channel power, crest factor, K and M parameters have very similar values, which shows modeling is independent of the amplifier properties. To sum up, presented 7-tone model is superior to the 5-tone model in terms of CCDF curve, distribution of instantaneous nonlinear power and parameter F. 7-tone model presented here is not unique. It is possible to find 7-tone models that present comparable performance. Moreover, while obtaining the 7-tone model, phase coefficients and tone spacing are not arranged in a sensitive way. For example, in the tuning process of the phase coefficients, 5-degree step is used and in the tuning process of the tone spacing, 0.1 MHz frequency step is used. Hence, it may be possible to obtain better representative 7-tone models than the presented 7-tone model by decreasing the phase and frequency steps.

4.1.4 9-Tone Model for WCDMA signal

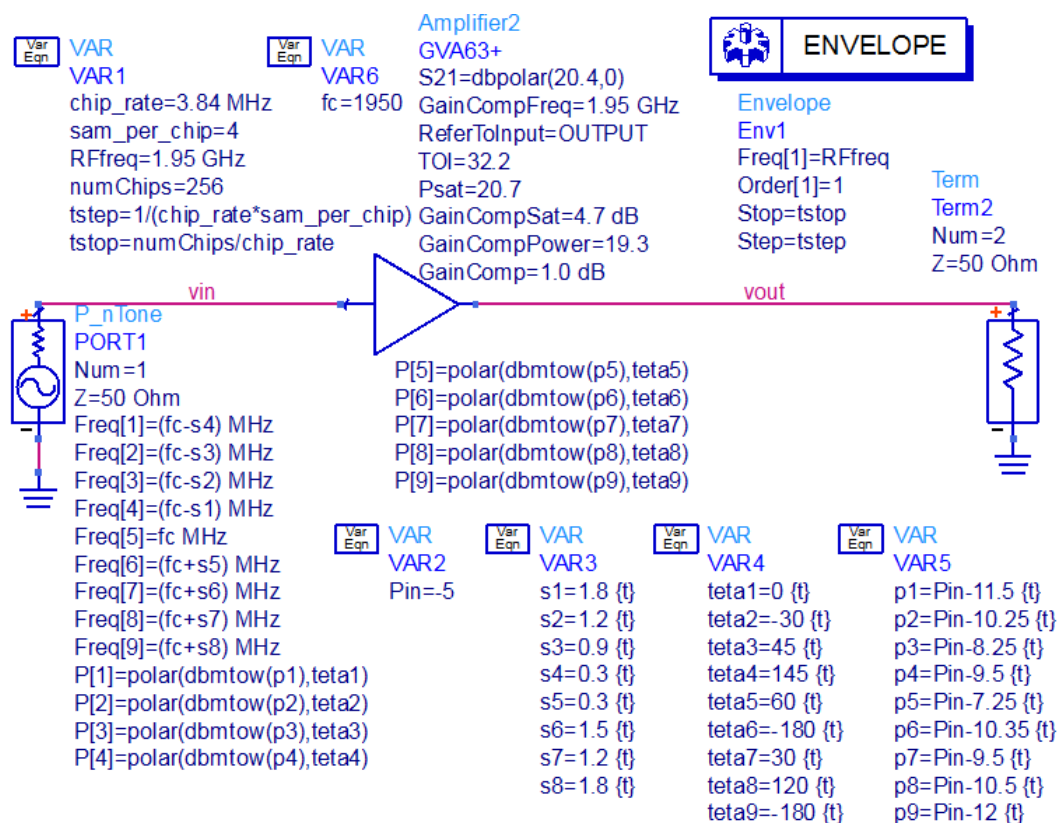


Figure 4-13 9-tone model schematic prepared in ADS

From Figure 4-13, power of the tones are -16.5 dBm, -15.25 dBm, -13.25 dBm, -14.5 dBm, -12.25 dBm, -15.35 dBm, -14.5 dBm, -15.5 dBm, -17 dBm and phase

coefficients are 0, -30, 45, 145, 60, -180, 30, 120 and -180 degrees. Four of the tones are placed 1.8, 1.2, 0.9 and 0.3 MHz left of the center tone and other four tones are placed 0.3, 1.5, 1.2 and 1.8 MHz right of the center tone. Tones are placed in such a way that all of the tones fall in to the 3.84 MHz channel bandwidth.

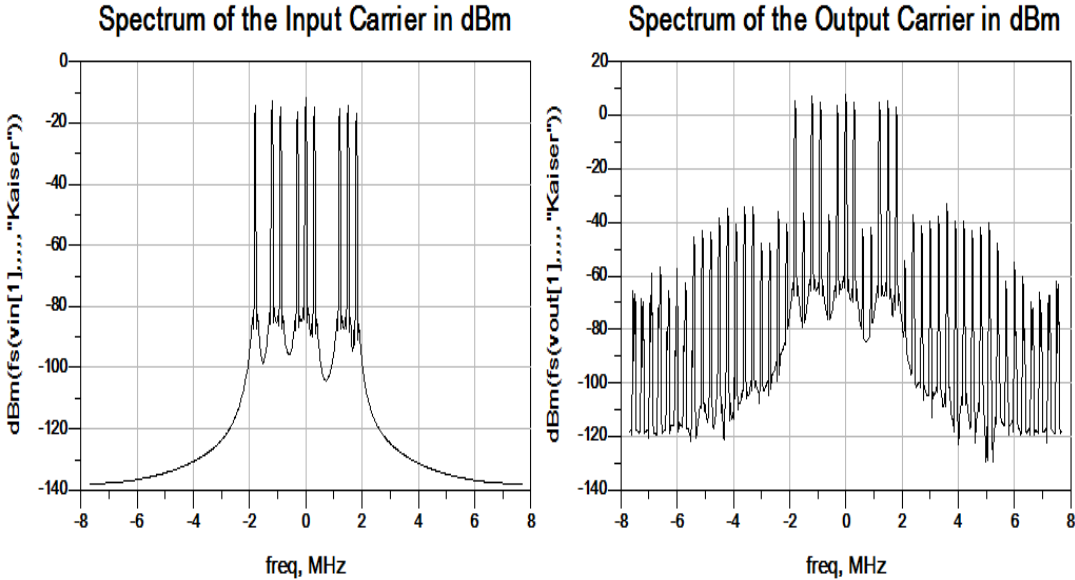


Figure 4-14 Baseband spectrum of 9-tone model and amplified (with GVA-63+ amplifier) 9-tone signal

From Figure 4-14, both undistorted 9-tone model and distorted 9-tone model could be observed. When input power is increased the distortion also increases. In the output spectrum it is possible to see both in-band and out of band components. Furthermore, similar to the 7-tone model, 9-tone model also represents the channel bandwidth of WCDMA signal well enough. 9-tone model presented here has a channel bandwidth of 3.6 MHz which is close to the 3.84 MHz.

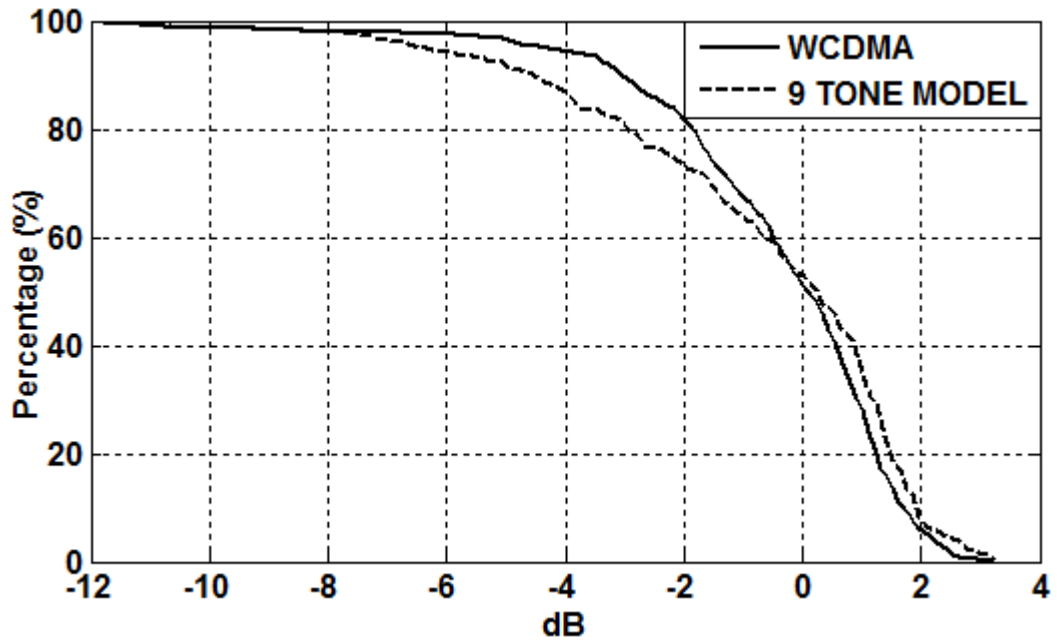


Figure 4-15 CCDF curves of 9-tone model and WCDMA signal

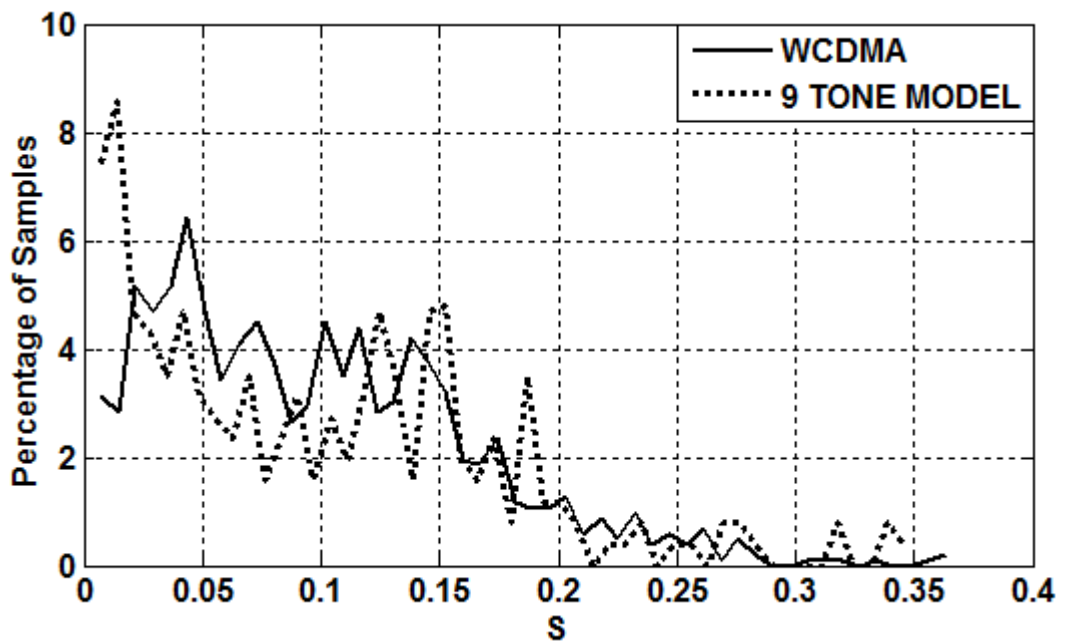


Figure 4-16 The distribution of instantaneous nonlinear power of WCDMA signal and its 9-tone model

As shown in Figure 4-15, crest factor of 9-tone model (3.245 dB) and crest factor of WCDMA signal (3.228 dB) are very close to each other. Moreover, CCDF curve of 9-tone model shows better characteristic than that of the 7-tone model. 9-tone model and WCDMA CCDF curves come very close to each other for the samples with low

power levels (samples with more than 7 dB less power than average power level, i.e., left of -7 dB in the x-axis). CCDF curve of 9-tone model also follow the CCDF curve of WCDMA signal well above the average power level (i.e., right side of 0 dB in x-axis). Between the -7 dB and 0 dB in the x-axis, curves are distinct, but still better than 3, 5 and 7-tone model. In Figure 4-16, distribution of instantaneous nonlinear power is plotted for WCDMA and 9-tone model. Distribution of term S for 9-tone model shows better characteristic than that of the 7-tone model. For very low values of S, there is an improvement with respect to 7-tone model. 9-tone model S distribution follows that of the WCDMA signal accurately. By comparing the Figure 4-15 and Figure 4-16 with Figure 4-11, Figure 4-12, Figure 4-7, Figure 4-8, Figure 4-3 and Figure 4-4, it could be concluded that with increasing tone number, more accurate models could be obtained in terms of CCDF and instantaneous nonlinear power distribution. Since, with increasing tone number more parameters are revealed which makes the multi-tone design more flexible.

Table 4-9 9-tone model parameters for different drive levels of GVA-63+

Pin		INPUT_ChannelPower_dBm		OUTPUT_ChannelPower_dBm	
	-10.000		-9.853		10.206
	-9.000		-8.853		11.186
	-8.000		-7.853		12.160
	-7.000		-6.853		13.125
	-6.000		-5.853		14.078
	-5.000		-4.853		15.013
	-4.000		-3.853		15.920
	-3.000		-2.853		16.781
	-2.000		-1.853		17.563
	-1.000		-0.853		18.205
	0.000		0.147		18.702
	1.000		1.147		19.095
	2.000		2.147		19.397
	3.000		3.147		19.634
	4.000		4.147		19.823
	5.000		5.147		19.973
Pin	M	K	F	Input_Crest_Factor	Output_Crest_Factor
-10.000	0.009	9.720	92.815	3.245	3.190
-9.000	0.015	15.404	185.190	3.245	3.172
-8.000	0.024	24.412	369.503	3.245	3.147
-7.000	0.038	38.687	737.255	3.245	3.112
-6.000	0.060	61.310	1.471E3	3.245	3.059
-5.000	0.095	97.157	2.935E3	3.245	2.978
-4.000	0.150	153.961	5.856E3	3.245	2.850
-3.000	0.238	243.965	1.168E4	3.245	2.556
-2.000	0.378	386.566	2.331E4	3.245	2.169
-1.000	0.598	612.480	4.652E4	3.245	1.718
0.000	0.948	970.348	9.281E4	3.245	1.482
1.000	1.501	1537.164	1.852E5	3.245	1.153
2.000	2.378	2434.782	3.695E5	3.245	0.913
3.000	3.766	3855.969	7.373E5	3.245	0.724
4.000	5.962	6105.536	1.471E6	3.245	0.637
5.000	9.439	9665.187	2.935E6	3.245	0.634

Table 4-10 9-tone model parameters for different drive levels of PMA-545G1+

Pin		INPUT_ChannelPower_dBm		OUTPUT_ChannelPower_dBm	
	-15.000		-14.853		11.112
	-14.000		-13.853		12.099
	-13.000		-12.853		13.083
	-12.000		-11.853		14.066
	-11.000		-10.853		15.047
	-10.000		-9.853		16.027
	-9.000		-8.853		17.005
	-8.000		-7.853		17.980
	-7.000		-6.853		18.944
	-6.000		-5.853		19.865
	-5.000		-4.853		20.692
	-4.000		-3.853		21.323
	-3.000		-2.853		21.827
	-2.000		-1.853		22.214
	-1.000		-0.853		22.511
	0.000		0.147		22.746
Pin	M	K	F	Input_Crest_Factor	Output_Crest_Factor
-15.000	0.013	13.235	139.836	3.245	3.208
-14.000	0.020	20.976	279.009	3.245	3.202
-13.000	0.032	33.244	556.695	3.245	3.198
-12.000	0.051	52.687	1.111E3	3.245	3.193
-11.000	0.082	83.502	2.216E3	3.245	3.190
-10.000	0.129	132.340	4.422E3	3.245	3.185
-9.000	0.205	209.739	8.823E3	3.245	3.175
-8.000	0.325	332.404	1.760E4	3.245	3.147
-7.000	0.514	526.804	3.513E4	3.245	3.059
-6.000	0.815	834.888	7.008E4	3.245	2.631
-5.000	1.292	1323.127	1.398E5	3.245	2.141
-4.000	2.048	2096.854	2.790E5	3.245	1.828
-3.000	3.245	3322.968	5.567E5	3.245	1.491
-2.000	5.142	5265.907	1.111E6	3.245	1.172
-1.000	8.149	8344.620	2.216E6	3.245	0.909
0.000	12.913	13222.780	4.422E6	3.245	0.720

Similar to 3-tone, 5-tone and 7-tone model, 9-tone model also has very close channel power, K and M values as shown in Table 4-9. Moreover, Parameter F shows an improvement and gets closer to F value calculated for WCDMA signal. When Table 4-9 is compared with Table 4-1, it is clear that modeling is valid for all input drive levels, as expected. Furthermore, when the same 9-tone model is applied to a different amplifier, results continue showing good agreement and this could be observed by comparing Table 4-10 with Table 4-3. Presented 9-tone model is not unique and models that will present similar performance could be found. Moreover, by decreasing the phase adjustment and tone spacing resolution, it is possible to obtain better 9-tone models for WCDMA signal.

4.2 Multi-Tone Models for CDMA Signal

In this part of the thesis, 5-tone, 7-tone and 9-tone model are developed to characterize a CDMA signal with certain statistical and channel properties. To find the coefficients of the tones, channel power, channel bandwidth, CCDF curve and nonlinear parameters K, F, M are considered. Results for each model are discussed and strong sides of the different models are depicted with reasoning.

4.2.1 5-Tone Model for CDMA signal

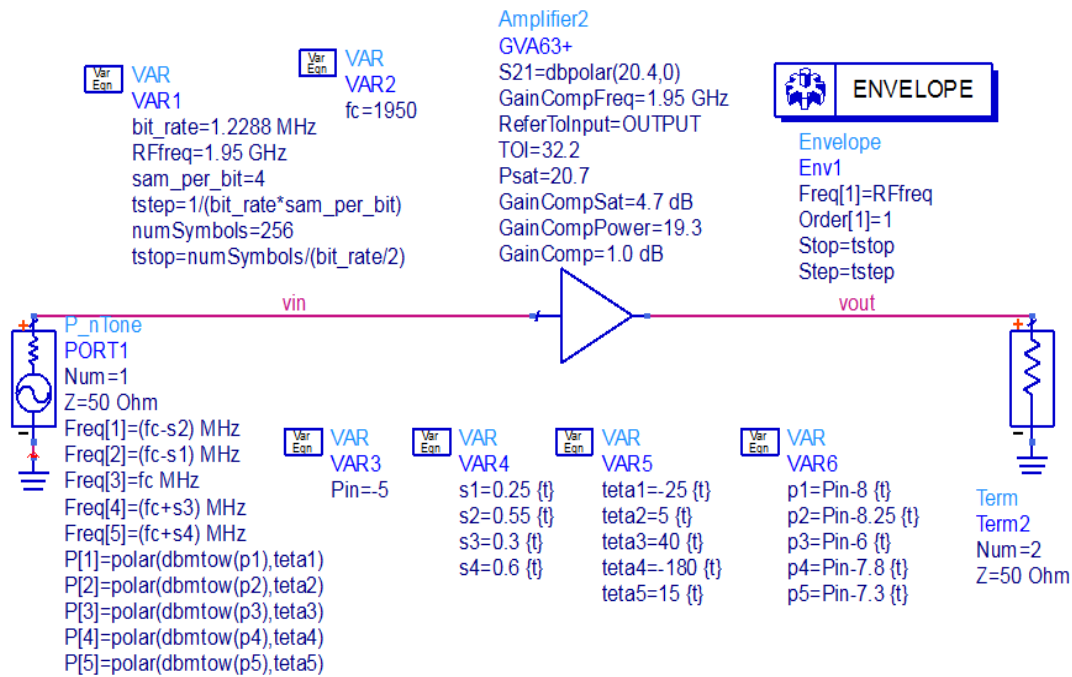


Figure 4-17 5-tone model schematic prepared in ADS

From Figure 4-17, power of the tones are -13 dBm, -13.25 dBm, -11 dBm, -12.8 dBm, -12.3 dBm, and phase coefficients are -25, 5, 40, -180 and 15 degrees. Two of the tones are placed 0.25 and 0.55 MHz left of the center tone and other two tones are placed 0.3 and 0.6 MHz right of the center tone. Tones are placed in such a way that all of the tones fall in to the 1.2288 MHz channel bandwidth.

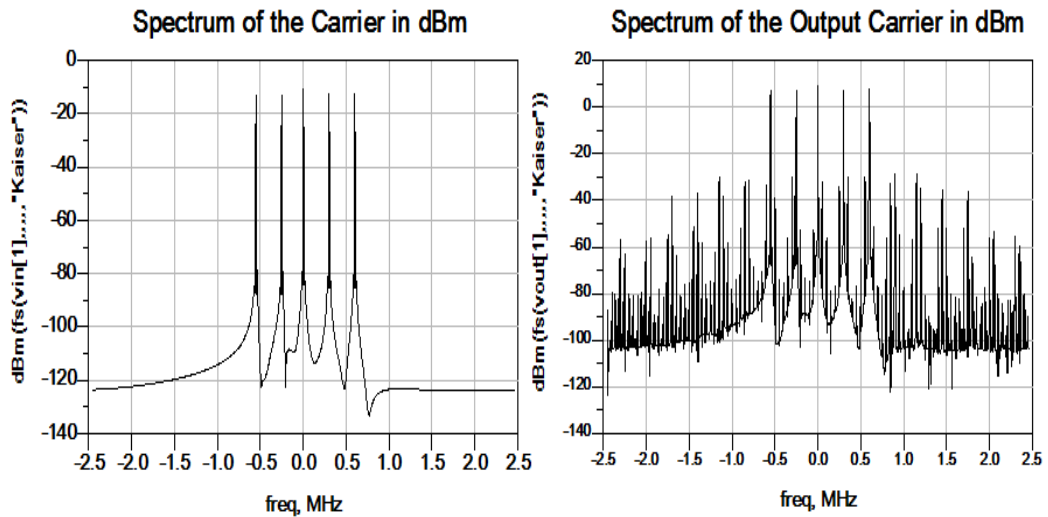


Figure 4-18 Baseband spectrum of 5-tone model (left) and amplified (with GVA-63+ amplifier) 5-tone signal (right)

From Figure 4-18, it is clear that channel bandwidth characteristics of the CDMA signal are represented well with 5-tone model. 5-tone model has a channel bandwidth of 1.15 MHz which is close to the 1.2288 MHz channel bandwidth of CDMA signal. Both un-distorted 5-tone model and distorted 5-tone model could be observed from Figure 4-18. When input power is increased, the distortion also increases. In the output spectrum it is possible to see both in-band and out of band components.

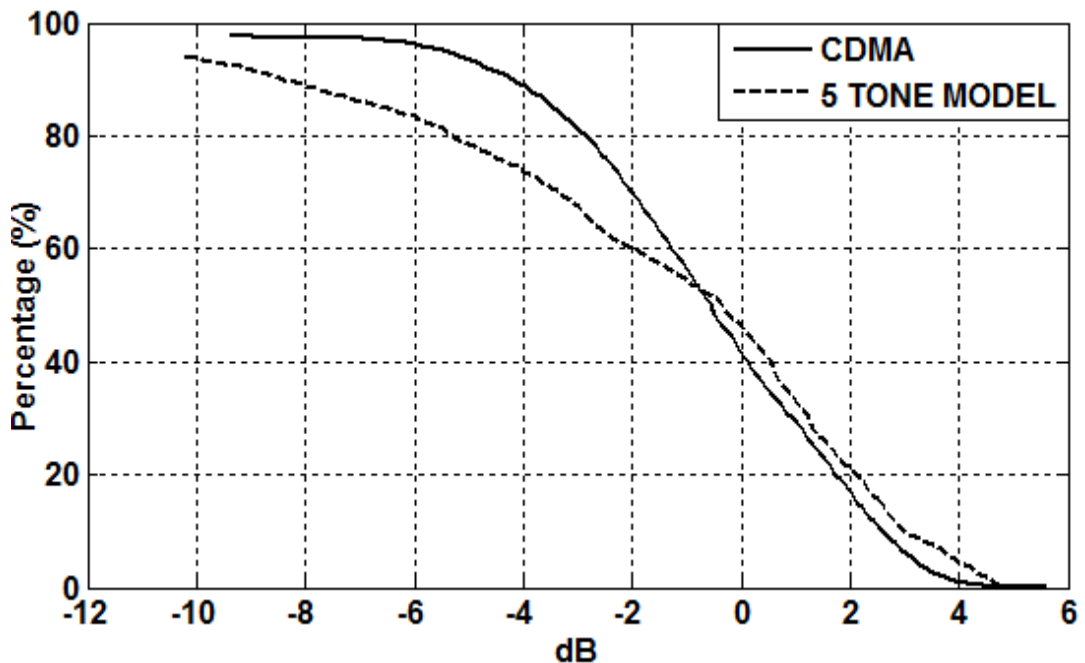


Figure 4-19 CCDF curves of 5-tone model and CDMA signal

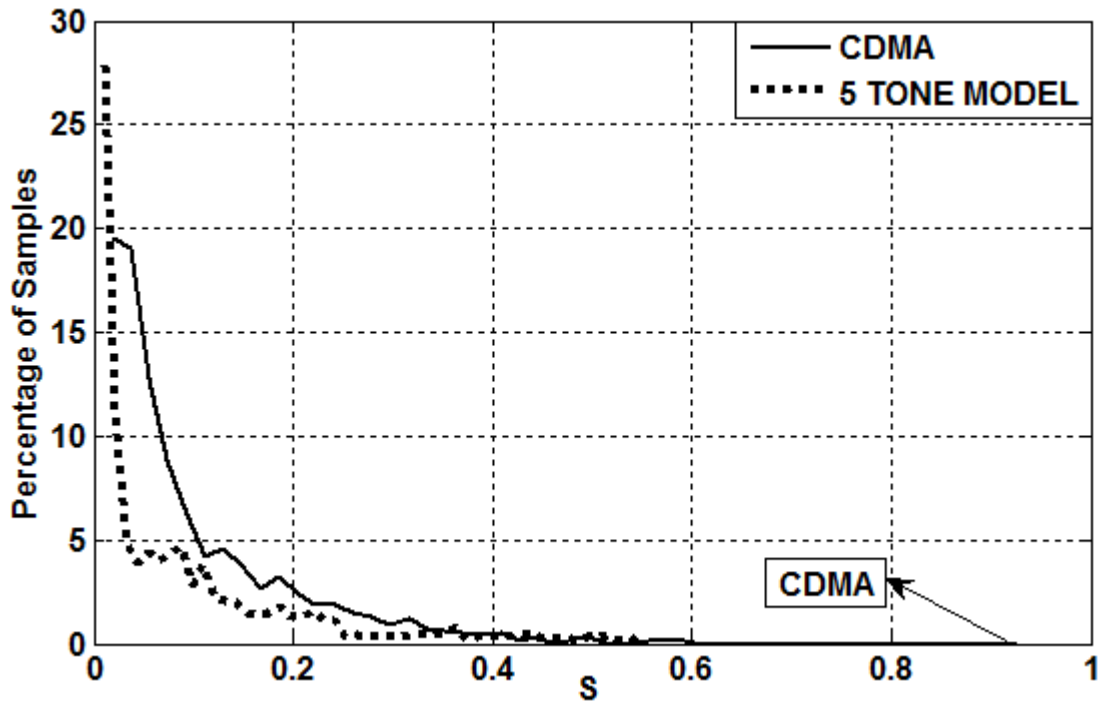


Figure 4-20 The distribution of instantaneous nonlinear power of CDMA signal and its 5-tone model

When Figure 4-19 is examined, it is observed that 5-tone model has a smaller crest factor (4.806 dB) than the CDMA waveform (5.628 dB). Moreover, CCDF curve of 5-tone model can't follow the CCDF curve of CDMA signal well below the average power level (i.e., left side of 0 dB in x-axis). In Figure 4-20, distribution of nonlinear term S is plotted for 5-tone model and CDMA signal. It is observed that maximum value of the S is a lot smaller for 5-tone model, from which it could be extracted that S term of the model signal focuses on its mid values. One can claim that with a better model, improved S distributions could be obtained as it will be proved with 7-tone and 9-tone model S distributions.

Table 4-11 5-tone model parameters for different drive levels of GVA-63+

Pin		INPUT_ChannelPower_dBm			OUTPUT_ChannelPower_dBm	
	-10.000			-10.403		9.912
	-9.000			-9.403		10.888
	-8.000			-8.403		11.855
	-7.000			-7.403		12.811
	-6.000			-6.403		13.749
	-5.000			-5.403		14.661
	-4.000			-4.403		15.524
	-3.000			-3.403		16.315
	-2.000			-2.403		17.006
	-1.000			-1.403		17.597
	0.000			-0.403		18.088
	1.000			0.597		18.493
	2.000			1.597		18.825
	3.000			2.597		19.104
	4.000			3.597		19.333
	5.000			4.597		19.520
Pin	M	K	F	Input_Crest_Factor	Output_Crest_Factor	
-10.000	0.009	18.944	439.297	4.806	4.715	
-9.000	0.015	30.025	876.513	4.806	4.684	
-8.000	0.023	47.586	1.749E3	4.806	4.639	
-7.000	0.037	75.417	3.489E3	4.806	4.573	
-6.000	0.058	119.527	6.962E3	4.806	4.471	
-5.000	0.092	189.436	1.389E4	4.806	4.311	
-4.000	0.147	300.231	2.772E4	4.806	3.937	
-3.000	0.232	475.824	5.530E4	4.806	3.489	
-2.000	0.368	754.112	1.103E5	4.806	3.023	
-1.000	0.584	1195.152	2.202E5	4.806	2.615	
0.000	0.925	1894.118	4.393E5	4.806	2.203	
1.000	1.466	3001.839	8.765E5	4.806	1.887	
2.000	2.323	4757.335	1.749E6	4.806	1.624	
3.000	3.681	7539.381	3.489E6	4.806	1.479	
4.000	5.834	11948.213	6.962E6	4.806	1.407	
5.000	9.246	18935.026	1.389E7	4.806	1.254	

Table 4-12 CDMA signal parameters for different drive levels of GVA-63+

Pin		INPUT_ChannelPower_dBm			OUTPUT_ChannelPower_dBm	
	-10.000			-10.027		10.294
	-9.000			-9.027		11.272
	-8.000			-8.027		12.242
	-7.000			-7.027		13.202
	-6.000			-6.027		14.146
	-5.000			-5.027		15.068
	-4.000			-4.027		15.951
	-3.000			-3.027		16.768
	-2.000			-2.027		17.488
	-1.000			-1.027		18.107
	0.000			-0.027		18.631
	1.000			0.973		19.059
	2.000			1.973		19.391
	3.000			2.973		19.640
	4.000			3.973		19.823
	5.000			4.973		19.958
Pin	M	K	F	Input_Crest_Factor	Output_Crest_Factor	
-10.000	0.009	18.838	398.326	5.628	5.465	
-9.000	0.015	29.857	794.765	5.628	5.406	
-8.000	0.023	47.320	1.586E3	5.628	5.319	
-7.000	0.037	74.997	3.164E3	5.628	5.186	
-6.000	0.058	118.861	6.313E3	5.628	4.978	
-5.000	0.092	188.382	1.260E4	5.628	4.503	
-4.000	0.146	298.563	2.513E4	5.628	3.926	
-3.000	0.231	473.189	5.015E4	5.628	3.290	
-2.000	0.366	749.949	1.001E5	5.628	2.739	
-1.000	0.580	1188.581	1.996E5	5.628	2.252	
0.000	0.920	1883.759	3.983E5	5.628	1.733	
1.000	1.458	2985.534	7.948E5	5.628	1.413	
2.000	2.310	4731.720	1.586E6	5.628	1.198	
3.000	3.662	7499.237	3.164E6	5.628	1.109	
4.000	5.803	11885.504	6.313E6	5.628	1.011	
5.000	9.198	18837.488	1.260E7	5.628	0.859	

While finding the suitable model, one of the main purposes is to make the channel power, channel bandwidth, average nonlinear power, total nonlinear power, out-of-band power and crest factor as close as possible to those of original waveform as it is told in previous sections. From Table 4-11 and Table 4-12, it could be observed that K and M parameters for 5-tone model are made very similar to those of CDMA signal for all input power levels. However while achieving K and M parameters' resemblance, crest factor of the 5-tone model and channel power are reduced. To get the same average and total nonlinear power, channel power is reduced approximately 0.4 dB. Furthermore, despite the decrease in channel power and crest factor, an increase in parameter F is also observed. To sum up, it could be said that 5-tone model preserves its validity when total and average nonlinear power is considered, but it can't satisfy the out-of-band power, instantaneous nonlinear power and CCDF characteristics of CDMA signal well enough.

Table 4-13 5-tone model parameters for different drive levels of PMA-545G1+

Pin		INPUT_ChannelPower_dBm		OUTPUT_ChannelPower_dBm	
	-15.000		-15.403		10.825
	-14.000		-14.403		11.810
	-13.000		-13.403		12.794
	-12.000		-12.403		13.777
	-11.000		-11.403		14.757
	-10.000		-10.403		15.736
	-9.000		-9.403		16.710
	-8.000		-8.403		17.669
	-7.000		-7.403		18.574
	-6.000		-6.403		19.395
	-5.000		-5.403		20.106
	-4.000		-4.403		20.703
	-3.000		-3.403		21.199
	-2.000		-2.403		21.600
	-1.000		-1.403		21.936
	0.000		-0.403		22.213
Pin	M	K	F	Input_Crest_Factor	Output_Crest_Factor
-15.000	0.013	25.794	661.907	4.806	4.753
-14.000	0.020	40.881	1.321E3	4.806	4.746
-13.000	0.032	64.792	2.635E3	4.806	4.741
-12.000	0.050	102.688	5.258E3	4.806	4.736
-11.000	0.079	162.749	1.049E4	4.806	4.729
-10.000	0.126	257.939	2.093E4	4.806	4.715
-9.000	0.200	408.804	4.176E4	4.806	4.677
-8.000	0.316	647.908	8.333E4	4.806	4.495
-7.000	0.501	1026.861	1.663E5	4.806	4.074
-6.000	0.795	1627.457	3.317E5	4.806	3.560
-5.000	1.259	2579.329	6.619E5	4.806	3.101
-4.000	1.996	4087.927	1.321E6	4.806	2.644
-3.000	3.164	6478.862	2.635E6	4.806	2.233
-2.000	5.014	10268.172	5.258E6	4.806	1.876
-1.000	7.946	16273.695	1.049E7	4.806	1.643
0.000	12.594	25791.555	2.093E7	4.806	1.526

With the same 5-tone model applied to a different amplifier configuration, it is expected to have similar results. When Table 4-13 and Table 4-14 are compared similar behaviors are observed, which proves validity of the model signal is independent of amplifier.

Table 4-14 CDMA signal parameters for different drive levels of PMA-545G1+

Pin		INPUT_ChannelPower_dBm		OUTPUT_ChannelPower_dBm	
	-15.000		-15.027		11.204
	-14.000		-14.027		12.190
	-13.000		-13.027		13.175
	-12.000		-12.027		14.157
	-11.000		-11.027		15.138
	-10.000		-10.027		16.117
	-9.000		-9.027		17.093
	-8.000		-8.027		18.059
	-7.000		-7.027		18.990
	-6.000		-6.027		19.839
	-5.000		-5.027		20.580
	-4.000		-4.027		21.217
	-3.000		-3.027		21.759
	-2.000		-2.027		22.189
	-1.000		-1.027		22.515
	0.000		-0.027		22.759
Pin	M	K	F	Input_Crest_Factor	Output_Crest_Factor
-15.000	0.013	25.648	600.121	5.628	5.546
-14.000	0.020	40.649	1.197E3	5.628	5.538
-13.000	0.031	64.424	2.389E3	5.628	5.531
-12.000	0.050	102.105	4.767E3	5.628	5.521
-11.000	0.079	161.825	9.511E3	5.628	5.502
-10.000	0.125	256.475	1.898E4	5.628	5.452
-9.000	0.198	406.485	3.787E4	5.628	5.182
-8.000	0.315	644.235	7.555E4	5.628	4.703
-7.000	0.499	1021.042	1.507E5	5.628	3.985
-6.000	0.790	1618.240	3.008E5	5.628	3.341
-5.000	1.252	2564.733	6.001E5	5.628	2.803
-4.000	1.985	4064.818	1.197E6	5.628	2.235
-3.000	3.146	6442.283	2.389E6	5.628	1.739
-2.000	4.985	10210.294	4.767E6	5.628	1.430
-1.000	7.901	16182.156	9.511E6	5.628	1.202
0.000	12.523	25646.857	1.898E7	5.628	1.173

4.2.2 7-Tone Model for CDMA signal

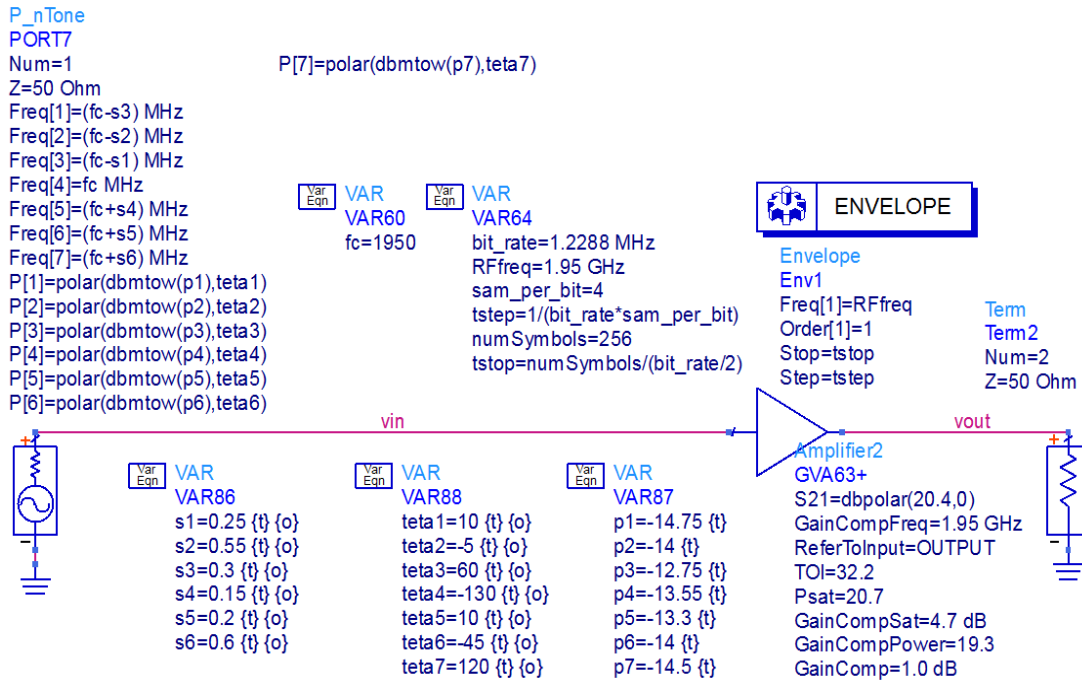


Figure 4-21 7-tone model schematic prepared in ADS

From Figure 4-21, power of the tones are -14.75 dBm, -14 dBm, -12.75 dBm, -13.55 dBm, -13.3 dBm, -14 dBm, -14.5 dBm (and phase coefficients are 10, -5, 60, -130, 10, -45 and 120 degrees. Three of the tones are placed 0.25, 0.55 and 0.3 MHz left of the center tone and other three tones are placed 0.15, 0.2 and 0.6 MHz right of the center tone. Tones are placed in such a way that all of the tones fall in to the 1.2288 MHz channel bandwidth.

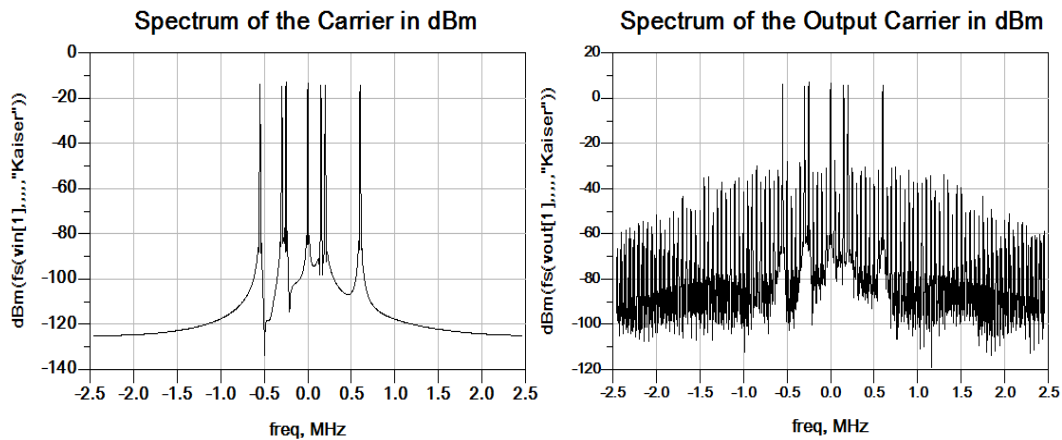


Figure 4-22 Baseband spectrum of 7-tone model (left) and amplified (with GVA-63+ amplifier) 7-tone model (right)

In Figure 4-22, baseband spectrum of the developed 7-tone model and amplified 7-tone model are shown. In band and out of band distortion are clearly observed for the amplified signal. It is important to note channel bandwidth of the 7-tone model (1.15 MHz) is approximated to channel bandwidth of the CDMA signal (1.2288 MHz) well enough similar to the 5-tone model case.

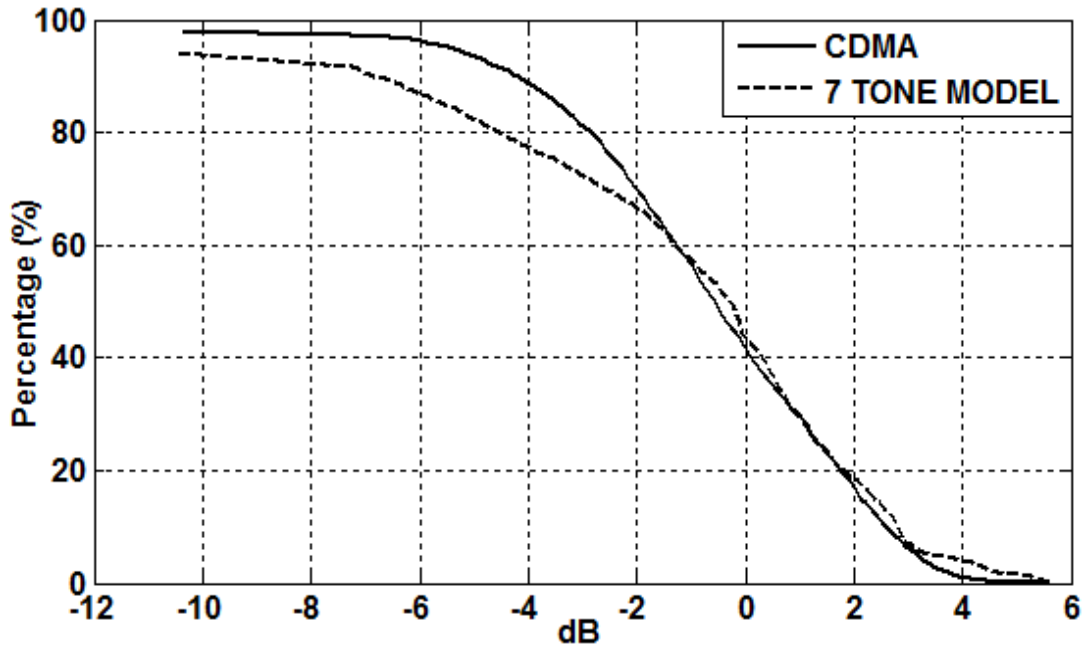


Figure 4-23 CCDF curves of 7-tone model and CDMA signal

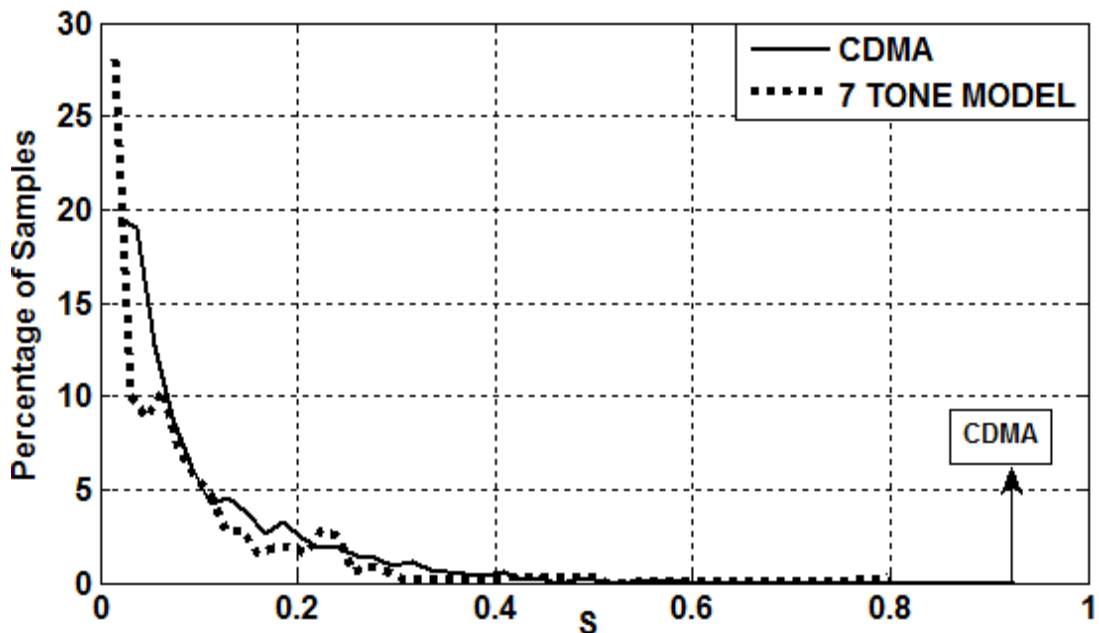


Figure 4-24 The distribution of instantaneous nonlinear power of CDMA signal and its 7-tone model

With 7-tone model, crest factor of the model is made very close to crest factor of CDMA waveform as it is observed in Figure 4-23. Furthermore when 7-tone model CCDF curve is compared with 5-tone model CDDF curve, it is clear that CCDF curve of the 7-tone model follows the CDMA CCDF curve better, but still they are distinct for the samples with low power levels (left of -2 dB in the x-axis). When S distribution of 7-tone model (Figure 4-24) is compared with S distribution of 5-tone model (Figure 4-20), it is observed that maximum value of S is made closer to the maximum value of S of the original waveform. Moreover, 7-tone model S distribution follows the CDMA S distribution better.

Table 4-15 7-tone model parameters for different drive levels of GVA-63+

Pin		INPUT_ChannelPower_dBm		OUTPUT_ChannelPower_dBm	
	-10.000		-10.337		9.979
	-9.000		-9.337		10.954
	-8.000		-8.337		11.922
	-7.000		-7.337		12.877
	-6.000		-6.337		13.816
	-5.000		-5.337		14.723
	-4.000		-4.337		15.587
	-3.000		-3.337		16.395
	-2.000		-2.337		17.118
	-1.000		-1.337		17.736
	0.000		-0.337		18.243
	1.000		0.663		18.649
	2.000		1.663		18.978
	3.000		2.663		19.243
	4.000		3.663		19.458
	5.000		4.663		19.629
Pin	M	K	F	Input_Crest_Factor	Output_Crest_Factor
-10.000	0.009	18.781	443.541	5.562	5.426
-9.000	0.015	29.766	884.981	5.562	5.378
-8.000	0.023	47.176	1.766E3	5.562	5.307
-7.000	0.037	74.769	3.523E3	5.562	5.199
-6.000	0.058	118.502	7.030E3	5.562	5.032
-5.000	0.092	187.814	1.403E4	5.562	4.653
-4.000	0.145	297.667	2.799E4	5.562	4.196
-3.000	0.230	471.775	5.584E4	5.562	3.637
-2.000	0.365	747.721	1.114E5	5.562	3.080
-1.000	0.579	1185.078	2.223E5	5.562	2.526
0.000	0.917	1878.262	4.435E5	5.562	2.015
1.000	1.454	2976.929	8.850E5	5.562	1.633
2.000	2.304	4718.298	1.766E6	5.562	1.351
3.000	3.652	7478.397	3.523E6	5.562	1.140
4.000	5.788	11853.341	7.030E6	5.562	1.095
5.000	9.174	18788.247	1.403E7	5.562	1.070

When Table 4-15 is compared with Table 4-11, it is observed that crest factor is made very close to the crest factor K of CDMA waveform. Furthermore, difference between channel powers of the multi-tone model and CDMA signal is decreased. K and M values also agree with the K and M values of the original waveform as in the

case of 5-tone model. Out of band power doesn't show an improvement with 7-tone model with respect to 5-tone model.

Table 4-16 7-tone model parameters for different drive levels of PMA-545G1+

Pin		INPUT_ChannelPower_dBm			OUTPUT_ChannelPower_dBm	
	-15.000			-15.337		10.892
	-14.000			-14.337		11.877
	-13.000			-13.337		12.861
	-12.000			-12.337		13.844
	-11.000			-11.337		14.824
	-10.000			-10.337		15.802
	-9.000			-9.337		16.772
	-8.000			-8.337		17.714
	-7.000			-7.337		18.622
	-6.000			-6.337		19.473
	-5.000			-5.337		20.223
	-4.000			-4.337		20.850
	-3.000			-3.337		21.357
	-2.000			-2.337		21.763
	-1.000			-1.337		22.090
	0.000			-0.337		22.356
Pin	M	K	F	Input_Crest_Factor	Output_Crest_Factor	
-15.000	0.012	25.571	668.302	5.562	5.490	
-14.000	0.020	40.527	1.333E3	5.562	5.483	
-13.000	0.031	64.232	2.661E3	5.562	5.476	
-12.000	0.050	101.800	5.309E3	5.562	5.468	
-11.000	0.079	161.343	1.059E4	5.562	5.453	
-10.000	0.125	255.711	2.113E4	5.562	5.416	
-9.000	0.198	405.275	4.217E4	5.562	5.256	
-8.000	0.314	642.318	8.413E4	5.562	4.812	
-7.000	0.497	1018.008	1.679E5	5.562	4.337	
-6.000	0.788	1613.437	3.349E5	5.562	3.701	
-5.000	1.249	2557.131	6.683E5	5.562	3.143	
-4.000	1.979	4052.794	1.333E6	5.562	2.510	
-3.000	3.136	6423.274	2.661E6	5.562	2.013	
-2.000	4.971	10180.260	5.309E6	5.562	1.635	
-1.000	7.878	16134.742	1.059E7	5.562	1.348	
0.000	12.486	25572.083	2.113E7	5.562	1.165	

With different amplifier configuration, 7-tone model shows still good agreement with CDMA signal, which could be clearly observed when Table 4-16 and Table 4-12 are compared. This shows validity of the model doesn't depend on amplifier properties.

4.2.3 9-Tone Model for CDMA signal



Figure 4-25 9-tone model schematic prepared in ADS

From Figure 4-25, power of the tones are -16.5 dBm, -13.5 dBm, -13.8 dBm, -15.55 dBm, -14.85 dBm, -14.5 dBm, -15.25 dBm, -16.25 dBm, -14 dBm and phase coefficients are 10, -5, 20, -150, 70, -50, 145, -170 and 20 degrees. Four of the tones are placed 0.15, 0.2, 0.4 and 0.55 MHz left of the center tone. Other four tones are placed 0.15, 0.25, 0.35 and 0.55 MHz right of the center tone. Tones are placed in such a way that all of the tones fall in to the 1.2288 MHz channel bandwidth. In Figure 4-26, baseband spectrum of the 9-tone model and amplified 9-tone model are shown. In band and out of band distortion are clearly observed. It is important to note that channel bandwidth of the 9-tone model (1.1 MHz) is approximated to channel bandwidth of the CDMA signal (1.2288 MHz) well enough similar to the 5-tone and 7-tone models.

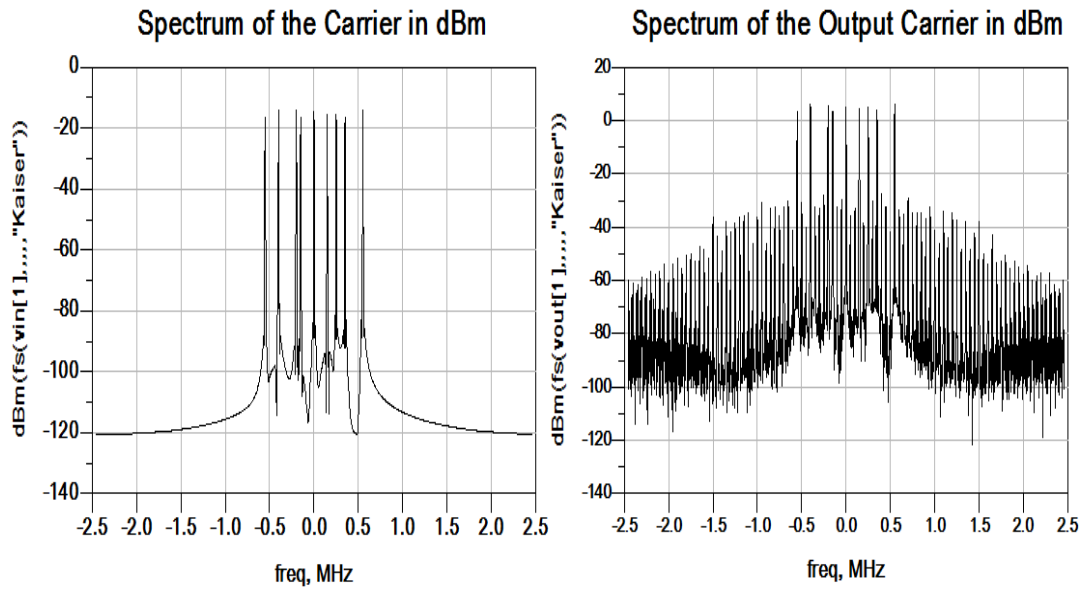


Figure 4-26 Baseband spectrum of 9-tone model representing CDMA signal and amplified (with GVA-63+ amplifier) 9-tone signal

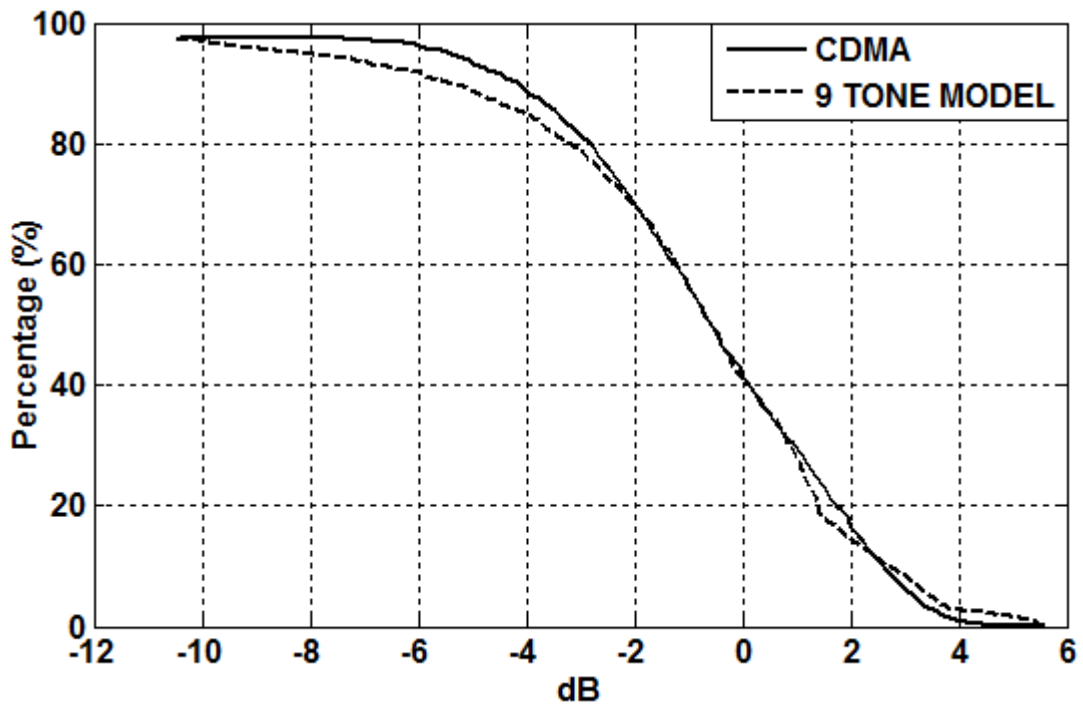


Figure 4-27 CCDF curves of 9-tone model and CDMA signal

CCDF curve of 9-tone model follows the CCDF curve of the CDMA signal with good agreement. Crest Factor of the 9-tone model (5.544 dB) is very close to the Crest Factor of the CDMA signal (5.628 db). When compared the 7-tone model

CCDF curve, an improvement is clearly observed for the samples with low power levels (left of -2 dB in the x-axis). Moreover, when Figure 4-28 is examined, instantaneous nonlinear power distribution of the 9-tone model shows good agreement with S distribution of the CDMA waveform, with only maximum value of S is about 10% smaller for 9-tone model. To sum up, if CDMA waveform is tried to be represented with more than 9-tone signal, it is obvious that better CCDF curves and S distributions could be obtained. However, it is important to note that with increasing number of tones, model complexity also increases, which makes analytical calculations more difficult. Furthermore, presented multi-tone models are not unique. With different sets of phase, amplitude and tone spacing, similar performances could be obtained. It may also be possible to obtain better models by adjusting the phase and spacing of tones more sensitively in the tuning process.

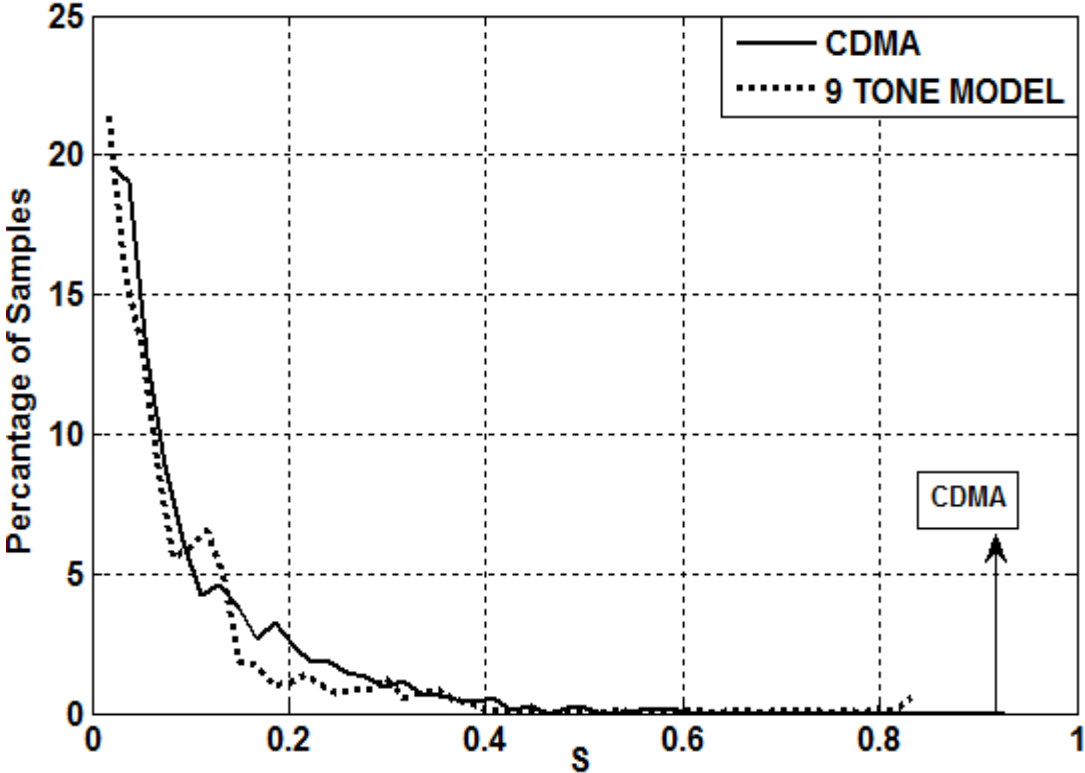


Figure 4-28 The distribution of instantaneous nonlinear power of CDMA signal and its 9-tone model

Table 4-17 9-tone model parameters for different drive levels of GVA-63+

Pin		INPUT_ChannelPower_dBm	OUTPUT_ChannelPower_dBm			
	-10.000	-10.255	10.063			
	-9.000	-9.255	11.039			
	-8.000	-8.255	12.008			
	-7.000	-7.255	12.965			
	-6.000	-6.255	13.905			
	-5.000	-5.255	14.814			
	-4.000	-4.255	15.685			
	-3.000	-3.255	16.504			
	-2.000	-2.255	17.239			
	-1.000	-1.255	17.878			
	0.000	-0.255	18.418			
	1.000	0.745	18.860			
	2.000	1.745	19.202			
	3.000	2.745	19.467			
	4.000	3.745	19.677			
	5.000	4.745	19.839			
Pin	M	K	F	Input_Crest_Factor	Output_Crest_Factor	
-10.000	0.009	18.872	445.724	5.544	5.400	
-9.000	0.015	29.910	889.336	5.544	5.349	
-8.000	0.023	47.405	1.774E3	5.544	5.274	
-7.000	0.037	75.131	3.541E3	5.544	5.160	
-6.000	0.058	119.073	7.064E3	5.544	4.982	
-5.000	0.092	188.716	1.410E4	5.544	4.570	
-4.000	0.146	299.091	2.812E4	5.544	4.114	
-3.000	0.231	474.019	5.611E4	5.544	3.616	
-2.000	0.367	751.254	1.120E5	5.544	2.989	
-1.000	0.581	1190.628	2.234E5	5.544	2.349	
0.000	0.921	1886.963	4.457E5	5.544	1.804	
1.000	1.460	2990.532	8.893E5	5.544	1.412	
2.000	2.314	4739.486	1.774E6	5.544	1.188	
3.000	3.668	7511.250	3.541E6	5.544	1.105	
4.000	5.812	11903.987	7.064E6	5.544	1.019	
5.000	9.212	18865.758	1.410E7	5.544	0.927	

Table 4-18 9-tone model parameters for different drive levels of PMA-545G1+

Pin		INPUT_ChannelPower_dBm	OUTPUT_ChannelPower_dBm			
	-15.000	-15.255	10.975			
	-14.000	-14.255	11.961			
	-13.000	-13.255	12.946			
	-12.000	-12.255	13.928			
	-11.000	-11.255	14.909			
	-10.000	-10.255	15.886			
	-9.000	-9.255	16.854			
	-8.000	-8.255	17.796			
	-7.000	-7.255	18.714			
	-6.000	-6.255	19.569			
	-5.000	-5.255	20.334			
	-4.000	-4.255	20.988			
	-3.000	-3.255	21.544			
	-2.000	-2.255	21.983			
	-1.000	-1.255	22.319			
	0.000	-0.255	22.582			
Pin	M	K	F	Input_Crest_Factor	Output_Crest_Factor	
-15.000	0.013	25.696	671.591	5.544	5.468	
-14.000	0.020	40.725	1.340E3	5.544	5.460	
-13.000	0.032	64.545	2.674E3	5.544	5.453	
-12.000	0.050	102.297	5.335E3	5.544	5.444	
-11.000	0.079	162.129	1.064E4	5.544	5.427	
-10.000	0.125	256.957	2.124E4	5.544	5.386	
-9.000	0.199	407.248	4.237E4	5.544	5.171	
-8.000	0.315	645.443	8.455E4	5.544	4.733	
-7.000	0.499	1022.954	1.687E5	5.544	4.308	
-6.000	0.792	1621.265	3.366E5	5.544	3.733	
-5.000	1.255	2569.517	6.716E5	5.544	2.997	
-4.000	1.988	4072.382	1.340E6	5.544	2.338	
-3.000	3.151	6454.233	2.674E6	5.544	1.803	
-2.000	4.995	10229.156	5.335E6	5.544	1.413	
-1.000	7.916	16211.899	1.064E7	5.544	1.191	
0.000	12.546	25693.698	2.124E7	5.544	1.144	

When Table 4-17 is compared with Table 4-15, it is observed that K, M, F and crest factor exhibit similar results. Only improvement is in the channel power. 9-tone model channel power is closer to CDMA channel power than that of the 7-tone model. Actual improvement with increasing number of tones lies behind the CCDF curve and instantaneous non-linear power distribution. As in the case of previous models, 9-tone model also shows similar results with different amplifier configuration, which is clearly observed when Table 4-18 and Table 4-14 are compared.

CHAPTER 5

EVM & BER MEASUREMENT

In previous parts, to measure the validity of the multi-tone signal, measurements for nonlinearity have been investigated for a single amplifier configuration. Histogram of nonlinear terms, complementary cumulative distribution function, adjacent channel power measurements have been emphasized for different signals. Although these types of measurements provide very critical information, they can't provide detailed information on modulation performance. It is very critical to know the effect of peak to average power ratio reduction, adjacent channel power increase at the output of an amplifier on communication signal modulation performance. Therefore, to obtain more detailed information in communication performance of the model signal, modulated signal analysis is necessary. There are many published researches to achieve extensive test coverage for communication signals by performing error vector magnitude and bit error rate measurements. In [26], EVM is used as figure of merit for effective evaluation of link quality. In [27], BER performance analysis on modulation techniques of WCDMA signal is investigated. In [28], analytical expressions are derived to compute the performance of 8-PSK signal in the presence of amplitude and phase distortion by calculating EVM, SER and SNR. In [29], EVM is offered with remarkable advantages as a conceptual figure of merit to characterize the distortions caused by elements of receiver's RF frontend.

In previous part of thesis, a WCDMA and CDMA signal have been modeled by using multi-tones with varying amplitude, phase, tone spacing and tone number. The purpose of the modeling was to make histogram of nonlinear terms, CCDF curves, channel bandwidth and channel power similar to each other. By making these

properties similar for multi-tone models and original waveform, it should be possible to obtain similar modulated signal performance. For this purpose, RMS EVM, Peak EVM and BER performance of the multicarrier communication signals and their multi-tone models are compared for a transmitter channel consisting of a single amplifier.

As shown in Figure 5-1, EVM is a measure of the difference between the expected complex voltage value of a demodulated symbol and the actual received symbol on a constellation diagram. It is expressed in dB or percentage. BER is a fractional number of errors in a transmitter chain. It just gives a pass or fail result for a transmitted sequence. Although both BER and EVM tell about transmitter quality, it is possible to say that EVM gives more detailed results for system performance. For a large number of transmitted symbol sequences, BER could be very small or a bit error could not be observed during the analysis. Therefore, the immunity of the system performance for different environments could not be estimated by just looking at the BER measurements. However, even if no bit error is observed, a certain level of EVM is measured due to several impairments and the immunity of the system performance could be estimated under more severe conditions.

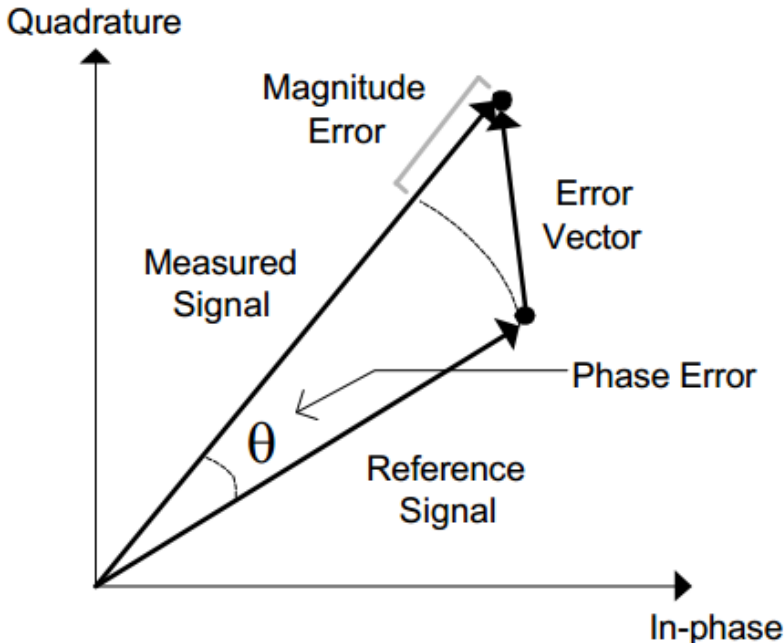


Figure 5-1 Magnitude and phase error components of error vector [28]

In this chapter, BER and EVM Analysis are performed in Matlab software and during the analysis noise contribution is ignored. It is also important to note that error correction algorithms are not performed during the analysis. Amplifier GVA-63+, which is used for simulations in previous chapter, is modeled by Ghorbani amplifier model by using the measured AM-AM and AM-PM characteristics of the amplifier. Modeled amplifier characteristics and measured characteristics are shown in Figure 5-3 and Figure 5-4. During the Matlab analysis following block diagram is used for BER and EVM measurement.

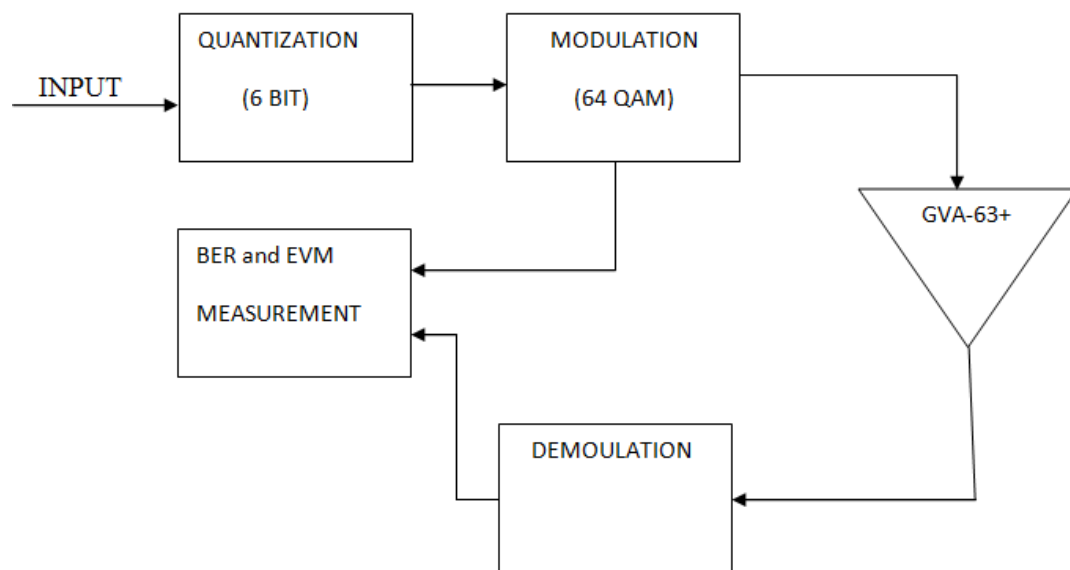


Figure 5-2 Block diagram representation for BER and EVM measurements

Input signal in Figure 5-2 is obtained from transient analysis of the waveforms in Agilent ADS simulation software. The sampled input waveform is exported from ADS and used in Matlab. Next, input signal is quantized by addressing the min level of the input signal as 0 (000000) and max level of the input signal as 63 (111111). Next, symbols are modulated using 64-QAM and presented to the amplifier. The reason for choosing high data rate modulation scheme is to perform the analysis under strict conditions. Since for low density constellations, immunity of the system to impairments such as amplifier nonlinearity is low. Moreover, multicarrier signals like WCDMA usually use high data rate modulation schemes due to bandwidth

efficiency. By using 64-QAM modulation, more realistic approach is obtained and symbols are made more susceptible to amplifier clipping effects.

It is known that the envelope of the input signal is varying with a certain envelope PAPR. Hence, for different drive levels and for different samples of the input signal, gain presented by the amplifier to that sample may differ according to closeness to the compression points. Therefore, normalization for gain is applied. In other words, gain is calculated for each sample of the input and maximum of that is made equal to 1. Gains of other samples are adjusted accordingly. By this way, for samples close to or above the compression points, gain is reduced and clipping effect of the amplifier is modeled. In the next step, amplified signal is demodulated and compared with the input stream presented to the amplifier for EVM and BER measurement. Indeed, BER and EVM measurements for the block diagram in Figure 5-2 include only amplifier clipping effect, but this would be adequate to compare the BER and EVM values of signals.

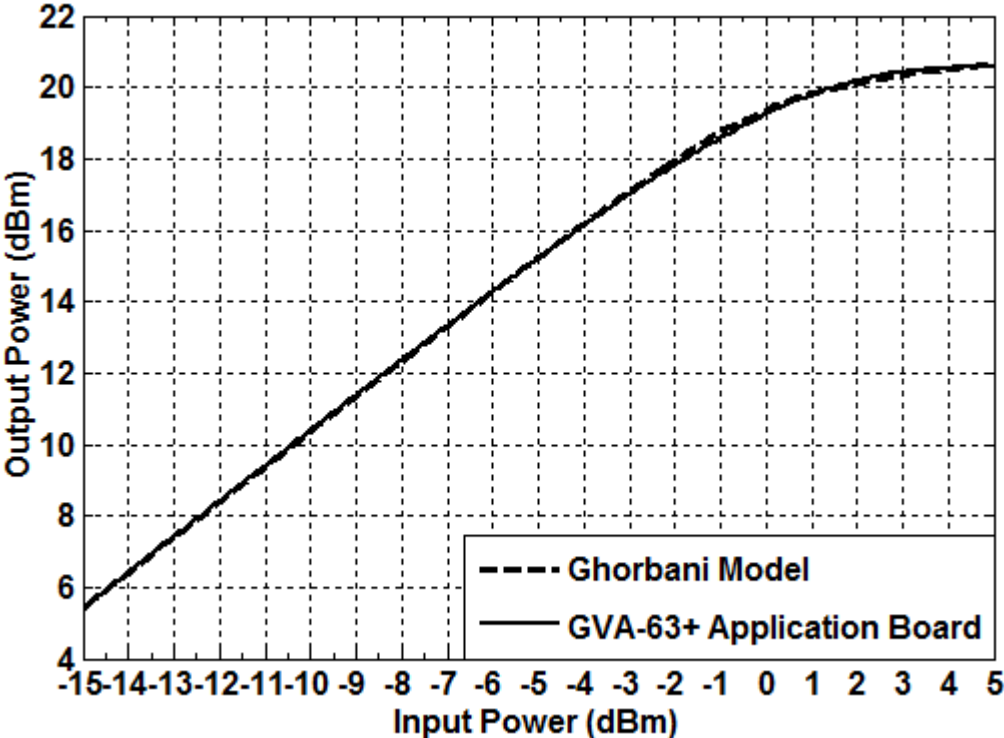


Figure 5-3 Comparison of the AM-AM characteristics of the GVA-63+ application board and model amplifier

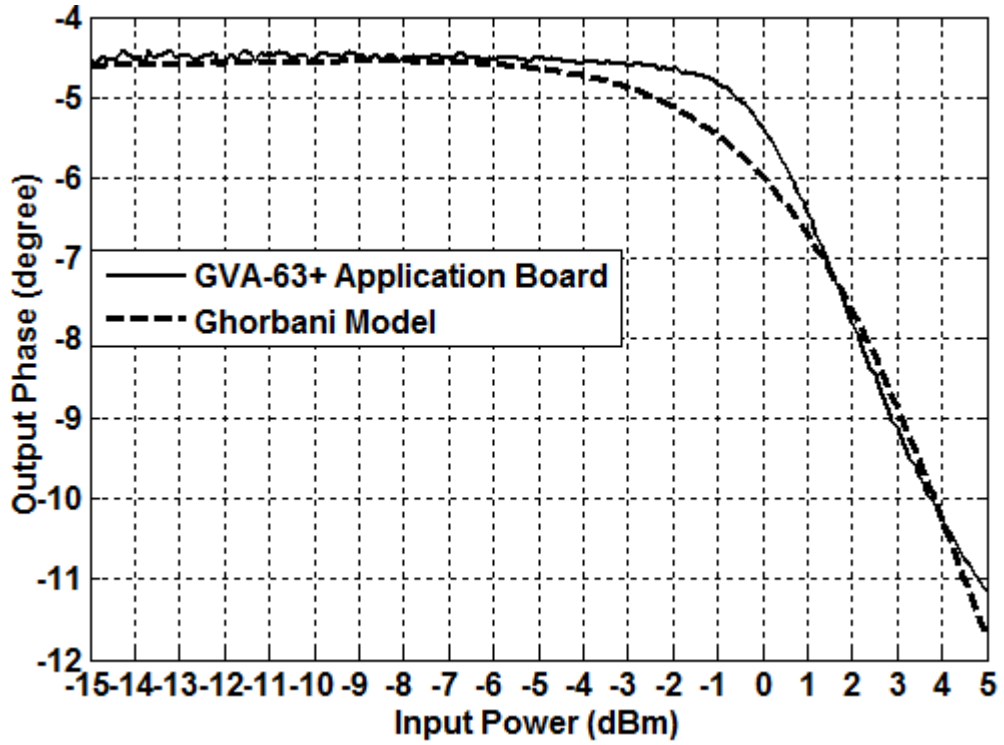


Figure 5-4 Comparison of the AM-PM characteristics of the GVA-63+ application board and model amplifier

In the previous chapter, WCDMA signal is modeled by using 3-tone, 5-tone, 7-tone and 9-tone models. CDMA signal is modeled by using 5-tone, 7-tone and 9-tone models. EVM and BER performance of all models are computed and compared to each other. EVM parameters could be provided in either % or dB. In this thesis, EVM parameters are given in %. RMS EVM is calculated with below formulation.

$$\text{RMS EVM} = \sqrt{\frac{\frac{1}{N} \sum_{k=1}^N (e_k)^2}{\frac{1}{N} \sum_{k=1}^N (I_k^2 + Q_k^2)}} \cdot 100 \quad (5.1)$$

In (5.1), e_k is the error vector for the k^{th} symbol and defined as

$$e_k = (I_k - I'_k)^2 + (Q_k - Q'_k)^2 \quad (5.2)$$

I_k is the in-phase measurement of the k^{th} symbol and Q_k is the quadrature-phase measurement of the k^{th} symbol. I'_k is the in-phase measurement of the k^{th} received symbol and Q'_k is the quadrature-phase measurement of the k^{th} received symbol. EVM is calculated for each symbol and maximum value is called as Max EVM. According to the 3GPP standards Max EVM should not exceed 17.5%. Percentile EVM is the EVM value below which x% of all EVM values lie. Throughout the EVM calculations, Percentile EVM is calculated according to 95% value. This value is chosen based on the standards for WCDMA signal.

5.1 SIMULATED BER and EVM RESULTS

Table 5- 1 EVM and BER results for CDMA signal for different power levels

Pin(dBm)	RMS EVM (%)	MAX EVM (%)	95th Percentile EVM	Total False Bits	BER
-10	0.3816	4.6917	0.7887	0	0
-9.5	0.4408	5.5518	0.9227	0	0
-9	0.5117	6.5693	1.0829	0	0
-8.5	0.5965	7.7702	1.2742	0	0
-8	0.6978	9.1841	1.5023	0	0
-7.5	0.8116	10.8435	1.7740	0	0
-7	0.9623	12.7834	2.0970	0	0
-6.5	1.1331	15.0409	2.4805	0	0
-6	1.3356	17.6530	2.9350	0	0
-5.5	1.5752	20.6542	3.4729	95	3.8637e-6
-5	1.8580	24.0734	4.1080	143	5.8158e-6
-4.5	2.1907	27.9286	4.8561	351	1.427e-5
-4	2.5808	32.2215	5.7344	2947	1.1986e-4
-3.5	3.0365	36.9308	6.7617	6455	2.6253e-4
-3	3.5664	42.0057	7.9582	30984	0.0013
-2.5	4.1792	47.3607	9.3439	50533	0.0021
-2	4.8834	52.8737	10.9333	56028	0.0023
-1.5	5.6870	58.3884	12.7343	70251	0.0029
-1	6.5967	63.7236	14.7667	122864	0.0050
-0.5	7.6170	68.688	17.0420	197251	0.0080
0	8.75	73.0989	19.6188	331517	0.0135

Table 5-2 EVM and BER results for 5-tone model of CDMA signal

Pin(dBm)	RMS EVM (%)	MAX EVM (%)	95th Percentile EVM	Total False Bits	BER
-10	0.4127	3.1365	0.9244	0	0
-9.5	0.4793	3.7071	1.0838	0	0
-9	0.5590	4.3848	1.2760	0	0
-8.5	0.6542	5.1884	1.5044	0	0
-8	0.7677	6.1395	1.7769	0	0
-7.5	0.9028	7.2631	2.1008	0	0
-7	1.0635	8.5871	2.4847	0	0
-6.5	1.2540	10.1425	2.9393	0	0
-6	1.4797	11.9634	3.4760	0	0
-5.5	1.7461	14.0858	4.1084	0	0
-5	2.0599	16.5464	4.8536	0	0
-4.5	2.4283	19.3805	5.7296	135	5.4905e-6
-4	2.8591	22.6186	6.7591	3672	1.4934e-4
-3.5	3.3607	26.2828	7.9623	3672	1.4934e-4
-3	3.9414	30.3805	9.3592	41003	0.0017
-2.5	4.6098	34.8989	10.9709	768181	0.0031
-2	5.3732	39.7978	12.8164	126265	0.0051
-1.5	6.2381	45.0043	14.9101	204828	0.0083
-1	7.2083	50.4096	17.2593	260093	0.0106
-0.5	8.2852	55.8698	19.8593	273234	0.0111
0	9.4665	61.2125	22.6916	369842	0.0150

Table 5-3 EVM and BER results for 7-tone model of CDMA signal

Pin(dBm)	RMS EVM (%)	MAX EVM (%)	95th Percentile EVM	Total False Bits	BER
-10	0.4050	4.1216	0.7543	0	0
-9.5	0.4701	4.8764	0.8895	0	0
-9	0.5479	5.7705	1.0503	0	0
-8.5	0.6408	6.8276	1.2417	0	0
-8	0.7515	8.0744	1.4672	0	0
-7.5	0.8832	9.5411	1.7351	0	0
-7	1.0395	11.2606	2.0488	0	0
-6.5	1.2247	13.2685	2.4217	0	0
-6	1.4435	15.6016	2.8644	0	0
-5.5	1.7013	18.2962	3.3874	0	0
-5	2.0041	21.3854	4.0032	2604	1.0591e-4
-4.5	2.3584	24.8951	4.7104	2604	1.0591e-4
-4	2.7713	28.8395	5.5298	13814	5.6182e-4
-3.5	3.25	33.2144	6.4710	30521	0.0012
-3	3.8017	37.991	7.5451	38266	0.0016
-2.5	4.4335	43.1099	8.7565	75207	0.0031
-2	5.1517	48.4760	10.2156	101206	0.0041
-1.5	5.9614	53.9580	11.8969	108087	0.0044
-1	6.8664	59.3932	13.7895	157363	0.0064
-0.5	7.8662	64.5973	15.9694	190590	0.0078
0	8.9664	69.3810	18.4399	329775	0.0134

Table 5-4 EVM and BER results for 9-tone model of CDMA signal

Pin(dBm)	RMS EVM (%)	MAX EVM (%)	95th Percentile EVM	Total False Bits	BER
-10	0.4115	4.2758	0.7502	0	0
-9.5	0.4775	5.0591	0.8771	0	0
-9	0.5564	5.9867	1.0285	0	0
-8.5	0.6506	7.0829	1.2094	0	0
-8	0.7629	8.3753	1.4251	0	0
-7.5	0.8963	9.8947	1.6822	0	0
-7	1.0547	11.679	1.9880	0	0
-6.5	1.2422	13.7519	2.3511	0	0
-6	1.4637	16.1628	2.7818	0	0
-5.5	1.7818	19.5473	3.2918	89	3.6197e-6
-5	2.0305	22.1270	3.8943	3028	1.2315e-4
-4.5	2.3884	25.7370	4.6045	3028	1.2315e-4
-4	2.8049	29.7849	5.4390	17379	7.0681e-4
-3.5	3.2873	34.2625	6.4163	28877	0.0012
-3	3.8426	39.1358	7.5501	38233	0.0016
-2.5	4.4776	44.3382	8.8623	85412	0.0035
-2	5.1985	49.7677	10.3740	110576	0.0045
-1.5	6.0102	55.2859	12.0978	113203	0.0046
-1	6.9163	60.7240	14.0422	156682	0.0064
-0.5	7.9186	65.8944	16.2270	174118	0.0071
0	9.0171	70.6078	18.6587	336402	0.0137

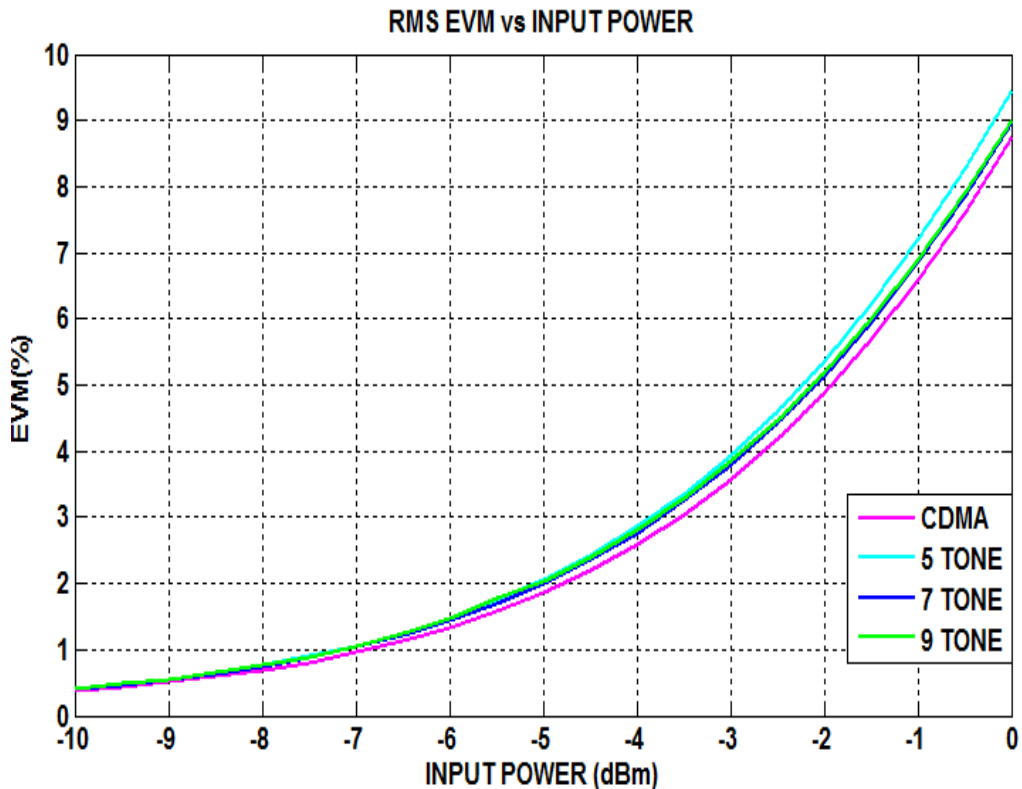


Figure 5-5 RMS EVM values of multi-tone signals and CDMA signal for different power levels

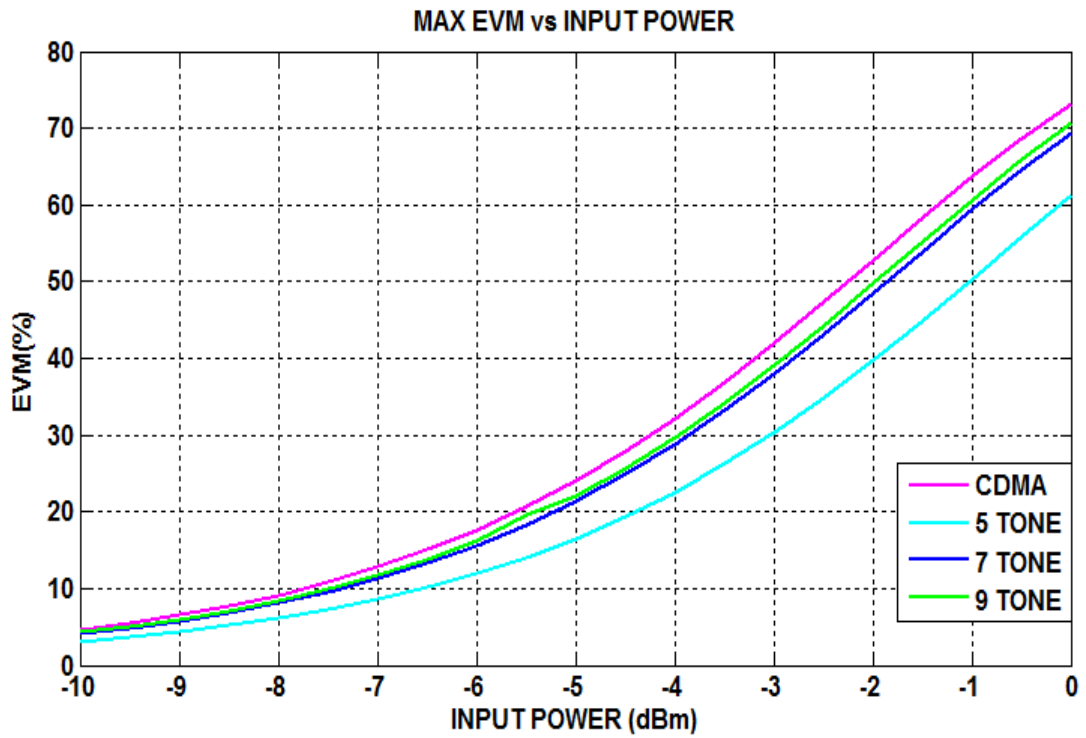


Figure 5-6 Max EVM values of multi-tone signals and CDMA signal for different power levels

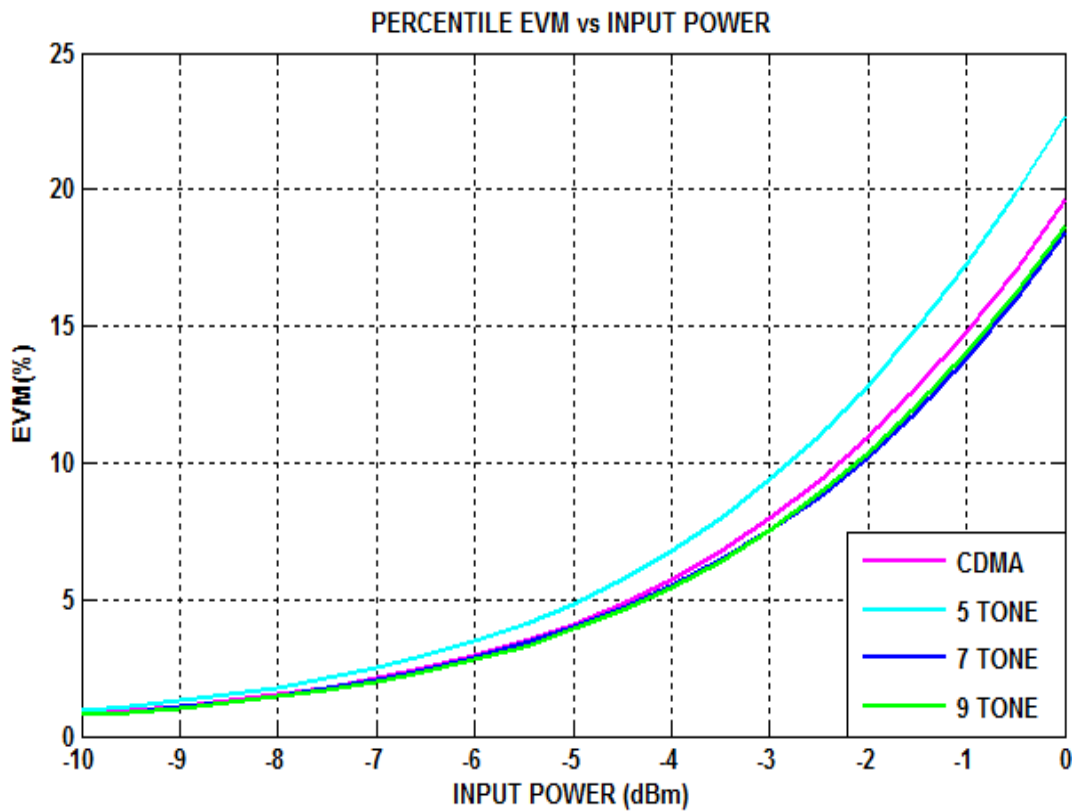


Figure 5-7 Percentile EVM values of multi-tone signals and CDMA signal for different power levels

In general, Max EVM could be related to crest factor of the signal. It is possible to say that if the channel powers of the two signals are the same, the one with lower crest factor should have smaller Max EVM value. In the previous chapter crest factor of the 5-tone model of CDMA signal was given as about 4.806 dB, whereas crest factor of the CDMA signal was given as 5.628 dB. Hence it is expected that 5-tone model has smaller Max EVM value when compared to CDMA signal. When RMS EVM value is considered, 5-tone model has larger RMS EVM value despite it has smaller crest factor. This is related to CCDF distribution of the waveform. Moreover, since the crest factor is less for the 5-tone model, bit error is observed for higher power levels. When input power is increased with 0.5 dB steps, bit error is observed first for -5.5 dBm power level for CDMA signal, whereas for 5-tone model, bit error is first observed for -4.5 dBm power level. 7-tone and 9-tone model crest factor is very close to the crest factor of the CDMA signal. When max EVM values in Table 4.3 and Table 4.4 are compared with max EVM values in Table 4.1, it is observed that they are close to each other. RMS EVM and percentile EVM values of the 7-tone and 9-tone model are also close to each other but 9-tone model is superior. Moreover, 9-tone model is superior to 7-tone model when bit error observation power level is considered. For 9-tone model, bit error rate is first observed at -5.5 dBm input power level as in the case of the CDMA signal, on the other hand, for 7-tone model bit error is observed first at -5 dBm power level. To sum up, it could be easily said that both 7-tone and 9-tone model could represent the modulation performance of the CDMA signal successfully with slight improvement on behalf of 9-tone model.

Table 5-5 EVM and BER results for WCDMA signal for different power levels

Pin(dbm)	RMS EVM (%)	MAX EVM (%)	95th Percentile EVM	Total False Bits	BER
-10	0.3924	2.3976	0.8926	0	0
-9.5	0.4517	2.2872	1.0372	0	0
-9	0.5229	3.3387	1.2103	0	0
-8.5	0.6082	3.9469	1.4176	0	0
-8	0.7102	4.6689	1.6651	0	0
-7.5	0.8320	5.5248	1.9607	0	0
-7	0.9774	6.5375	2.3129	0	0
-6.5	1.1506	7.7330	2.7321	0	0
-6	1.3567	9.1410	3.2303	0	0
-5.5	1.6013	10.7939	3.8216	0	0
-5	1.8912	12.7212	4.5221	0	0
-4.5	2.2340	14.9781	5.3505	0	0
-4	2.6385	17.5842	6.3278	0	0
-3.5	3.1143	20.5809	7.4778	212	1.2311e-5
-3	3.6722	23.9981	8.8266	585	3.3972e-5
-2.5	4.3236	27.8555	10.4027	998	5.7956e-5
-2	5.0808	32.1567	12.2348	23981	0.0014
-1.5	5.9558	36.8830	14.3513	53527	0.0031
-1	6.9601	41.9862	16.7799	153069	0.0089
-0.5	8.1038	47.3834	19.5388	238244	0.0138
0	9.3942	52.9547	22.6436	280058	0.0163

Table 5-6 EVM and BER results for 3-tone model of WCDMA signal

Pin(dbm)	RMS EVM (%)	MAX EVM (%)	95th Percentile EVM	Total False Bits	BER
-10	0.4253	2.7407	1.0088	0	0
-9.5	0.4941	3.2367	1.1771	0	0
-9	0.5764	3.8257	1.3787	0	0
-8.5	0.6748	4.5255	1.6196	0	0
-8	0.7921	5.3550	1.9070	0	0
-7.5	0.9318	6.3366	2.2496	0	0
-7	1.0979	7.4956	2.6574	0	0
-6.5	1.2951	8.8607	3.1421	0	0
-6	1.5286	10.4635	3.7172	0	0
-5.5	1.8046	12.3385	4.3986	0	0
-5	2.1298	14.5221	5.2044	0	0
-4.5	2.5120	17.0508	6.1550	0	0
-4	2.9594	19.9556	7.2735	1172	6.806e-5
-3.5	3.4809	23.2779	8.5853	4567	2.6521e-4
-3	4.0857	27.0255	10.1177	5403	3.1376e-4
-2.5	4.7826	31.2068	11.8991	56513	0.0033
-2	5.58	35.8044	13.9582	93611	0.0054
-1.5	6.4856	40.7729	16.3151	157465	0.0091
-1	7.5008	46.0328	18.9534	213455	0.0124
-0.5	8.6297	51.4688	21.9208	269125	0.0156
0	9.8681	56.9307	25.2615	288492	0.0168

Table 5-7 EVM and BER results for 5-tone model of WCDMA signal

Pin(dbm)	RMS EVM (%)	MAX EVM (%)	95th Percentile EVM	Total False Bits	BER
-10	0.4083	2.1140	0.9534	0	0
-9.5	0.4725	2.4900	1.1190	0	0
-9	0.5494	2.9381	1.3161	0	0
-8.5	0.6413	3.4713	1.5512	0	0
-8	0.7513	4.1048	1.8312	0	0
-7.5	0.8825	4.8566	2.1642	0	0
-7	1.0388	5.7471	2.5597	0	0
-6.5	1.2247	6.7998	3.0288	0	0
-6	1.4455	8.0415	3.5844	0	0
-5.5	1.7073	9.5020	4.2401	0	0
-5	2.0170	11.2142	5.0135	0	0
-4.5	2.3825	13.2134	5.9216	0	0
-4	2.8126	15.5361	6.9853	0	0
-3.5	3.3172	18.2184	8.2251	0	0
-3	3.9067	21.2930	9.6627	4738	2.7515e-4
-2.5	4.5924	24.7856	11.3191	4738	2.7515e-4
-2	5.3853	28.7098	13.2118	46479	0.0027
-1.5	6.2960	33.0613	15.3550	132215	0.0077
-1	7.3339	37.8108	17.7526	168508	0.0098
-0.5	8.5056	42.8988	20.3983	320129	0.0186
0	9.8141	48.2301	23.2684	414381	0.0241

Table 5-8 EVM and BER results for 7-tone model of WCDMA signal

Pin(dbm)	RMS EVM (%)	MAX EVM (%)	95th Percentile EVM	Total False Bits	BER
-10	0.4068	2.1783	0.8594	0	0
-9.5	0.4700	2.5663	0.9978	0	0
-9	0.5458	3.0286	1.1632	0	0
-8.5	0.6365	3.5787	1.3615	0	0
-8	0.7449	4.2322	1.5983	0	0
-7.5	0.8743	5.0075	1.8813	0	0
-7	1.0286	5.9257	2.2182	0	0
-6.5	1.2122	7.0108	2.6199	0	0
-6	1.4303	8.2904	3.0968	0	0
-5.5	1.6890	9.7949	3.6630	0	0
-5	1.9953	11.5579	4.3345	0	0
-4.5	2.3570	13.6153	5.1288	0	0
-4	2.7830	16.0041	6.0660	0	0
-3.5	3.2832	18.7605	7.1691	0	0
-3	3.8683	21.9169	8.4634	3644	2.1161e-4
-2.5	4.5497	25.4981	9.9763	3644	2.1161e-4
-2	5.3390	29.5161	11.7345	40710	0.0024
-1.5	6.2474	33.9638	13.7619	116463	0.0068
-1	7.2850	38.8085	16.0864	156393	0.0091
-0.5	8.4596	43.9856	18.7260	303351	0.0176
0	9.7757	49.3949	21.7158	400773	0.0233

Table 5-9 EVM and BER results for 9-tone model of WCDMA signal

Pin(dBm)	RMS EVM (%)	M EVM (%)	95th Percentile EVM	Total False Bits	BER
-10	0.4023	2.2896	0.8759	0	0
-9.5	0.4642	2.6987	1.0175	0	0
-9	0.5383	3.1860	1.1872	0	0
-8.5	0.6271	3.7656	1.3902	0	0
-8	0.7333	4.4539	1.6329	0	0
-7.5	0.8601	5.2702	1.9225	0	0
-7	1.0113	6.2364	2.2677	0	0
-6.5	1.1913	7.3777	2.6785	0	0
-6	1.4052	8.7226	3.1668	0	0
-5.5	1.6591	10.3027	3.7464	0	0
-5	1.9596	12.1527	4.4331	0	0
-4.5	2.3147	14.3090	5.2452	0	0
-4	2.7332	16.8091	6.2036	0	0
-3.5	3.2247	19.6888	7.3314	56	3.252e-6
-3	3.8002	22.9796	8.6543	3162	1.8362e-4
-2.5	4.4709	26.7037	10.2002	3162	1.8362e-4
-2	5.2486	30.8692	11.9978	36784	0.0021
-1.5	6.1449	35.4631	14.0761	76897	0.0045
-1	7.1704	40.4449	16.4527	164388	0.0095
-0.5	8.3337	45.7410	19.1510	289658	0.0168
0	9.6405	51.2409	22.1897	354917	0.0206

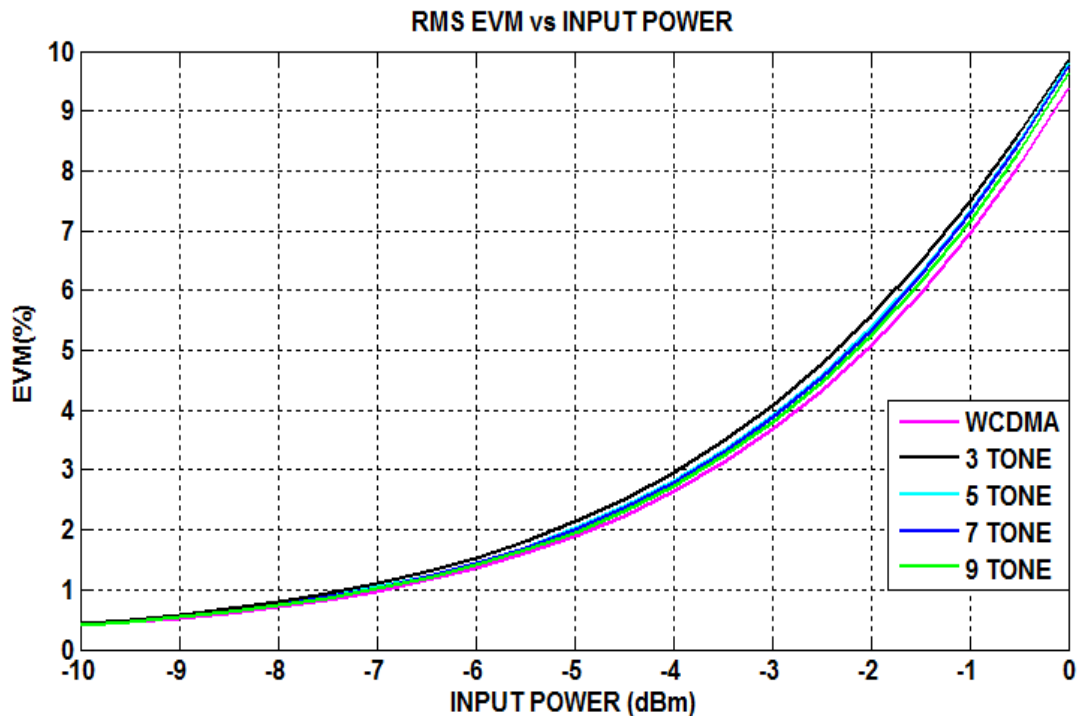


Figure 5-8 RMS EVM values of multi-tone signals and WCDMA signal for different power levels

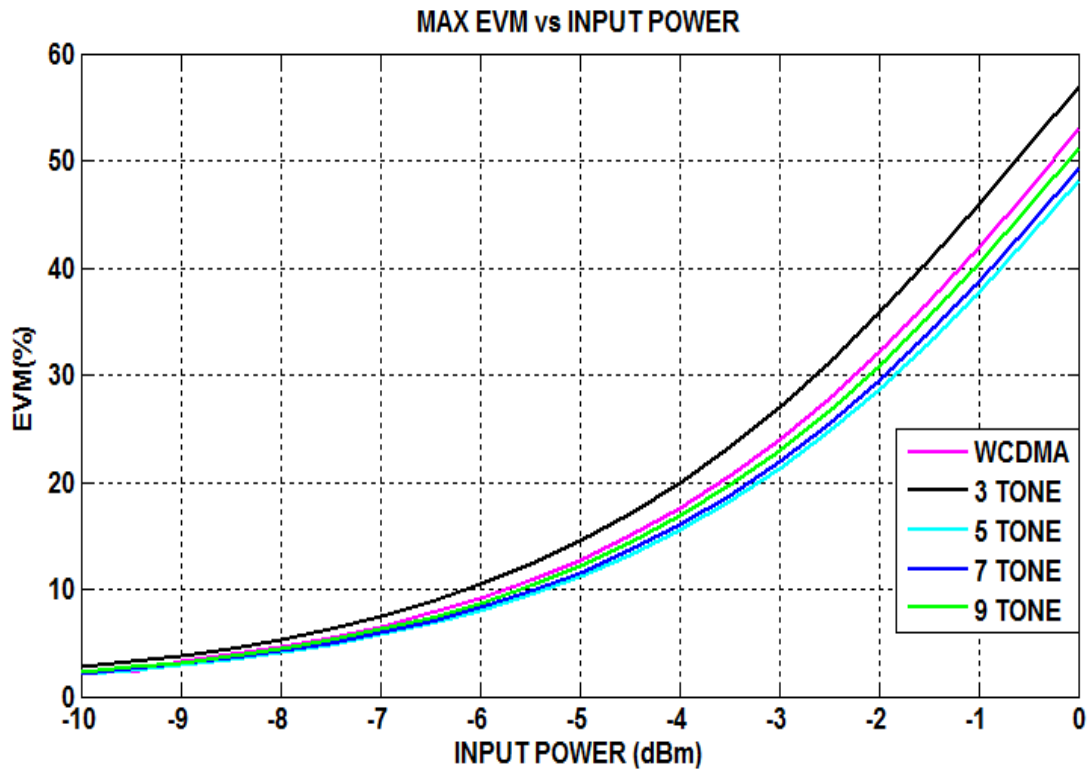


Figure 5-9 Max EVM values of multi-tone signals and WCDMA signal for different power levels

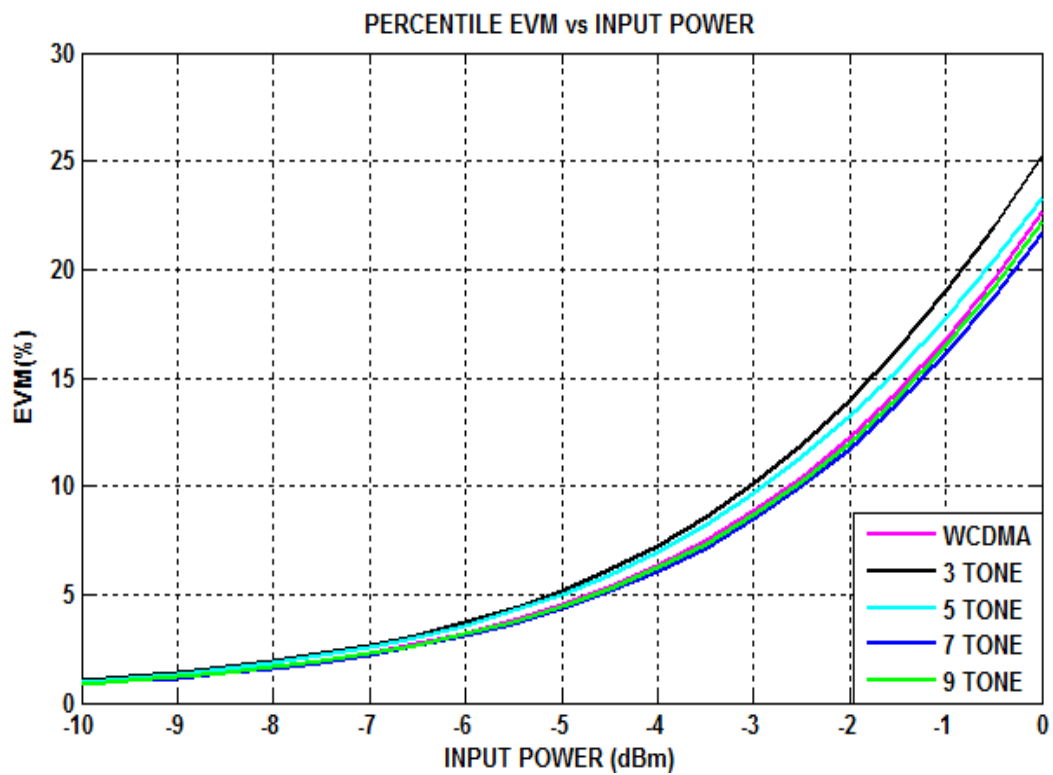


Figure 5-10 Percentile EVM values of multi-tone signals and WCDMA signal for different power levels

In the previous chapter, it was stated that 3-tone model of the WCDMA signal has higher crest factor than that of WCDM signal. That is why 3-tone model has higher Max EVM values for same level of input power. Due to same reason, observation of bit error rate occurs for lower level of input power. In 3-tone model, bit error is first observed for the power level of -4 dBm, whereas for WCDMA signal bit error is first observed for the power level of -3.5 dBm. 5-tone, 7-tone and 9-tone signals have almost identical crest factor with WCDMA signal. Therefore, max EVM value is similar for both 5-tone, 7-tone and 9-tone signals, but it could be said 9-tone model is superior in terms of max EVM. When RMS EVM values are compared, acceptable values are observed for 5-tone, 7-tone and 9-tone model when compared to RMS EVM value of the WCDMA signal, but again 9 tone signal is one step ahead. When bit error observation power level is considered, 9-tone model shows better characteristics. Bit error rate is first observed for -3.5 dBm power level for both WCDMA and 9-tone model. The reason why 9-tone model is one step ahead when compared to other models is that its CCDF curve is better approximated to CCDF curve of WCDMA signal than other models. Although 9-tone model shows better characteristics in terms of modulation performance, 5-tone and 7-tone model also exhibit acceptable performance up to a point.

In short, if channel power and crest factor are represented well enough for the model signal, it is possible to say that Max EVM characteristics of the model signal will be very similar to that of the original waveform. With increasing number of tones, better models are found in terms of RMS EVM, however, with a fewer number of tones RMS EVM may also be represented within an acceptable range. Hence, when modulation properties of a waveform are considered, models with a fewer number of tones may be sufficient.

CHAPTER 6

CONCLUSION & FUTURE WORK

In this thesis, difficulties in analytical implementation of complex and random signals are mentioned. To overcome the analytical implementation problem, utilization of multi-tone signals that would sufficiently characterize the behavior of complex and random signals is suggested.

A CDMA and a WCDMA signal that have different characteristics are modeled by multi-tone signals with variable amplitude and phase coefficients by using Agilent Advanced Design System simulation program. The purpose of using two different types of signals is to show that any signal's behavior could be approximated by multi-tone signals no matter how hard it is. Moreover, number of tones and spacing between tones are also proposed as parameters for the multi-tone signals. Effect of each parameter to model signal is investigated. It is emphasized that choice of number of tones has utmost importance as starting point of proposed models. For both CDMA and WCDMA signal, models with different number of tones are proposed. It is proved that with increasing number of tones better results could be obtained. However it is important to note that with increasing number of tones complexity of the multi-tone signal also increases. In other words, analytical expression of the output of a complex system with multi-tone signal excitation becomes difficult with increasing number of tones.

To decide the validity of the proposed multi-tone models, CCDF curves, channel bandwidth and channel power of the proposed model signals are compared to those of CDMA and WCDMA signal. Furthermore, in-band distortion power, out of band distortion power and total distortion power of the multi-tone model signal in a nonlinear amplifier configuration are tried to made as close as possible to distortion

powers of CDMA and WCDMA signal in the same nonlinear amplifier configuration. Two different amplifiers' performance are measured by making single and 2-tone measurements. From these measurements, linear gain, P_{1dB} , P_{sat} and OIP3 values are calculated. These parameters are embedded into the amplifier unit provided by Agilent ADS simulation program. Simulations are made for different power levels to prove that model signals are valid for any power level. Moreover, the purpose of using two different amplifiers with different characteristics is to demonstrate validity of proposed model signal is independent of the amplifier.

In the final part of the thesis, modulation performance of the proposed models is investigated by BER and EVM analysis in a noise free, single amplifier configuration. Transient simulations for different power levels are made in Agilent ADS. Input and output waveforms are exported and used in the developed Matlab script. Amplifier is modeled by using Ghorbani memoryless model. To decide the model parameters AM-AM and AM-PM performance of a real amplifier are measured. By this way, compression characteristics and output phase shift with increasing drive level are included in the analysis. Analysis are made from large back off input power levels to the input power levels that would highly saturate the amplifier. For both CDMA and WCDMA signal, multi-tone models with different number of tones are analyzed. It is demonstrated that modulation performance of the model signal increases if CCDF curve is approximated more closely.

To get rid of the amplifier clipping and nonlinearity effect, the simplest but most inefficient solution is to operate the amplifier at least peak to average ratio less than maximum output power. For large peak to average ratio signals, this results in excessive heat dissipation and short lived battery issues. Recently, for mobile devices new transmitter topologies have been investigated especially for high peak to average ratio communication signals like CDMA and WCDMA. One of the basic ideas behind these topologies is to convert the varying envelope high peak to average ratio signal to a constant envelope signal before the amplification stage. Cartesian transmitter and polar transmitter topologies employ this procedure. In a polar transmitter, envelope of the signal is passed through a Delta Sigma modulator to obtain a constant envelope signal. Then, carrier is modulated by phase of the signal

and product of constant envelope signal with phase modulated carrier is sent to the amplification stage. Since input of the amplifier is constant envelope signal, it allows the amplifier to operate in saturation region without loss of information. After passing through the amplified signal from a band pass filter, a replica of the input signal could be obtained. In this study, it is shown that envelope characteristics of CDMA and WCDMA signal could be modeled with a certain success by using sufficient number of multi-tone signals. This is proved in Chapter 4 by providing complementary cumulative distribution functions of model and original signals. In other words, by arranging the parameters of multi-tone signal, how often a certain power level is encountered could be mimicked from the original signal. Therefore if some statistical information and some channel properties are provided for an arbitrary communication signal, such as histogram, CCDF curve, channel power, center frequency and channel bandwidth, it is possible to obtain a multi-tone signal that has same statistical information and channel properties. After modeling the arbitrary communication signal with multi-tones, it could be used in a polar transmitter architecture. The performance of the polar transmitter with multi-tone input waveform gives enough information about final performance of the polar transmitter with communication signal that is trying to be modeled.

Another topology to operate an amplifier beyond the compression points is Envelope elimination and restoration (EER) technique. In this technique envelope information is extracted from the input signal by an envelope detector and the detected signal is used to modulate the supply which feeds the drain of the output stage amplifier. EER technique presents good linearity behavior with high efficiency over a broad input power range. Since envelope statistics of a communication signal could be modeled within acceptable range by multi-tone signals, performance of the EER with multi-tone stimuli gives certain information about the performance of the EER with communication signal that is trying to be modeled.

In summary, possible future research activities could include investigation of performance of polar transmitter and EER architecture with multi-tone excitation that represents a communication signal with known statistical properties and channel characteristics.

REFERENCES

- [1] A. Mutlu, “Multi-tone Representation of Arbitrary Waveforms and Application to the Analysis of Non-linear Amplifiers and Feedforward Linearizers”, M.S. thesis, Dept. of Electrical and Electronics Eng., Middle East Technical Univ., Ankara, Turkey, 2005.
- [2] K. A. Remley, “Multisine Excitation for ACPR Measurements”, IEEE MTT-S Digest, pp. 2141-2144, 2003.
- [3] J. C. Pedro, “A Glimpse on Behavioral Modeling for Microwave Transistors”, in Wireless and Microwave Technology Conference, April 7-9, 2013, pp. 1-6
- [4] M. Honkanen and Sven-Gustav Haggman, “New Aspects on Nonlinear Power Amplifier Modeling in Radio Communication System Simulations”, in Personal, Indoor and Mobile Radio Communications, Sep 1-4, 1997, vol. 3, pp. 844-848.
- [5] J. Kim and K. Konstantinou, “Digital Predistortion of Wideband Signals Based on Power Amplifier Model with Memory”, IEEE, vol. 37, no. 23, November 2001.
- [6] Application Note: An Insight Intermodulation Distortion Measurement Method Using IFR2026A/B MultiSource Generator, Aeroflex Corporation, NY, 2007.
- [7] J. Karki. (2003) Calculating Noise Figure and Third-Order Intercept in ADCs. Texas Instruments Corporation, Available: <http://www.ti.com/lit/an/slyt090/slyt090.pdf>
- [8] J.-S. Yuan, Y. Wang, J. Steighner, H. D. Yen, S. L. Jang, G. W. Huang and W. K. Yeh, “Reliability Analysis of Phemt Power Amplifier with an On-Chip Linearizer”, Microelectronics Reliability, vol. 53, pp. 878-884, June 2013.

- [9] R. Sorace, R. Reines, N. Carlson, M. Glasgow, T. Novak and K. Conte, "AM/PM Distortion in Nonlinear Circuits", in Vehicular Technology Conference, Sep. 26-29, 2004, vol. 6, pp. 3994-3996.
- [10] Application Note: ACPR Measurements Using the ME7840A Power Amplifier Test System (PATS), Anritsu, KNG, February 2001.
- [11] S. E. Ramanujam, "Intermodulation Distortion Modeling and Measurement Techniques for GaN Hemt Characterization" Ph.D. dissertation, Dept. of Electrical Eng. and Computer Science, Kassel Univ., Kassel, Germany, 2008.
- [12] Yong-Sub Lee, Mun-Woo and Yoon-Ha Jeong, "High-Efficiency Doherty Amplifier Using GaN Hemt Class-F Cells for WCDMA Applications", in Microwave and Millimeter Wave Technology, April 21-24, 2008, pp. 270-273.
- [13] S. Wood, R. Pengelly, "A High Efficiency Doherty Amplifier with Digital Predistortion for Wimax", High Frequency Electronics, pp. 18-28, 2008.
- [14] Xiaodong Li and Leonard J. Cimini, "Effect of Clipping and Filtering on the Performance of OFDM", in Vehicular Technology Conference, May 4-7, 1997, vol. 3, pp. 1634-1638.
- [15] Ashraf A. Eltholth, Adel R. Mekhail, A. Elshirbini, M. I. Dessouki and A. I. Abdelfattah, "Modeling the Effect of Clipping and Power Amplifier Nonlinearities on OFDM Systems", Ubiquitous Computing and Communication Journal, vol. 3, no. 1, pp. 54-59.
- [16] D. Falconer, T. Kolze, Y. Leiba, J. Liebetreu, "Proposed System Impairment Models", IEEE 802.16.1pc-00/15, February 2000.
- [17] X. Li, C. M. Liu, Y. Xu and F. Li, "Obtaining Polynomial Coefficients from Intercept Points of RF Power Amplifiers", Electronics Letters, vol. 48, no. 19, pp. 1238-1240, September 2012.

- [18] P. Jaunten, "Modeling of Amplifier Nonlinearities I: Memoryless Models", October 2003, unpublished.
- [19] P. Jantunen, "Modelling of Nonlinear Power Amplifiers for Wireless Communications", M.S. thesis, Dept. of Electrical and Communications Eng., Helsinki University of Technology, Helsinki, Finland, 2004.
- [20] A. H. Coskun, A. Mutlu, S. Demir, "A Multi-Tone Model of Complex Enveloped Signals and Its Application in Feedforward Circuit Analysis", IEEE Tran. Microwave Theory and Techniques, vol. 53, pp. 2171-2178, June 2005.
- [21] N. B. Carvalho and J. C. Pedro, "Multi-Tone Intermodulation Distortion Performance of 3rd Order Microwave Circuits", in Microwave Symposium Digest, June 13-19, 1999, vol. 2, pp. 763-766.
- [22] R. Hajji, F. Beanregard, "Multi-Tone Power and Intermodulation Load-Pull Characterization of Microwave Transistors Suitable for Linear SSPA's Design", IEEE Tran. Microwave Theory and Techniques, vol. 45, pp. 1093-1099, July, 1997
- [23] N. Boulejfen, A. Harguem and F. M. Ghannouchi, "New Closed-Form Expressions for the Prediction of Multi-Tone Intermodulation Distortion in Fifth-Order Nonlinear RF Circuits/Systems", IEEE Tran. Microwave Theory and Techniques, vol. 52, pp. 121-132, January 2004.
- [24] J. C. Pedro and N. B. Carvalho, "On the Use of Multi-Tone Techniques for Assessing RF Components' Intermodulation Distortion", IEEE Tran. Microwave Theory and Techniques, vol. 47, pp. 2393-2402, December 1999.
- [25] Application Note: Characterizing Digitally Modulated Signals with CCDF Curves", Agilent Technologies, CA, 2000.
- [26] R. Hassun, M. Flaherty, R. Matreci, M. Taylor, "Effective Evaluation of Link Quality Using Error Vector Magnitude Techniques", in Wireless Communications Conference, August 11-13, 1997, pp. 89-94.

- [27] M. A. Masud, M. Samsuzzaman, M. A. Rahman, “Bit Error Rate Performance Analysis on Modulation Techniques of Wideband Code Division Multiple Access”, *Journal of Telecommunications*, vol. 1, pp. 22-29, March 2010.
- [28] J. L Pinto, I.Darwazeh, “Error Vector Magnitude Relation to Magnitude and Phase Distortion in 8-PSK Systems”, *Electronic Letters*, vol. 37, pp. 437-438, March 2001.
- [29] M. A. Hackl, S. Freisleben, R. Heddergott, W. Xu, “Error Vector Magnitude as a Figure of Merit for CDMA Receiver Design”, unpublished.

APPENDICES

MATLAB SCRIPTS

Script#1: Obtaining CCDF curves from simulated Envelope signals

```
clear all;close all; clc;
a=load('CDMA_ESG_REV_mag_vin[1].txt');
%load magnitude of Envelope of CDMA signal obtained from Agilent ADS
Software
mag=a(:,2);
c=load('9Tone_mag_vin[1].txt');
%load magnitude of Envelope of 9 Tone Model obtained from Agilent ADS
mag_model=c(:,2);
[dimx,dimy]=size(mag);
%Calculate power with reference impedance 1 ohm for CDMA and 9 tone model
refpower_wave=mag.*mag;
refpower_wave_model=mag_model.*mag_model;
sum_power=0;
sum_power_model=0;
for k=1:dimx
sum_power=sum_power+refpower_wave(k);
end
for k=1:dimx
sum_power_model=sum_power_model+refpower_wave_model(k);
end
%Calculate Peak Power and Mean Power for CDMA and its 9 tone Model
peak_pow=max(refpower_wave);
peak_pow_model=max(refpower_wave_model);
mean_pow=sum_power/dimx;
mean_pow_model=sum_power_model/dimx;
peaktoaverage=0.5*(db(peak_pow)-db(mean_pow));
peaktoaverage_model=0.5*(db(peak_pow_model)-db(mean_pow_model));
db_norm_refpower_wave=0.5*db(refpower_wave/mean_pow);

db_norm_refpower_wave_model=0.5*db(refpower_wave_model/mean_pow_model);
```

Script#1 continues

```
span=16;
span_aralik=0.1;
point=span/span_aralik;
x_axis2=[max(db_norm_refpower_wave_model)-
point*span_aralik:span_aralik:max(db_norm_refpower_wave_model)];
x_axis1=[max(db_norm_refpower_wave)-
point*span_aralik:span_aralik:max(db_norm_refpower_wave)];
count=0;
probability_vector=zeros(point+1,1);
probability_vector_model=zeros(point+1,1);
for t=1:point+1
    count=0;
    for k=1:dimx
        if db_norm_refpower_wave(k) >= x_axis1(t)
            count=count+1;
        end
        probability_vector(t)=count/dimx;
    end
end
%Count the number of samples for each interval and calculate probability vector
for CDMA signal
for t=1:point+1
    count=0;
    for k=1:dimx
        if db_norm_refpower_wave_model(k) >= x_axis2(t)
            count=count+1;
        end
        probability_vector_model(t)=count/dimx;
    end
end
%Count the number of samples for each interval and calculate probability vector
for 9 Tone Model
%Plot and Compare CCDF curves of CDMA signal and its 9 Tone Model
plot(x_axis1,probability_vector(:,1),'r',x_axis2,probability_vector_model(:,1),'b')
    xlabel('dB');
    ylabel('Probability');
    title('CCDF Curves of 9 Tone Model and CDMA Signal');
    legend('CDMA','9 Tone Model');
    grid on;
```

Script#2: Obtaining histogram for instantaneous nonlinear power, S

```

clear all; close all; clc
array1=load('CDMA_S_Term.txt');
%Load S values from ADS software for CDMA and 9 tone model signal
array2=load('9Tone_S_Term.txt');
CDMA_S=array1(:,2);
MultiTone_S=array2(:,2);
[Total_Sample_Count,n] = size(array1);
%Find minimum and maximum values of S for CDMA and 9 Tone Model and
%calculate increment value for S for CDMA and 9 Tone Model and segment S
%with calculated increment value to obtain data_start_CDMA_S and
MultiTone_S
min_CDMA_S=min(CDMA_S);
    min_MultiTone_S=min(MultiTone_S);
max_CDMA_S=max(CDMA_S);
    max_MultiTone_S=max(MultiTone_S);
data_segment=50;
data_start_CDMA_S=zeros(1,data_segment+1);
    data_start_MultiTone_S=zeros(1,data_segment+1);
count_sample_CDMA_S=zeros(1,data_segment);
    count_sample_MultiTone_S=zeros(1,data_segment);
increment_CDMA_S=(max_CDMA_S-min_CDMA_S)/data_segment;
    increment_MultiTone_S=(max_MultiTone_S-
min_MultiTone_S)/data_segment;
data_start_CDMA_S(1)=min_CDMA_S;
    data_start_MultiTone_S(1)=min_MultiTone_S;
display_array_CDMA_S=zeros(Total_Sample_Count,data_segment);
    display_array_MultiTone_S=zeros(Total_Sample_Count,data_segment);
for a=2:data_segment+1;
    data_start_CDMA_S(a)=data_start_CDMA_S(a-1)+increment_CDMA_S;
    data_start_MultiTone_S(a)=data_start_MultiTone_S(a-
1)+increment_MultiTone_S;
end
data_start_CDMA_S(data_segment+1)=data_start_CDMA_S(data_segment+1)+
1;
data_start_MultiTone_S(data_segment+1)=data_start_MultiTone_S(data_segmen
t+1)+1;
%Calculate the number of samples for each segment for CDMA signal
for j=1:Total_Sample_Count
for k=1:data_segment
if data_start_CDMA_S(k)<=CDMA_S(j) &&
CDMA_S(j)<=data_start_CDMA_S(k+1)
    count_sample_CDMA_S(k)=count_sample_CDMA_S(k)+1;
    display_array_CDMA_S(j,k)=CDMA_S(j);
end
end
end

```

Script#2 continues

```

for j=1:Total_Sample_Count
for k=1:data_segment
if data_start_MultiTone_S(k)<=MultiTone_S(j) &&
MultiTone_S(j)<=data_start_MultiTone_S(k+1)
count_sample_MultiTone_S(k)=count_sample_MultiTone_S(k)+1;
    display_array_MultiTone_S(j,k)=MultiTone_S(j);
end
end
end
data_start_CDMA_S(data_segment+1)=data_start_CDMA_S(data_segment+1)-
1;
data_start_MultiTone_S(data_segment+1)=data_start_MultiTone_S(data_segmen
t+1)-1;
%Calculate the percentage of samples for CDMA signal and its 9 Tone Model
percentage_sample_CDMA=zeros(1,data_segment);
    percentage_sample_MultiTone=zeros(1,data_segment);
for i=1:data_segment
percentage_sample_CDMA(i)=(count_sample_CDMA_S(i)/Total_Sample_Coun
t)*100;
percentage_sample_MultiTone(i)=(count_sample_MultiTone_S(i)/Total_Sample
_Count)*100;
end
%Obtain the x-axes for plots for CDMA and its 9 Tone Model
x_axis_CDMA=zeros(1,data_segment);
    x_axis_MULTITONE=zeros(1,data_segment);
for i=1:data_segment
    x_axis_CDMA(i)=data_start_CDMA_S(i+1);
    x_axis_MULTITONE(i)=data_start_MultiTone_S(i+1);
end
%Plot number of samples and percentage of samples vs S for the signals
figure;
plot(x_axis_CDMA,count_sample_CDMA_S,'r',x_axis_MULTITONE,count_sa
mple_MultiTone_S,'b');
title('number of Samples vs S');
legend('CDMA','MULTITONE');
xlabel('S');
ylabel('number of Samples');
grid on;
figure;
plot(x_axis_CDMA,percentage_sample_CDMA,'r',x_axis_MULTITONE,percenta
ge_sample_MultiTone,'b');
title('Percentage of Samples vs S');
legend('CDMA','MULTITONE');
xlabel('S');
ylabel('Percentage of Samples');
grid on;

```

Script#3 Modulation Performance Analysis

```

close all;clear all;clc;
%Ghorbani model parameters for amplitude
x1f = -44.5938;
x2f = 3.9688;
x3f = 7.7813;
x4f = 10.5313;
%Ghorbani model parameters for phase
y1f = -131.8516;
y2f = 3.5898;
y3f = 8.4805;
y4f = 1.8242;
%Load simulated transient data for CDMA signal
message = load('Pin is -10 dBm.txt');
wave = message(:,2);
[dimy,q] = size(message);
ampv = zeros(dimy,1);
ampp = zeros(dimy,1);
clear message;
%Obtain amplified signal using Ghorbani Model Parameters
for i = 1:dimy
if wave(i)>= 0
    ampv(i) = (x1f*(wave(i).^x2f)/((1+x3f*wave(i).^x2f ))+
x4f*wave(i);
    ampp(i) = (y1f*(wave(i).^y2f)/((1+y3f*wave(i).^y2f ) )+
y4f*wave(i);
else
    wave(i) = -1*wave(i);
    ampv(i) = (x1f*(wave(i).^x2f)/((1+x3f*wave(i).^x2f ))+
x4f*wave(i);
    ampv(i) = -1*ampv(i);
    ampp(i) = (y1f*(wave(i).^y2f)/((1+y3f*wave(i).^y2f ) )+
y4f*wave(i);
    ampp(i) = -1*ampp(i);
    wave(i) = -1*wave(i);
end
end
%Calculate Gain For Each Sample
gainvector = zeros(dimy,1);
for i = 1:dimy
gainvector(i) = ampv(i)/wave(i);
end
clear ampv;

```

Script#3 continues

```
%Normalize the Gain to make maximum gain equal to 1
maxgain=max(gainvector);
for i = 1:dimy
gainvector(i)=gainvector(i)/maxgain;
end
Tx_Message=wave;
q=6;
%Quantize the waveform with 2^q levels
stepp = (max(wave)-min(wave))/(2^q);
min_val = min(wave);
max_val = max(wave);
new_level = zeros(1,2^q);
for i = 1:2^q
    new_level(i) = i-1;
end
quantization_level = zeros(1,2^q+1);
quantization_level(1) = min_val;
quantization_level(2^q+1) = max_val;
for a=2:2^q;
    quantization_level(a) = quantization_level(a-1)+stepp;
end
for j=1:dimy
for k=1:2^q
if quantization_level(k)<=wave(j) && wave(j)<=quantization_level(k+1)
    Tx_Message(j)=new_level(k);
break;
end
end
end
bin_Tx_message = de2bi(Tx_Message,q,'left-msb');
% M-QAM MDOULATION
h_qam_mod = modem.qammod('M', 2^q, 'PHASEOFFSET', 0,
'SYMBOLORDER', 'GRAY', 'INPUTTYPE', 'INTEGER');
```

Script#3 continues

```
%Constellation Diagram
hScope = commscope.ScatterPlot; % Create a scatter plot scope
hScope.Constellation = h_qam_mod.Constellation;
h_qam_Demod = modem.qamdemod(h_qam_mod);
Modulated_Tx_Message = modulate(h_qam_mod,Tx_Message);
clear Tx_Message;
% update(hScope, Modulated_Tx_Message)
%Amplified Signal in Phasor Domain
amplified_message=zeros(dimy,1);
for j=1:dimy
    amplified_message(j) =
Modulated_Tx_Message(j)*gainvector(j)*(cosd(ampp(j))+1i*sind(ampp(j)));
end
clear ampp;
update(hScope, amplified_message)
%Receiver Part
Rx_Message=transpose(demodulate(h_qam_Demod,amplified_message));
% measurements, and symbol count
hEVM = comm.EVM('MaximumEVMOutputPort',true,...
'XPercentileEVMOutputPort', true, 'XPercentileValue', 90,...
'SymbolCountOutputPort', true);
[RMSEVM,MaxEVM,PercentileEVM,NumSym] =
step(hEVM,Modulated_Tx_Message,amplified_message)
clear Modulated_Tx_Message;
clear amplified_message;

bin_Rx_message = de2bi(Rx_Message,q,'left-msb');
clear Rx_Message;
[Total_False_Bits,BER] = biterr(bin_Tx_message,bin_Rx_message)
[Total_False_Symbols,SER] = symerr(bin_Tx_message,bin_Rx_message)
clear bin_Tx_message;
clear bin_Rx_message;
```